nanomaterials

MDPI

Review

Influence of the Surface Functionalization on the Fate and Performance of Mesoporous Silica Nanoparticles

Miguel Gisbert-Garzarán [1,2,*] and María Vallet-Regí [1,2,*]

[1] Departamento de Química en Ciencias Farmacéuticas, Universidad Complutense de Madrid, Instituto de Investigación Sanitaria Hospital 12 de Octubre i + 12, Plaza Ramón y Cajal s/n, 28040 Madrid, Spain

[2] Networking Research Center on Bioengineering, Biomaterials and Nanomedicine (CIBER-BBN), 28029 Madrid, Spain

* Correspondence: migisber@ucm.es (M.G.-G.); vallet@ucm.es (M.V.-R.); Tel.: +34-91-394-1843 (M.G.-G. & M.V.-R.)

Received: 13 April 2020; Accepted: 24 April 2020; Published: 9 May 2020

Abstract: Mesoporous silica nanoparticles have been broadly applied as drug delivery systems owing to their exquisite features, such as excellent textural properties or biocompatibility. However, there are various biological barriers that prevent their proper translation into the clinic, including: (1) lack of selectivity toward tumor tissues, (2) lack of selectivity for tumoral cells and (3) endosomal sequestration of the particles upon internalization. In addition, their open porous structure may lead to premature drug release, consequently affecting healthy tissues and decreasing the efficacy of the treatment. First, this review will provide a comprehensive and systematic overview of the different approximations that have been implemented into mesoporous silica nanoparticles to overcome each of such biological barriers. Afterward, the potential premature and non-specific drug release from these mesoporous nanocarriers will be addressed by introducing the concept of stimuli-responsive gatekeepers, which endow the particles with on-demand and localized drug delivery.

Keywords: mesoporous silica nanoparticles; cancer; drug delivery; targeting; biological barriers; endosomal escape; stimuli-responsive; controlled drug release; nanomedicine

1. Introduction

In the last few decades, the application of nanotechnology to medicine, the so-called nanomedicine, has attracted much interest among the scientific community, and it is expected to revolutionize the biotechnological and healthcare industries in the near future [1–3]. In this sense, the efforts of many nanotechnologists have been headed toward the development of nanoparticles for the treatment and/or diagnosis of several diseases [4–6]. From a general point of view, those nanoparticles can be classified as organic or inorganic. Organic nanocarriers include liposomes [7], polymeric micelles [8] or polymeric nanoparticles [9], whereas examples of inorganic nanocarriers are metal [10], carbon [11] and silica nanoparticles, which have attracted great attention owing to their excellent properties [12].

Bulk ordered mesoporous silica materials were first reported in the early 90s by researchers from Waseda University [13] and the Mobil Oil Corporation [14]. They have been employed in a number of fields, including catalysis [15,16] or energy storage [17,18], among others. In addition, these materials have been extensively applied for biomedical purposes, especially since Vallet-Regí and coworkers first reported these materials as convenient carriers for therapeutic payloads [19].

Because these bulk mesoporous silica materials exhibited remarkable physico-chemical properties and promising biomedical applications, their translation to the nanoscale dimension was promptly achieved. These efforts led to mesoporous silica nanoparticles (MSNs) offering (a) tunable pore size distributions and high pore volumes (2–30 nm and ca. 1 cm^3/g, respectively), (b) high specific surface areas (up to 1500 cm^2/g), (c) high density of silanol groups on the surface, (d) robust silica framework that allows harsh reaction conditions and (e) great biocompatibility [20,21].

Silica is "generally recognized as safe" by the US Food and Drug Administration (FDA) and it is often used as dietary supplement and as excipient in drug formulations [12,22]. Silica can be found as crystalline or amorphous materials, as MSNs are. Compared to the crystalline form, amorphous silica is rapidly cleared from the lungs, which would account for its lower toxicity [23]. Amorphous silica nanoparticles can be engineered into porous or nonporous silica nanoparticles. Both types of particles are hydrolytically degraded over time into water-soluble, biocompatible silicic acid, which is eventually excreted in the urine [24]. However, it should be mentioned that porous silica nanoparticles degrade faster than their nonporous counterparts, which would facilitate their excretion. This phenomenon has been ascribed to presence of mesopores and the larger surface area of the former [25]. Moreover, the degradation rate of porous silica can be tuned by functionalizing the surface with different functionalities thanks to the creation of a protective barrier [26]. Furthermore, it has been shown that MSNs can also be degraded within cells [27–29].

Given the suitability of MSNs to be applied for biomedical applications, much emphasis should be placed on the surface, as it constitutes the frontline of the nanocarrier. It is involved in all the interactions with the surrounding biological milieu and, consequently, it should be conveniently engineered to avoid any potential issues derived from the administration of the particles. In this regard, presenting a surface full of silanol groups is a feature of major importance, since they can be easily derivatized to other functional groups (amine, carboxylic acid, thiol, etc.) to then introduce additional molecular structures with many different functionalities.

As a result of all the excellent properties described above, MSNs have been applied for the treatment of a number of diseases, such as infection and osteoporotic scenarios [30,31], heart diseases [32–34], ophthalmological diseases [35,36] or diabetes [37,38], among others. In particular, most of the efforts have been headed towards the development of nanocarriers for cancer treatment, which is one of the leading causes of death worldwide [39].

Ideally, drug-loaded nanoparticles should accumulate only in the tumor. However, the several barriers that nanoparticles have to face when administered may not only prevent their successful translation into the clinic, but also reduce the efficacy of the treatments. In fact, a recent meta-analysis argued that less than 1% of the administered nanoparticles finally reached the tumor [40]. Figure 1 illustrates relevant barriers that nanoparticles have to face when administered to a patient.

As observed in Figure 1, MSNs should be able to: (a) accumulate preferentially in the tumors, (b) internalize selectively in cancer cells and (c) achieve endosomal escape to exert their therapeutic action. In addition, drug-loaded MSNs should be able to release their cargo only inside the tumoral cells. To obtain such behavior, researchers have focused on the development of stimuli-responsive gatekeepers. These structures are able to block the pore entrances until some specific stimulus is applied, leading to the drug release.

This review is intended to provide a description on how the surface functionalization of MSNs influences their performance as drug delivery carriers for cancer treatment. The review is sequentially organized according to the journey that MSNs would have when administered systemically to a patient. First, different strategies to enhance the accumulation of MSNs in tumoral tissues will be presented. Then, the different targeting moieties that confer the particles selective recognition of tumoral cells will be described. Afterward, various strategies for achieving the endosomal escape will be outlined. Finally, different strategies to prevent premature drug release and achieve on-demand stimuli-responsive drug delivery will be presented.

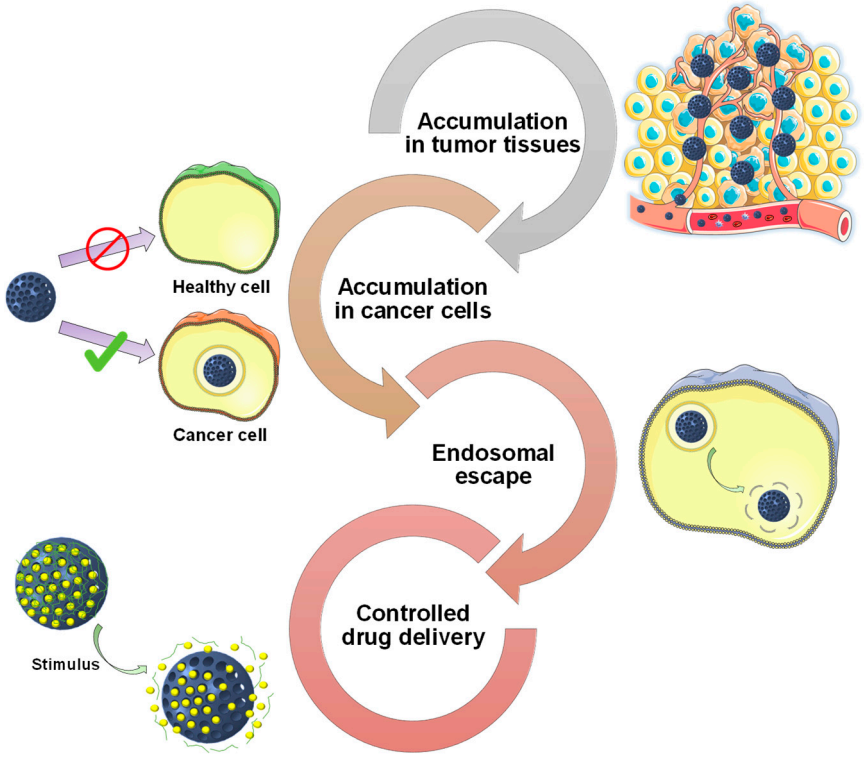

Figure 1. Schematic representation of relevant barriers that mesoporous silica nanoparticles (MSNs) have to face when administered to a patient. These barriers include potential premature release and different biological barriers, such as lack of accumulation in tumor tissues, lack of accumulation in cancer cells and sequestration in the endo-lysosomes.

2. Targeting Tumor Tissues

While achieving preferential cellular uptake in cancer cells is of major importance, maximizing the amount of nanoparticles delivered to the tumoral tissues still needs to be addressed. In this sense, the use of passive and active strategies to promote the accumulation of particles constitutes a promising tool for the effective delivery of chemotherapeutics to the tumors.

2.1. Passive Targeting of Tumor Tissues

2.1.1. Enhanced Permeability and Retention Effect

The first steps towards the development nanocarriers for cancer treatment were the findings that Maeda and coworkers reported in 1986. They found that proteins above 40 kDa spontaneously accumulated in tumoral tissues and remained there for long periods of time [41]. They observed that solid tumors present impaired blood vessels, with 200–2000 nm endothelial cell-cell gaps, and poor lymphatic drainage, as a consequence of their rapid growth. As a consequence of such physiology, nanoparticles tend to leak out from the tumor vessels and accumulate in the tumors (Figure 2).

This effect is known as enhanced permeability and retention (EPR) effect and it is the basis of some commercialized nanomedicines [42]. As observed in Figure 2, only tumor blood vessels show such impaired development and, consequently, the EPR effect constitute a differential feature for the delivery of nanoparticles to tumors [43].

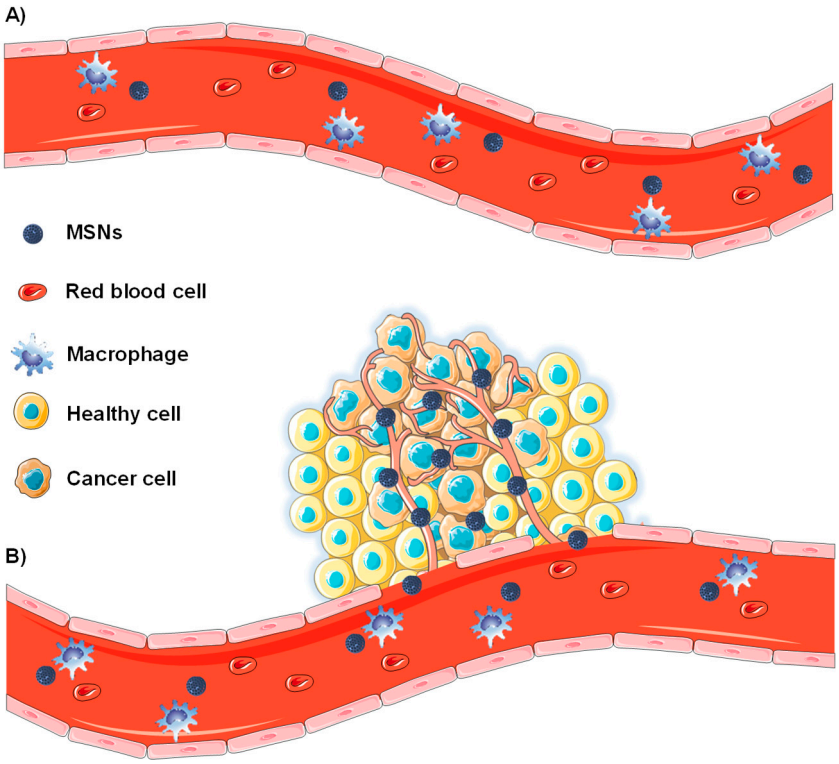

Figure 2. Schematic representation of the enhanced permeability and retention effect. (**A**) Normal blood vessels do not present fenestrations and MSNs remain in the bloodstream. (**B**) Tumor tissues present defective blood vessels and MSNs can leak out from them through the endothelial gap-gap and accumulate in the tumor.

2.1.2. Nanoparticle Features Affecting the Biodistribution of MSNs

In order for the carriers to accumulate in the tumor, it is still necessary to avoid renal clearance and removal from the bloodstream by the mononuclear phagocyte system (MPS). Regarding clearance, in vivo animal studies have shown that MSNs are mainly excreted in the urine, especially during the first two days. Furthermore, 7-nm silica nanoparticles (c-dots) have been approved by the FDA for imaging purposes and the human clinical trials have demonstrated that they are well tolerated and mainly excreted through the kidneys [24].

Features such as their size, shape or surface characteristics directly affect the final fate of the particles. With regard to the size, it is agreed that particles must be at least 10 nm in diameter to bypass renal clearance and smaller than 400 nm, so they can extravasate and diffuse into the tumor. Nonetheless, the precise size to balance those factors along with the eventual cellular uptake of the carriers is controversial. In this respect, some authors consider a size of ca. 100 nm or below as the most effective [44], while others propose a size of ca. 300 nm [45].

The biodistribution and the interaction with cells are also influenced by the shape of the carriers. Unlike their spherical counterparts, rod-like nanoparticles circulate longer in the bloodstream, being at the same time more prone to diverge closer to the vessel walls, enhancing their extravasation [46,47]. Nonetheless, it is unclear whether non-spherical particles present greater cellular internalization than their spherical counterparts [48,49].

In addition to size and shape, the surface characteristics also play an important role. There are some plasma proteins, known as opsonins, whose function is to adhere to foreign bodies so they can be easily recognized by the organism and removed from the bloodstream by the MPS. In consequence, when nanoparticles are exposed to biological fluids, these proteins are rapidly deposited onto the surface, forming a protein corona that provides a biological entity to the particles and triggers their removal [50]. That protein adsorption can be minimized if the surface is conveniently engineered (Figure 3).

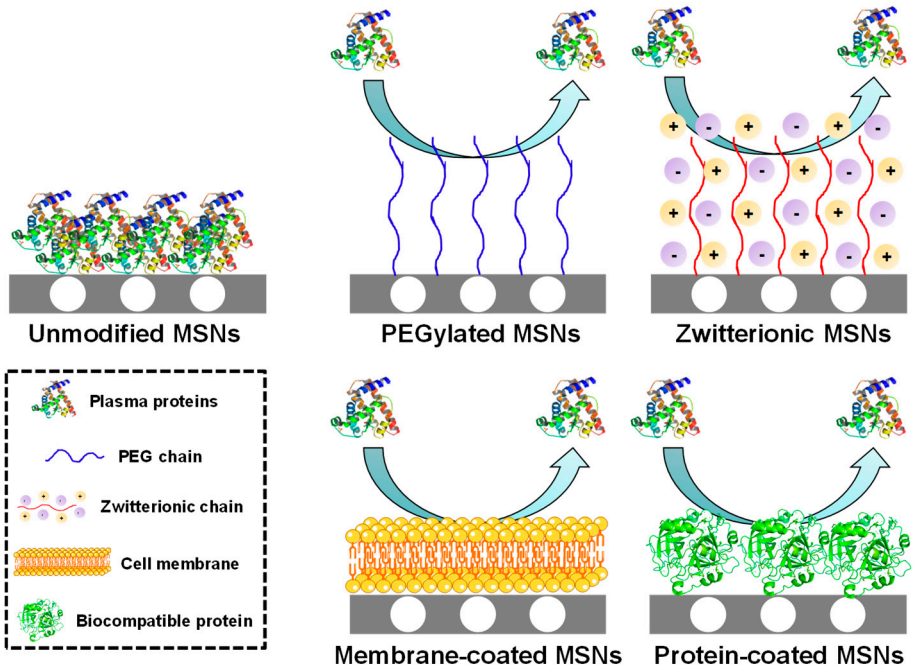

Figure 3. Schematic representation of the strategies employed to minimize protein adsorption and subsequent nanoparticle removal from the bloodstream. Unmodified MSNs tend to adsorb plasma protein, thereby triggering their clearance, whereas functionalized nanoparticles repel plasma protein and achieve longer circulation time.

A common strategy consists in the use of polyethylene glycol (PEG), which is a hydrophilic polymer that creates a hydration layer around the particles, reducing protein adsorption and improving their colloidal stability [51], as demonstrated using MSNs [52,53]. An alternative strategy involves functionalizing the surface with zwitterionic moieties (equal number of positive and negative charges). In this manner, the surface presents zero net charge, which creates a hydration layer that prevents opsonization [54], as it has been shown for different zwitterionic MSNs [55–57]. In addition to those purely chemical approaches, the use of red blood cell membrane coatings onto MSNs has been proved to be useful for preventing immune response and enhancing the circulation time [58]. Furthermore, coating the MSNs with cancer cell membranes not only enhances their circulation time, but also promotes the internalization in such cancer cells [59–61]. Finally, functionalizing MSNs with biocompatible proteins has been proved to reduce macrophage activation and minimize the immune response [62,63].

2.2. Active Targeting of Tumor Tissues

As mentioned above, the EPR effect constitutes a reliable approximation to the passive accumulation of particles in tumors. However, its magnitude highly depends on the particularities of the patient and the tumor [64]. For instance, it is very pronounced in Kaposi sarcoma and multiple myeloma, whereas pancreatic cancer barely exhibits EPR-mediated accumulation [65]. That non-universality of the EPR effect has fueled the development of active approaches to improve the delivery of nanoparticles to the tumor tissues. Examples of this strategy include the use of tumor-tropic peptides and tumor-tropic cells, among others.

2.2.1. Tumor-Tropic Peptides

Tumor-tropic peptides are cyclic peptides that have been observed to trigger the spontaneous accumulation of MSNs in tumoral tissues at the same time that promote their penetration toward inner areas of the tumor [66–68]. This phenomenon is consequence of an existing endocytic transcytosis

pathway in tumor endothelial cells that can be activated by such peptides. The most relevant example is the iRGD peptide, which is composed by the integrin-binding RGD (arginine-glycine-aspartate) peptidic sequence and the neuropilin-1 binding motif. The RGD sequence first binds the overexpressed $\alpha\beta$ integrin present on the membrane of tumor endothelial cells. After that, a proteolytic cleavage exposes the neuropilin-1 motif (previously inactive), which interacts with the NRP-1 receptor and initiates a trans-tissue transport pathway [69,70]. This approach is not restricted to using the RGD motif, and it can be tuned to target alternative receptors (e.g., iNGR peptide [71]).

2.2.2. Cells with Migratory Properties

On the other hand, there are some types of cells with migratory properties, including different bacteria and mesenchymal stem cells, among others [72–74]. For instance, there are bacteria that move toward hypoxic areas, as inner areas of tumors are [75,76]. In this sense, it has been shown that MSNs can be attached to the bacteria wall. Then, such bacteria can move toward inner areas of a 3D tumoral matrix model, carrying the particles and showing great efficacy in killing cancer cells [77].

Mesenchymal cells show inherent migratory properties in response to injury or inflammation and their main advantage is their low or non-immune response. In this manner, nanoparticles are first internalized within these cells to then be spontaneously delivered to the tumoral tissues without exposing them to the biological milieu, thereby minimizing any potential immune response against the particles, as demonstrated using MSNs [78–80].

2.3. Enhanced Penetration in the Tumoral Mass

Aside from targeting the tumoral mass, nanoparticles should diffuse toward inner areas of the tumor to reach and eliminate all cancer cells. The extracellular matrix is predominantly composed of a highly interconnected network of collagen and other components such as hyaluronic acid (HA), elastin, laminin and proteoglycans. Besides, tumors present elevated interstitial pressure [81,82]. As a result, nanoparticles penetration and diffusion are hindered, thereby decreasing the efficacy of the treatment.

2.3.1. Proteolytic Enzymes

Some authors have proposed the use of proteolytic enzymes, as they are able to digest the components of the extracellular matrix, therefore decreasing its stiffness and enhancing nanoparticle penetration. For instance, the surface modification of MSNs with bromelain enhances their diffusion in the tumoral mass, compared to the uncoated particles [83]. However, this strategy has some limitations, as enzymes may degrade and lose their catalytic activity on their way to the tumor. In this regard, our group recently reported the encapsulation of collagenase within a degradable polymeric mesh. This coating remained unaffected at physiological pH, preserving the catalytic activity of the enzyme. However, the capsule degraded at acid pH, releasing the enzyme and enhancing the penetration of MSNs in a 3D tumoral matrix model thanks to the collagen digestion [84,85].

It is agreed that smaller nanoparticles penetrate deeper in the tumors, although those with larger size present greater circulation time. For that reason, a nice strategy to address both concerns consists in designing nanoparticles able to undergo a larger-to-smaller size change upon arrival to the tumoral mass [86]. In this regard, a recent article proposed the synthesis of small 40 nm MSNs that were then engineered as large nanocarriers through the use of 3-arm PEG. MSNs were connected using a peptidic sequence (GPLGIAGQ) cleavable by metalloproteinases (MMPs), which are overexpressed in the extracellular tumoral matrix. Hence, the particles only reduced their size once in the tumor, enhancing the initial accumulation and subsequent penetration in the tumor [87].

2.3.2. Ultrasounds

An alternative strategy to enhance the penetration of particles in tumors consists in the use of localized ultrasound (US) [88]. The rationale for using US relies on the inertial cavitation phenomenon. Cavitation is the oscillation of gas bubbles in a fluid, which can be stable (expanding and contracting

around a given radius) or instable if the pressure is high enough (inertial cavitation). In the latter scenario, the bubbles grow unstably and collapse violently during compression, effect that can be taken advantage of for impelling the particles, favoring their extravasation and subsequent penetration in the tumoral mass [89]. It this sense, it has been observed that applying US leads to increased tumor vascular disruption and deeper particle penetration [90]. However, our group has demonstrated that too high pressure might be needed to obtain significant penetration. In this regard, it has been shown that co-administering MSNs with submicrometric cavitation nuclei leads to enhanced diffusion of the particles in an agarose model upon application of clinically suitable US frequency [91].

3. Targeting Cancer Cells

As stated above, the shape and size of nanocarriers not only determine their extravasation but also affects their interaction with cells. In addition to these parameters, the surface charge also plays an important role. Because of the negatively charged cell membrane, cationic nanoparticles show greater uptake, albeit being more prone to undergo opsonization and subsequent clearance [92,93]. However, there is evidence that positive nanoparticles tend to accumulate in the periphery of the tumor whereas those negatively charged tend to penetrate deeper owing to the repulsion with cell membranes [94]. Nonetheless, even if the previously mentioned factors were optimized, nanoparticles might still be internalized by healthy cells. For that reason, there has been much research on how to specifically recognize cancer cells as well as on how to optimize intracellular trafficking.

A widely employed strategy for the selective targeting of cancer cells consists in the functionalization of the surface targeting ligands that are able to bind specific receptors that are overexpressed only on the membrane of tumoral cells. The ligand density on the particles is a parameter of key importance. For instance, too high ligand density would account for (a) reduced particle stealth character (i.e., increased clearance), (b) increased particle size (i.e., reduced accumulation in the tumor via EPR effect), (c) steric hindrance of closely packed ligands (i.e., reduced nanoparticle binding ability) and (d) high number of cells receptors used per particle (i.e., reduced cellular uptake) [95]. Examples of such targeting agents include antibodies, aptamers, peptides, proteins, saccharides and small molecules (Figure 4).

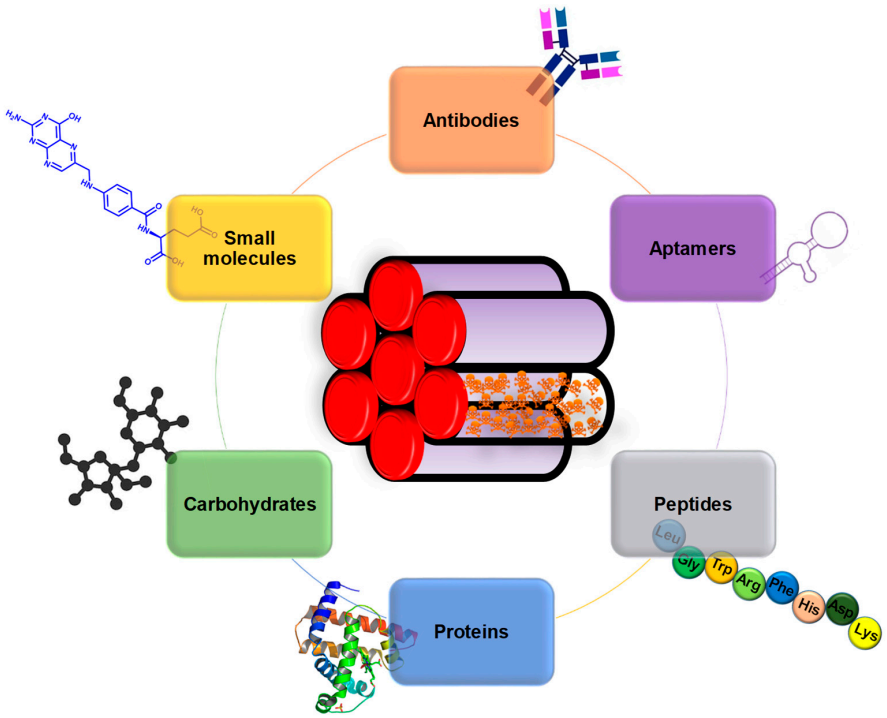

Figure 4. Schematic representation of targeting ligands employed for MSNs-based targeted drug delivery.

Such targeting agents can be implemented into MSNs following different configurations, endowing the particles with many different targeting possibilities. A schematic representation of the strategies most commonly employed to target cancer cells with MSNs is shown in Figure 5.

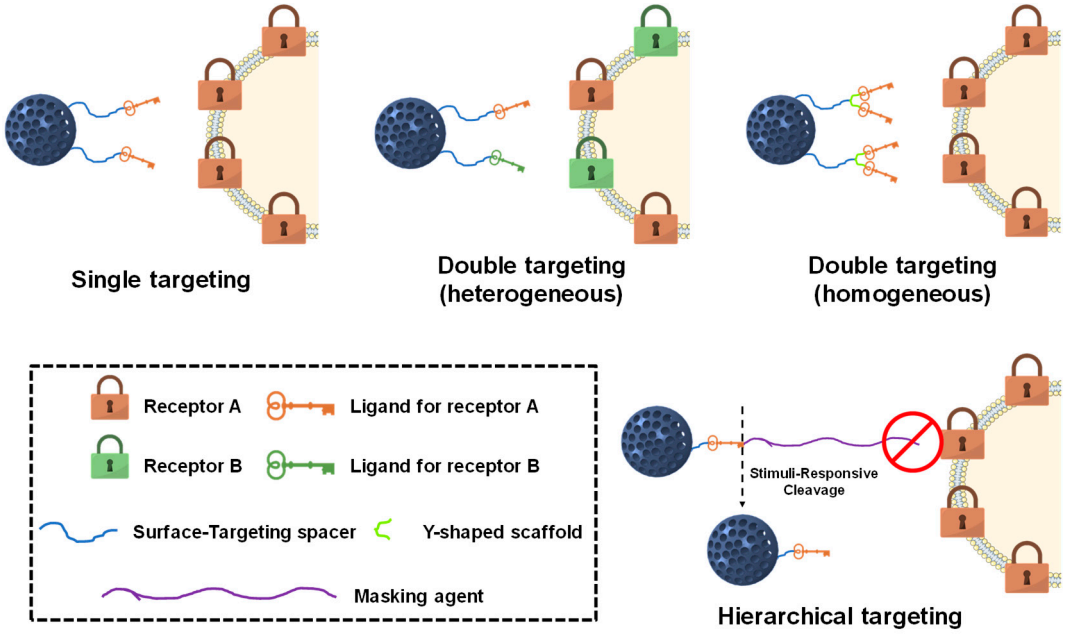

Figure 5. Schematic representation of the most common targeting approaches using MSNs.

3.1. Single Targeting

The simplest approximation involves the direct attachment of those targeting ligands to the surface of MSNs. In this manner, the targeting ligands are permanently exposed and can interact with the surrounding environment.

3.1.1. Antibodies

Antibodies bind specific antigens located on the membrane of cancer cells with extremely high specificity. For instance, trastuzumab, an FDA-approved monoclonal antibody that targets the HER2 receptor, has been extensively conjugated with MSNs, endowing them with remarkable targeting ability toward SK-BR3 [96–98] and BT-474 [98–100] breast cancer cells. Similarly, the FDA has also approved a monoclonal antibody for targeting the CD44 receptor, whose grafting to MSNs results in enhanced cellular uptake in MCF-7 breast cancer cells [101].

TRC105, a monoclonal antibody in clinical trials that binds the CD105 membrane protein, has also proved to be useful for improving the internalization of MSNs 4T1 breast cancer cells [102–104]. A monoclonal antibody for targeting the EpCAM transmembrane protein has also been FDA-approved, and it has been grafted to MSNs to enhance their efficacy against Y79 retinoblastoma cells [105]. Another monoclonal antibody that is currently in clinical trials is TAB-004. This compound targets the MUC1 transmembrane glycoprotein, which is overexpressed in most of cancer cells, and its conjugation with MSNs has yielded excellent results targeting murine breast cancer cells expressing the human form of MUC1 [106].

Finally, cetuximab, which is a monoclonal antibody also approved by the FDA, has been grafted to MSNs to selectively target overexpressed EGFR receptors in MCF-7 breast cancer [107], PC9 non-small lung cancer [108] and in a number of pancreatic cancer cell lines [109]. Even though they are highly effective in binding such receptors, their high production cost and potential undesired immune response have fueled the research of alternative targeting agents.

3.1.2. Aptamers

Aptamers are single-stranded DNA, RNA or unnatural oligonucleotides able to adopt tertiary conformations that exhibit affinity for various types of targets. These structures show specificity comparable to that of antibodies, besides being non-immunogenic and easy to synthesize [110]. For instance, the EpCAM protein can also be targeted using conveniently engineered aptamers. In this regard, modifying the surface of MSNs with such aptamer increases their selectivity toward Huh-7 liver cancer cells [111], HepG2 hepatic cancer cells [112] and different colon cancer cells [113,114]. Similarly, the MUC1 protein can also be targeted using aptamers, increasing the ability of MSNs to inhibit the proliferation of MDA-MB-231 [115] and MCF-7 breast cancer cells [116]. The AS1411 aptamer was the first aptamer to enter clinical trials, and it has been proved to be effective in targeting the nucleolin receptor of HeLa [117], SKOV-3 ovarian cancer cells [118] and MCF-7 breast cancer cells [119–121] with MSNs. Additional examples of aptamer-targeted MSNs are those using the YQ26 or HB5 aptamers, which show high selectivity for END-positive [122] and HER2-positive [123] cancer cells, respectively.

3.1.3. Peptides

The use of cell-penetrating peptides has attracted much attention owing to their ability to cross biological membranes [124]. The exact mechanism remains not fully understood but there are some proposed mechanisms [125]. For instance, the functionalization of MSNs with the TAT peptide provides great cellular uptake and further targets the nanoparticles to the cell nucleus [126]. Another example is the functionalization of MSNs with the KALA peptide, which is able to mediate the internalization and subsequent endosomal escape of nanoparticles [127].

The examples described so far rely on nonspecific internalization mechanisms, meaning that those particles could be internalized by both tumoral and healthy cells. For that reason, researchers have focused on identifying specific peptidic sequences that provide specific binding of overexpressed cellular receptors. For instance, functionalizing the surface with the RGD peptide is useful for promoting the internalization of MSNs in cells overexpressing αβ-integrin, such as many cancer cells [128–132] or the tumor endothelium [133]. The CD13 receptor, which is upregulated in glioma cells, can be efficiently targeted using NGR-functionalized MSNs [134,135]. Moreover, MSNs bearing this peptide are more prone target brain endothelial cells and cross the blood-brain-barrier [136]. In addition to those wide spectrum peptides, MSNs can be functionalized with peptides that show affinity for receptors present only on very specific cell lines. Examples of these peptides include NAPamide (targets the melanocortin-1 receptor of melanoma cells) [137], Bld-1 (targets formyl peptide receptor-1 of bladder cancer cells) [138] or IL-13 (targets the IL-13R-α2 receptor of glioma cells) [139].

3.1.4. Proteins

Proteins also have a relevant role in targeting cancer cells. For instance, transferrin is a protein that mediates iron cellular uptake and its receptor is highly overexpressed in many cancer cells. In this sense, transferrin-targeted MSNs show enhanced cellular uptake in HT1080 fibrosarcoma [140], HepG2 hepatocellular carcinoma [141], Huh-7 liver cancer cells [142], MDA-MB-231 breast cancer cells [143], C6 glioma cells [144] and MIA PaCa-2 pancreatic cancer cells [145]. A unique feature of pancreatic cancer cells is the presence of upregulated urokinase plasminogen activator receptors, which can be efficiently targeted by modifying the surface of MSNs with the serine protease urokinase plasminogen activator [146]. Lectins show affinity for aberrantly overexpressed carbohydrates on the membrane of cancer cells. In this regard, concanavalin A-coated MSNs present superior internalization in cells overexpressing sialic acid residues [147], whereas *Aleuria aurantia* promotes the internalization of MSNs in colon adenocarcinoma cells upregulating the sialyl-Lewis X antigen [148].

3.1.5. Carbohydrates

These biomolecules have also been explored as targeting agents owing to their ability to interact in a very specific manner with overexpressed lectin proteins present on the cell membrane. For instance, the asialoglycoprotein receptor can be targeted using MSNs functionalized with galactose [149] or lactobionic acid [150–153]. In addition, the conjugation of glucose derivatives with MSNs are useful for targeting overexpressed GLUT receptors [154,155]. The CD44 receptor can also be targeted using carbohydrates, and it has been shown that modifying the surface of MSNs with HA [156–159] or chondroitin sulfate [160–162] promotes the cellular uptake in CD44-positive cancer cells.

3.1.6. Small Molecules

There are also some small molecules that are commercially available or easy to synthesize that can be employed to target overexpressed cellular receptors. For instance, cancer cells need huge amounts of vitamins as a consequence of their accelerated metabolism and many of their receptors are highly overexpressed [163]. Examples are the use of folic acid (vitamin B9) [164–172] and biotin (vitamin B7) [173–175], whose conjugation with nanoparticles enhances their cellular uptake in a number of cancer cell lines. Additionally, it seems that cobalamin (vitamin B12) could have a role in enhancing cellular uptake [176].

Commercially available boronic acids bind sialic acid residues [177]. For that reason, they can be employed to target MSNs to HepG2 cells showing aberrant overexpression of such residues [178]. Besides, boronic acid-functionalized MSNs are useful for detecting the presence of glycosylated proteins, which have a role in the initiation and progression of tumors [179]. In addition, highly specific cancer cell targeting can be accomplished by synthesizing small molecules with great affinity for a very specific receptor. For instance, the norepinephrine transporter is highly overexpressed in neuroblastoma cells and can be efficiently targeted using MSNs containing benzylguanidine analogues [180]. A summary of all the above-mentioned approximations is shown in Table 1.

Table 1. Summary of all the targeting agents implemented into MSNs.

Targeting Agent	Membrane Receptor	Cell Line	Reference
Antibodies			
Trastuzumab	HER2	SK-BR3, BT-474	[96–100]
Anti-CD44	CD44	MCF-7	[101]
TRC105	CD105	4T1	[102–104]
Anti-EpCAM	EpCAM	Y79	[105]
TAB-004	MUC1	MMT	[106]
Cetuximab	EGFR	MCF-7, PC9, AsPC-1, PANC-1, MIA PaCa-2	[107–109]
Aptamers			
EpCAM	EpCAM	Huh-7, HepG2, SW620, SW480	[111–114]
MUC1	MUC1	MDA-MB-231, MCF-7	[115,116]
AS1411	NCL	HeLa, SKOV-3, MCF-7	[117–121]
YQ26	END	HEK293	[122]
HB5	HER2	SK-BR-3	[123]
Peptides			
TAT	Importin α/β	HeLa	[126]
KALA	-	A549, HeLa	[127]
RGD	$\alpha_v\beta_3$-integrin	MDA-MB-231, HeLa, UMR-106, PC-3, 4T1, HUVEC	[128–133,181]
NGR	CD13	C6, NCI-H1299, BCEC	[134,135]
NAPamide	Melanocortin-1	#17 (melanoma cancer cells)	[137]
Bld-1	FPR-1	HT-1376	[138]
IL-13	IL-13R-α2	U87	[139]

Table 1. *Cont.*

Targeting Agent	Membrane Receptor	Cell Line	Reference
Proteins			
Transferrin	TfR	HT1080, HepG2, Huh-7, MDA-MB-231, C6, MIA PaCa-2	[140–145]
Urokinase plasminogen activator	UPAR	S2-VP10	[146]
Concanavalin A	Sialic acids	HOS	[147]
Aleuria Auranti	Sialyl-Lewis X antigen	DLD-1	[148]
Carbohydrates			
Galactose	ASGPR	HepG2, SMMC-7721	[149]
Lactobionic acid			[150–153]
Glucose derivatives	GLUT	Y79, HeLa, A549	[154,155]
Hyaluronic acid	CD44	MDA-MB-231, HCT-116, HeLa, MCF-7	[156–159]
Chondroitin sulfate			[160–162]
Small Molecules			
Folic acid	FR-α	PANC-1, LS174T, LnCAP, KB, HeLa, Y79, A549, NCI-H1299	[164–172]
Biotin	BR	A549, HeLa, NB-4	[173–175]
Boronic acid	Sialic acids	HepG2	[178]
Benzylguanidine derivatives	NET	NB-1691	[180]

Membrane receptors. **HER2** (Human epidermal growth factor receptor 2); **CD44** (Cluster of differentiation 44, glycoprotein); **CD105/END** (Endoglin protein); **EpCAM** (Epithelial cell adhesion molecule); **MUC1** (Mucin 1 protein); **EGFR** (Epidermal growth factor receptor 1); **NCL** (Nucleolin protein); **CD13** (Aminopeptidase N enzyme); **FPR-1** (Formyl peptide receptor 1); **IL-13R-α2** (Interleukin-13 receptor α2); **TfR** (Transferrin receptor); **UPAR** (Urokinase plasminogen activator receptor); **ASGPR** (asialoglycoprotein receptor); **GLUT** (Glucose transporter); **FR-α** (Folic acid receptor); **BR** (Biotin receptor); **NET** (Norepinephrine transporter). **Cell lines**. **Breast**. SK-BR3 (adenocarcinoma); BT-474 (ductal carcinoma); MCF-7 (invasive ductal carcinoma); MDA-MB-231 (adenocarcinoma); 4T1 (mouse breast cancer that simulates stage IV human breast cancer); MMT (mouse breast cancer). **Lung**. PC9 (adenocarcinoma); A549 (adenocarcinoma); NCI-H1299 (large cell carcinoma). **Pancreas**. AsPC-1 (ductal adenocarcinoma); PANC-1 (ductal carcinoma); MIA PaCa-2 (ductal carcinoma); S2VP10 (ductal adenocarcinoma). **Colon**. SW620 (adenocarcinoma); SW480 (adenocarcinoma); DLD-1 (adenocarcinoma); HCT-116 (carcinoma); LS174T (adenocarcinoma). **Liver**. Huh-7 (hepatocellular carcinoma); HepG2 (hepatoblastoma). **Ovary**. SKOV-3 (ovarian serous cystadenocarcinoma). **Prostate**. PC-3 (carcinoma); LnCAP (carcinoma). **Endocervix**. HeLa (papillomavirus-related endocervical adenocarcinoma); SMMC-7721 (papillomavirus-related endocervical adenocarcinoma); KB (papillomavirus-related endocervical adenocarcinoma). **Bone**. HT-1080 (fibrosarcoma); HOS (osteosarcoma); NB-4 (acute promyelocytic leukemia); UMR-106 (rat osteosarcoma). **Brain**. NB-1691 (neuroblastoma); BCEC (brain capillary endothelial cells); C6 (rat malignant glioma). **Eyes**. Y79 (retinoblastoma). **Kidney**. HEK293 (embryonic human kidney cells). **Bladder**. HT-1376 (carcinoma). **Endothelium**. HUVEC (human umbilical vein endothelial cells).

3.2. Dual Targeting

The previously mentioned active targeting agents can be combined in a single carrier so that the final nanoparticle presents exceptional targeting capacities for various cellular receptors. Nanoparticles synthesized following this philosophy are referred to as dual-targeted nanocarriers. In this manner, MSNs can be engineered so they show selectivity not only for tumoral cells but also for the tumor vasculature or certain subcellular compartments.

3.2.1. Membrane Dual Targeting

The first strategy consists in using only membrane targeting agents. For instance, the combined use of HA and the RGD peptide has been shown to promote the cellular uptake of MSNs in ovarian cancer thanks to the simultaneous targeting of CD44 and αβ-integrin [181,182]. Similarly, targeting HeLa cells using both biotin and folic acid results in slightly better internalization rates than each one alone [183]. Besides, grafting the monoclonal antibody bevacizumab to MSNs bearing the EpCAM aptamer provides superior cellular uptake compared to the group containing only the aptamer [184]. However, our group recently demonstrated that using heterogeneous double targeting moieties not always provides the best results. In this case, a benzylguanidine analog with high affinity for

the norepinephrine receptor of neuroblastoma was implemented in a Y-shaped, flexible scaffold, demonstrating extraordinary targeting capacity compared to any other combination [185].

3.2.2. Sequential Dual Targeting

Another approach involves the use of targeting agents showing not only selectivity for cancer cells but also for other parts of the tumor. For instance, the co-conjugation of both RGD and TAT peptides on MSNs leads to sequential vascular-membrane-organelle targeting. In this manner, nanoparticles first bind the tumor vasculature to then be internalized by the tumoral cells owing to the cooperative behavior of both targeting agents. Once inside the tumoral cell, TAT drives the MSNs into the nucleus to achieve great cytotoxicity [186]. Another strategy to accumulate the particles in the nucleus consists in modifying the surface of MSNs with folic acid and dexamethasone. In this manner, folic acid first triggers the cellular uptake of the particles, which then undergo nuclear translocation thanks to the dexamethasone molecules [187]. Mitochondria can also be targeted using small molecules. For instance, MSNs can be engineered to first target the CD44 receptor using HA, which would then degrade in the lysosomes, exposing a triphenylphosphonium (TPP) derivative with strong mitochondrial affinity [188].

3.2.3. Janus Dual Targeting

In addition to the previous approaches, in which the targeting agents were randomly distributed along the surface, the use of Janus nanoparticles (nanoparticles that present two hemispheres, each one with different reactivity) provides further possibilities. For instance, it is possible to decorate one hemisphere with HA to target CD44 and the other one with masked positive charges that are only exposed at the acid pH of the tumoral matrix, improving the internalization in A549 lung cancer cells [189]. Besides, our group recently reported Janus MSNs with one hemisphere bearing folic acid and the other one presenting a TPP derivative, demonstrating superior cell internalization and subsequent mitochondrial targeting [190].

3.3. Hierarchical Targeting

As stated in Section 2.1, nanoparticles are usually modified with PEG to endow them with stealth properties. However, the targeting moieties are usually attached to the end of the PEG chain in many of the available systems. This strategy entails two main issues. First, despite the fact that normal cells do not show overexpressed levels of the previously mentioned receptors, they still present some of them. In consequence, nanoparticles bearing the targeting moieties anchored to the PEG chains might lead to non-specific targeting of healthy tissues. Second, because those targeting agents are directly exposed to the surrounding biological milieu, they might decrease the stealth character of the particles, consequently triggering their clearance.

Considering the facts exposed above, some researchers have explored the use of hierarchically-targeted nanocarriers, where the targeting agents are masked by PEG chains. In this manner, the stealth character of the nanoparticles is preserved on their way to the tumor. In addition, PEG chains difficult the cellular internalization of nanoparticles, so off-target is minimized [191]. Finally, PEG chains are detached upon arrival to the tumoral mass, thereby exposing the targeting agents and triggering the drug release.

3.3.1. pH-Responsive Hierarchical Targeting

The most extended approximation is based on using benzoic imine bonds, which are known to be hydrolyzed at the slightly acidic pH of the tumoral matrix (pH 6.4–6.8) [192]. A common approach consists in forming acid-labile benzoic imine bonds between MSNs presenting free NH_2 groups and an aldehyde PEG. In this way, the positively charged groups are exposed only in the tumor, triggering the cellular uptake through electrostatic interactions [193–195]. This method can also be employed to mask the RGD peptide, combining stealth properties and subsequent pH-mediated active targeting [196].

Similarly, positive charges can be generated using a thermally-cleavable bond between PEG and the amino groups on the surface [197].

3.3.2. Enzyme-Responsive Hierarchical Targeting

As stated in Section 2.3, levels of MMPs are upregulated in the tumoral matrix and can be employed for cleaving specific peptidic sequences. For instance, MSNs can be decorated with HA and further functionalized a MMP-sensitive PEGylated gelatin. In this way, the particles would accumulate in the tumor and then MMPs would cleave the PEGylated gelatin, exposing the targeting to CD44 to trigger the cellular uptake [198]. A similar strategy can be employed to engineer hierarchical folic acid-targeted MSNs [199]. The RGD peptide can also be masked using a MMP-sensitive peptidic sequence, which would be cleaved along with the stealthy coating only in the tumor tissue, thereby triggering the specific binding of αβ-integrin [200,201].

The different strategies for achieving dual and hierarchical targeting described in Sections 3.2 and 3.3 are summarized in Table 2.

Table 2. Summary of the different strategies implemented into MSNs for achieving dual or hierarchical targeting.

Targeting Agents	Approach	Cell line	Reference
Dual Targeting			
Hyaluronic acid + RGD Biotin + Folic acid Bevacizumab + EpCAM aptamer	Two different membrane targeting agents	SKOV-3 HeLa SW480	[181,182] [183] [184]
Benzylguanidine derivatives	Y-shaped scaffold using the same membrane targeting agent	NB-1691	[185]
RGD + TAT	Sequential vascular-membrane-organelle targeting	HeLa	[186]
Folic acid + Dexamethasone Hyaluronic acid + Triphenylphosphonium	Sequential membrane-organelle targeting	HeLa MGC-803	[187] [188]
Hyaluronic acid + Positive charge	Janus dual membrane targeting	A549	[189]
Folic acid + TPP	Janus membrane-organelle targeting	LnCAP	[190]
Hierarchical Targeting			
Positive charge RGD	pH-responsive benzoic imine bond	HepG2, HeLa U87	[193–195] [196]
Positive charge	Thermally-cleavable bond	HOS	[197]
Hyaluronic acid Folic acid	MMP-2-degradable gelatin	MDA-MB-231 HT-29	[198] [199]
RGD	RGD masked with MMP-2-clevable peptide sequence	4T1, HT-29	[200,201]

Cell lines. **Breast**. MDA-MB-231 (adenocarcinoma); 4T1 (mouse breast cancer that simulates stage IV human breast cancer); MMT (mouse breast cancer). **Lung**. A549 (adenocarcinoma). **Colon**. SW480 (adenocarcinoma); HT-29 (adenocarcinoma). **Liver**. HepG2 (hepatoblastoma). **Ovary**. SKOV-3 (ovarian serous cystadenocarcinoma). **Prostate**. LnCAP (carcinoma). **Endocervix**. HeLa (papillomavirus-related endocervical adenocarcinoma); **Bone**. HOS (osteosarcoma). **Brain**. NB-1691 (neuroblastoma); U87 (glioblastoma). **Stomach**. MGC-803 (adenocarcinoma).

4. Achieving Endosomal Escape

In addition to being preferentially internalized, nanoparticles should be able to release their payload properly in the cytoplasm. However, nanoparticles that are taken up through the endocytic pathway may be sequestered in the acid endo-lysosomes, which might degrade nanoparticles payload. Besides, membrane impermeable and/or poorly membrane permeable therapeutics need to be properly

released into the cytoplasm to exert their action. In this sense, the development of nanoparticles with ability to achieve endosomal escape has received much attention (Figure 6) [202].

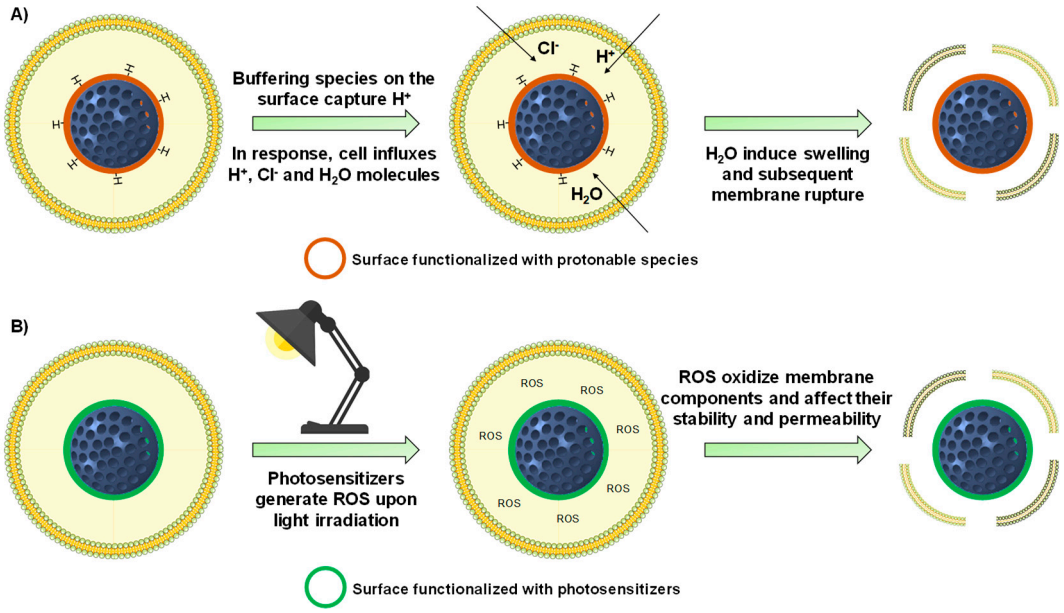

Figure 6. Schematic representation of the most employed strategies employed to induce the endosomal escape of MSNs. (**A**) The protonable species on the surface of the particles capture the protons of the vesicle. To counteract that basification, cell influxes protons, chloride ions and water, which induces the swelling and eventual endo-lysosomal rupture. (**B**) MSNs functionalized with photosensitizers are able to generate reactive oxygen species (ROS) upon light irradiation. These ROS can oxidize the lipid membrane of the endo-lysosomes, leading to a loss of stability and enhancement of the permeability of the lipid bilayer, triggering nanoparticle escape.

4.1. Internally-Triggered Endosomal Escape

4.1.1. Proton Sponge Effect

The first approach consists in taking advantage of the acidic environment found in the endocytic pathway (pH 4.5–6.5) [203]. MSNs can be functionalized using macromolecules that show buffering capacity at that acidic pH, which would lead to the disruption of the endosomes/lysosomes via the "proton sponge effect". This membrane rupture would be consequence of the cell influxing protons along with chloride ions and water to counteract the capture of protons by the particles. In this manner, the water molecules would make the endo-lysosomes to swell, eventually leading the release of the particles into the cytoplasm [202].

For instance, coating the surface of MSNs with poly(amidoamine) dendrimers results in the endosomal escape of the particles, owing to their great buffering capacity [204]. A similar example consists in the use of polyethyleneimine (PEI), a macromolecule with a huge number of protonable amino groups that can mediate the endosomal escape of MSNs [205,206]. However, it should be mentioned that it remains unclear whether PEI-mediated escape is actually consequence of its buffering capacity [207]. Because PEI-coated MSNs are positively charged, PEI can be employed to first load negatively charged nucleic acids within the polymeric mess and then induce the endosomal escape for effective therapeutic action. Examples of nucleic acids transfected using this approach include small interfering RNA (siRNA) [208–210] and short hairpin RNA (shRNA) [211]. In addition, it is known that PEI can be cytotoxic, depending on their molecular weight and conformation (linear, branched) [212]. For that purpose, PEI-coated MSNs can be further coated with poly(methyl vinyl ether-co-maleic acid) to yield more biocompatible nanoparticles with endosomal escape capabilities [213].

Amino acids and peptides also find application in the field of endosomal escape. For instance histidine, whose imidazole ring has a pKa of ca. 6 [214], shows buffering capacity at the pH of the endocytic pathway. For instance, it can be polymerized to engineer a pH-responsive gatekeeper for MSNs with potential endosomal escape capabilities [215]. Similarly, the surface of the particles can be modified with only the imidazole motif, which allows the effective delivery of plasmids into the cytoplasm [216]. Additionally, histidine can be incorporated within other sequences of amino acids. For instance, histidine-rich fusogenic peptides promote the destabilization of the vesicle membrane by both the proton sponge effect and fusion events with the peptide [217,218]. In addition, histidine motifs can be engineered with RGD targeting peptides to achieve both membrane targeting and endosomal escape of MSNs [219].

4.1.2. Other Mechanisms for Destabilizing the Endo-Lysosomal Membrane

As stated in Section 4, cell-penetrating peptides are able to cross biological membranes. For that reason, the KALA peptide can also be employed as a means of crossing the endo-lysosomal membrane [127]. Besides, it is possible to mask their positive charge so the surface of MSNs is negatively charged in the bloodstream and clearance is minimized. However, at the acid pH of the endo-lysosomes the positive charges are recovered, triggering the endosomal escape. Examples include the use of masked polylysine [220] and TAT peptide [221]. Another approach involves the use of MSNs functionalized with lysine-containing α-helical peptides, which are able to act at the same time as gatekeepers and endosomolytic agents [222]. Finally, the escape of MSNs can also be accomplished by functionalizing the surface with TPP derivatives, which are highly cationic and lipophilic small molecules able to destabilize the endo-lysosomal membrane. [190,223,224].

4.2. Externally-Triggered Endosomal Escape

A second strategy for inducing endosomal escape consists in grafting macrocycles (porphyrins and phthalocyanines) to the surface of the particles to then irradiate the MSNs with a given wavelength. When these materials are exposed to light, those macromolecules generate reactive oxygen species (ROS), which are known to destabilize the membrane of the endo-lysosomes [225]. Examples of photosensitizers are porphyrins and phthalocyanines. The porphyrin PpIX generates ROS upon 405 nm ultraviolet light irradiation, and it has been proved to mediate the endosomal escape of MSNs coated with biocompatible supported lipid bilayers [226,227]. Porphyrins can also generate ROS upon visible light application [228]. Similarly, the phthalocyanine $AsPCs_{2a}$ generate ROS upon irradiation with 639 nm near-infrared light, and its grafting to MSNs has been shown to be effective in triggering their endosomal escape [229,230]. Finally, indocyanine green can be loaded within the mesopores of MSNs and generate ROS upon 780 nm light excitation, leading to the endosomal escape of the particles [231].

5. Functional Groups Determine Drug Loading and Release

The outstanding textural properties of MSNs allow the loading of large amounts of therapeutics, process easily accomplished thanks to their open porous structure. However, for the very same reason, the loaded molecules might prematurely diffuse out of the pores and affect healthy tissues. Both the loading and release kinetics are governed by the interactions between such molecules and the silanol groups of the particles. Hence, tuning the functional groups present in the particles provides a first manner to improve drug loading and control premature release. In consequence, mesoporous silica matrices should be conveniently modified according to the drug to be stored.

Overall, the loading process of polar drugs can be improved using polar functional groups. Conversely, the loading of hydrophobic compounds increases in the presence of nonpolar moieties [232]. For instance, NH_2-functionalized mesoporous silica materials provide considerably higher loading and more sustained release of alendronate [233,234]. Similar behavior is found for erythromycin when the particles are functionalized with long alkyl chains [235] and ipriflavone in the presence of phenyl groups [236], thanks to the appearance of hydrophobic interactions.

With regard to antitumoral drugs, introduction of SH groups increases the storage of cisplatin [237] and mitoxantrone [238]. Doxorubicin loading in MSNs is enhanced after functionalization with COOH or PO_3^- groups, although that of paclitaxel is not improved after modifying the particles with phenyl groups [239]. Moreover, functionalization with NH_2 or CN groups provides the greatest loading of 5-fluorouracil in MSNs [240]. In addition, the amount of gemcitabine loaded increases if MSNs are modified with a carboxylic acid derivative of piperazine [241].

Periodic mesoporous organosilica nanoparticles (PMONs), which are composed of bridged organoalkoxysilanes, offer increased loading capacity of antitumoral drugs owing to their higher hydrophobicity and isoelectric point. For instance, PMONs containing porphyrin-ethylene bridged moieties provide extraordinary loading of gemcitabine [242]. Similarly, the use of precursors bearing ethylene-bis(propyl)disulfide [243] or oxamide-phenylene moieties [244] yields PMONs with remarkable DOX loading capacity.

6. Stimuli-Responsive Drug Delivery

Modifying the interactions between the silica matrix and the guest molecules provides a first manner to diminish premature release. A step head involves the use of stimuli-responsive gatekeepers, which are structures able to open the mesopores on-demand in response to the application of a particular stimulus (Figure 7).

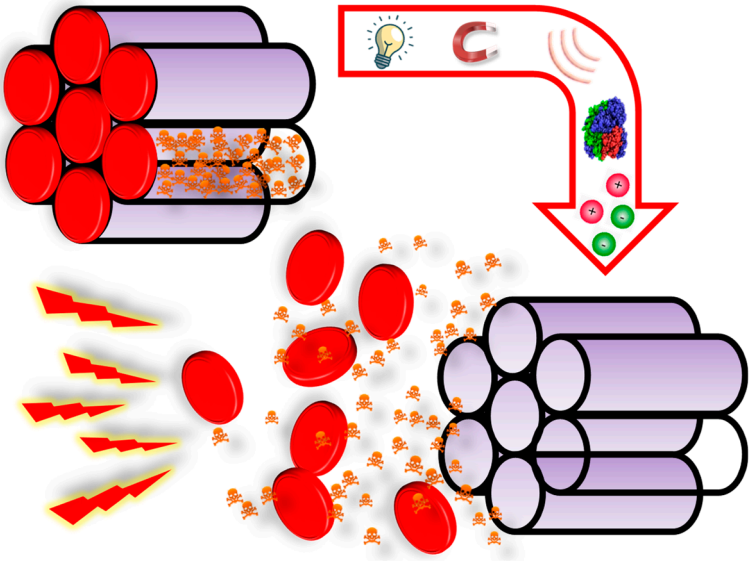

Figure 7. Schematic representation of how stimuli-responsive mesoporous materials work. The gatekeepers close the pore entrances and avoid premature release until some specific stimulus is applied. The stimuli can be applied from inside (e.g., pH, redox species, enzymes) or outside the patient (e.g., light, US, magnetic fields).

As shown in Figure 7, the origin of stimuli can internal or external. The use of internal stimuli relies on some relevant biological markers being upregulated/downregulated in tumor tissues (e.g., pH, redox species, enzymes). In this manner, the pore entrances of the particles would remain closed under physiological conditions, whereas the tumor microenvironment (inside or outside cancer cells) would trigger the drug release. On the other hand, external stimuli-responsive MSNs only allow drug release when the stimulus is applied from the outside using specific equipment (e.g., light, US, magnetic fields).

6.1. pH-Responsive MSNs

A unique feature of tumor tissues is the slightly acidic pH of the tumoral matrix, which has been quantified to be within the range 6.4–6.8 [192]. This subtle acidification is consequence of a process

known as Warburg effect, which states that most cancer cells (or any proliferating cell) produce energy through the aerobic glycolysis process regardless of the presence of oxygen, leading to the secretion of large amounts of acidic lactate [245]. Such acidification plays a major role in cancer progression because (a) it promotes cancer cell migration ad radioresistance, (b) it disturbs the metabolism and function of T-cells and (c) it provokes chronic inflammation in tumor tissues by enhancing interleukin production by macrophages and T-cells [246].

In addition, there are some intracellular compartments and organelles that present slight differences in pH with respect to that of the cytoplasm, which is nearly neutral. In this sense, nanoparticles can be internalized in cells through the endocytic pathway, which results in the formation of vesicles containing the particles. These vesicles, whose function is degrading compounds no longer useful for the cells, are acidic in nature and evolve from the endocytic vesicles (pH 6.5) to the lysosomes (pH 4.5–5) [247].

Such differences in pH can be employed to trigger the drug release from pH-responsive mesoporous nanoparticles. The most common strategies to design such systems involve the use of: (1) acid-labile bonds, (2) pH-degradable gatekeepers, (3) pH-operated nanovalves, (4) polymers that undergo conformational changes upon variations in pH, (5) biomolecules that vary their charge or conformation upon changes in pH and (6) polyelectrolytes.

6.1.1. Acid-Labile Bonds

The simplest approximation consists in grafting different types of gatekeepers through acid-labile bonds. These linkers are stable at physiological pH but rapidly hydrolyze when pH drops. For instance, hydrazone bonds are cleaved at pH 5 and can be employed to close the mesopores with gold nanoparticles [248,249], HA [250] or charge-reversal polymers [251]. Acetal bonds hydrolyze at pH 5 as well and find application as acid-responsive linkers between MSNs and small metal nanoparticles [252,253], graphene quantum dots (QDs) [254], polymeric coatings [255,256] and proteins [147]. Boronate esters are also interesting because they are known to undergo reversible hydrolysis at acid pH [257] and can be employed to design MSNs with on-off release behavior using small gold [258] and Fe_3O_4 nanoparticles [259], ZnS nanocrystals [260] or lactobionic acid [261] as gatekeepers. Imine bond-based compounds find application as crosslinking agents and allow the formation of acid pH-responsive protective layers that disassemble when pH drops. Examples are the combination chitosan with dialdehyde starch [262], dextrin with tetraethylenepentamine [263] or glutaraldehyde with polyethyleneimine [264].

6.1.2. pH-Degradable Gatekeepers

Another approach is based on the use of acid-degradable gatekeepers that close the mesopores at physiological pH and degrade in the acidic subcellular compartments, triggering the drug release. For instance, small degradable nanoparticles can be employed as pore blockers. Examples include ZnO QD, whose degradation generates cytotoxic Zn^{2+} ions [265–268] and MnO nanoparticles that generate manganese ions upon dissolution that can be used for imaging [269,270]. In addition, MSNs can be coated with a layer of MgAl-hydrotalcite, which is known to degrade at acid pH [271].

There are various examples of organic gatekeepers that decompose upon pH variations as well. For instance, MSNs can be functionalized with a polydopamine layer that remains stable at physiological pH but degrade when pH drops [272]. Another approximation consists in functionalizing the particles with self-immolative moieties, which are molecules or macromolecules that present a cleavable trigger that initiate the self-degradation of the structure upon application of a very specific stimulus [273]. Such self-immolative structures endow MSNs with responsiveness to either basic [274] or acid pH [275]. In fact, the latter have been recently implemented into pH-responsive mesoporous carbon nanoparticles, validating in vivo the pH-responsiveness of such self-immolative polyurethanes [276].

6.1.3. pH-Operated Nanovalves

There are some examples of MSNs gated using the so-called nanovalves, which are supramolecular gatekeepers able to close the pores upon interaction with a stalk grafted on the surface. A first strategy involves the use of triazine derivatives as stalks and 5-fluorouracil-based compounds as caps, which are able to close the pore entrances thanks to hydrogen bonding interactions. However, at acid pH the interaction weakens and cytotoxic 5-fluorouracil is released along with a loaded cytotoxic, leading to high cytotoxicity [277]. Another strategy involves the use of biocompatible cyclodextrins (CD). They present a hydrophilic outer surface and a hydrophobic cavity with which the stalk interacts. The interaction is stable at physiological pH and the CD tightly close the pore entrances. However, it weakens at acid pH, triggering the drug release. Examples of stalks employed to accomplish pH-mediated drug delivery are amine-based stalks [278–280] and complementary base pairs [281].

6.1.4. Conformation-Changing Polymers

This kind of polymers are collapsed on the surface at a given pH, blocking the pore entrances. However, upon a variation in pH the ionizable groups of the polymer acquire net charge and repulsion forces among the chains appear. Hence, the polymeric layer changes its hydrophobicity and adopt a more extended conformation that permits the drug release. Cationic polymers showing this behavior protonate at acid pH and can be employed to design gates that open only in the acidic endo-lysosomes. Examples include amino-based acrylates and methacrylates [282,283], polyamine-based polymers/dendrimers [284–286] and poly(*n*-vinylpyridine) [230,287,288]. On the other hand, anionic polymers, such as poly(acrylic acid) and poly(methacrylic acid), protonate at neutral pH, closing the pores at acid pH and being excellent candidates for oral drug delivery [289–291].

6.1.5. pH-Responsive Biomolecules

Likewise, some biomolecules undergo reversible changes upon variations in pH. For instance, MSNs can be functionalized with polypeptides containing protonable groups that would only allow drug release at a given pH. In this sense, poly(L-histidine) [215] protonates at acid pH, whereas poly(L-aspartic acid) [292] and succinylated poly(ε-lysine) [293] protonate at physiological pH and might be useful for oral drug delivery. Additionally, such pH variations can reversibly modify the 3D structure of peptides, proteins and DNA strands to allow the drug release only at acid [294–297] or physiological pH [298,299].

6.1.6. Polyelectrolytes

Another approach consists in the use of polyelectrolytes, which are polymers bearing ionizable cationic or anionic groups. Such polyelectrolytes can be directly deposited on the surface, forming a single polymeric layer that interacts with the nanoparticle surface. In this manner, variations in pH would lead to electrostatic repulsions that would weaken the interaction with the surface, opening the pores. The surface must be accordingly functionalized, i.e., positively charged for anionic and negatively charged for cationic polymers. Examples include coating the surface with PEI, poly(2-diethylamino ethyl methacrylate) [300], poly(vinyl pyridine) [301], polyanionic poly(acrylic acid-co-itaconic acid) [302] and chitosan, which is particularly interesting because it swells reversibly at acid pH, leading to on-off systems [303–306]. Furthermore, polyelectrolytes can be disposed forming multilayers that are destabilized upon variations in pH, initiating the drug release. Examples are the combination of poly(allylamine hydrochloride) with poly(styrene sulfonate) [307,308] and chitosan with sodium alginate [309,310]. Table 3 summarizes the different pH-responsive approximations described in Section 6.1.

Table 3. Different strategies implemented into MSNs for achieving pH-responsive drug delivery.

Approach	Description	Reference
Acid-Labile Bonds		
Hydrazone bond Acetal bond Boronate ester bond	pH-responsive bonds that find application as linkers between MSNs and different gatekeepers	[248,249,251] [147,252–256] [258–261]
Imine bond	pH-responsive bond useful as cross-linking agent	[262–264]
pH-Degradable Gatekeepers		
Inorganic nanoparticles	Small nanoparticles that degrade at acid pH, generating different ions with therapeutic applications	[265–271]
Polymers	Polymeric coatings that decompose into their building blocks upon changes in pH	[272,274–276]
pH-Operated Nanovalves		
Stalk + Cap	Supramolecular structures that close and open the pores thanks to the interaction with stalks grafted on the surface	[277–281]
Conformation-Changing Polymers		
Cationic	Polymers that are collapsed on the surface of the particles when deprotonated (pores closed) and undergo a conformational change when pH varies (pores open)	[230,282–288]
Anionic		[289–291]
pH-Responsive Biomolecules		
Polypeptides	Large peptidic chains containing protonable groups that exhibit collapsed-to-extended behavior upon pH variations	[215,292,293]
Nucleic acids and proteins	Macromolecules that modify their 3D structure upon variations in pH	[294–299]
Polyelectrolytes		
Monolayers	Charged polymers that close the pores by forming a monolayer through electrostatic interactions	[300–306]
Multilayers	Arrangement of multiple charged layers on the surface of the particles to close the pore entrances	[307–310]

6.2. Redox-Responsive MSNs

Unlike healthy cells, where the production of reactive oxygen species (ROS) and antioxidants is balanced, ROS levels in cancer cells are upregulated due to the altered metabolism, some genetic mutations and mitochondrial dysfunction. To counteract this and prevent apoptosis, cancer cells present elevated levels of ROS scavengers, being the most representative the tripeptide glutathione (γ-glutamyl-cysteinyl-glycine, GSH) [311], although the redox-active nature of the endocytic pathway has also been reported [312]. GSH, which participates in the metabolism of many molecules in healthy cells [313], also plays an important role in cancer progression and may contribute to increase radio- and chemoresistance of cancer cells [314]. GSH is mainly located in the mitochondria and cytoplasm, and its upregulated levels (2–10 mM in the cytosol vs. 2–20 μM in the extracellular microenvironment) can be employed to trigger the drug release from redox-responsive mesoporous nanoparticles [315].

Such systems are commonly engineered using different gatekeepers grafted using GSH-cleavable disulfide bonds. In this manner, the pores remain closed outside the cells (bloodstream and tumoral matrix), whereas the overexpressed GSH triggers the release once in the cytoplasm. Examples of gatekeepers attached using disulfide bonds are: (1) proteins, (2) small nanoparticles and nanovalves and (3) polymers and small molecules. In addition to being useful as cleavable linkers for grafting gatekeepers, disulfide bonds can be introduced throughout the framework of PMONs,

yielding biodegradable silica nanoparticles in which drug release and degradation are triggered by the presence of overexpressed reductive species [243,316,317].

6.2.1. Proteins

Owing to their large size, proteins are effective in blocking the mesopores when grafted viaredox-responsive bonds. For instance, biocompatible bovine serum albumin (BSA) can be doped with Gd to act at the same time as gatekeeper and magnetic resonance imaging agent [318]. Similarly, transferrin can be employed as both gatekeeper and targeting agent [142]. Cytochrome c, which is an apoptotic protease, can be employed as gatekeeper as well, leading to enhanced doxorubicin delivery and protein-mediated therapeutic effect [319].

6.2.2. Small Nanoparticles and Nanovalves

The pore entrances of MSNs can additionally be sealed by grafting small nanoparticles (4–6 nm) to the surface via disulfide bond. Examples of this approach are the use of carbon dots [320,321], gold nanoparticles [322], silver nanoparticles [323] and cerium oxide nanoparticles [324] as gatekeepers.

The stalks that interact with supramolecular nanovalves can be grafted to the surface of the particles through disulfide bonds, yielding pH- and redox-responsive MSNs. In this manner, enhanced drug release can be observed when MSNs reach the cytoplasm and GSH completely removes the β-CD caps [325,326]. A nice feature of β-CDs is that not only they serve as gatekeeper, but also provide possibilities for further functionalization, including PEGylation [327] and grafting of targeting agents [149,201,328,329].

6.2.3. Polymers and Small Molecules

Disulfide bonds can also be employed to graft bulky polymers to the surface of MSNs. In this regard, cationic polymers such as chitosan [330] and PEI [209,331] have been grafted through redox-responsive bonds to engineer gatekeepers that also serve as gene transfection vectors. Additional examples of gatekeepers grafted through disulfide bonds are naturally occurring polymers, such as HA [158,332] and collagen [152], and synthetic polymers, such as poly(acrylic acid) [333] and poly(glycicyl methacrylate) [334].

Similarly, the pore entrances can be sealed using small disulfide-bridged molecules [335]. Besides, grafting peptides containing hydrophobic / bulky components and targeting units through disulfide bonds provides on-demand drug release and selective recognition of cancer cells [135,196,336,337]. An additional strategy involves grafting stearic acid molecules using GSH-sensitive bonds because such molecules can directly close the mesopores through hydrophobic interactions among them [338]. Moreover, stearic acid can be employed to attach an amphiphilic targeting peptide thanks to their hydrophobic nature, providing both gatekeeping and targeting features [339].

6.3. Enzyme-Responsive MSNs

A characteristic feature of tumor environments is the overexpression of certain enzymes with proteolytic behavior. For that reason, designing mesoporous nanomatrices functionalized with gatekeepers degradable by such enzymes has attracted much attention. These materials would avoid premature release in the bloodstream, whereas the payload would be release once in the tumor microenvironment upon enzymatic degradation of the pore blockers. The most targeted enzymes are: (1) cathepsin b (CatB) and (2) various metalloproteinases (MMPs). Besides, (3) the use of some other proteolytic enzymes has also been explored.

6.3.1. Cathepsin B

CatB is a lysosomal proteolytic enzyme which is overexpressed in many cancer cells [340]. In consequence, it can be employed to trigger the drug release from MSNs once they have been

internalized through the endocytic pathway. In this sense, MSNs can be capped using large peptides containing repeating units of a CatB-sensitive sequence (GIVRAK) [341]. Similarly, a short CatB-sensitive peptidic sequence (PGFK) can be employed to mask a cationic cell penetrating peptide with a negative complementary chain. In this manner, such interacting chains close the pore entrances until CatB cleaves the sensitive bond along with the negative chain, exposing the positively peptide and targeting the cell nucleus [342]. In addition, such CatB-responsive sequences can be employed for attaching bulky gatekeepers to the surface of MSNs. Examples of such linking sequences are GFLG for attaching α-CDs [343] and CRRGGKKGGKKRK for grafting gold nanoclusters [344]. Besides, MSNs can be coated with poly(glutamic acid), which is able to prevent drug release unless the polymeric coating is degraded by lysosomal CatB [345].

6.3.2. Metalloproteinases

Some MMPs are overexpressed in the tumoral matrix of certain tumors and can be employed to cleave specific peptidic sequences. For instance, the use of peptides containing the MMP-2-responsive PLGVR sequence as gatekeepers for MSNs results in significant drug release only the presence of that enzyme [346,347]. In addition, such responsive sequences can be employed to graft gold nanoparticles and inhibit premature drug release [348]. Similarly, a MMP-9-responsive sequence (RSWMGLP) can be employed to attach avidin to the surface of MSNs, allowing the drug release only in the tumoral matrix [349]. Besides, MSNs can be coated with a MMP-9-sensitive gelatin, so that drug release would only take place upon enzymatic degradation of the polymeric layer [350]. Finally, the pore entrance of MSNs can also be sealed by grafting BSA using a MMP-13-responsive sequence (PLGLAR), because this enzyme has been found to be overexpressed in the tumor microenvironment of liver cancer [351].

6.3.3. Other Enzymes

Aside from serving as targeting agents for the CD44 receptor, HA [156,158,352] and chondroitin sulfate [160,162] can be employed as gatekeepers for enzyme-responsive MSNs, as they are both degraded by hyaluronidase, an enzyme that can be found in the lysosomes. Trypsin is an enzyme that has been found to be overexpressed in liver cancer scenarios. In this respect, it has been shown that the presence of trypsin can degrade BSA in BSA-coated MSNs, triggering the co-delivery of doxorubicin and bilirubin [353].

Similarly, alkaline phosphatase is found in tumor scenarios and can be employed to degrade an ATP coating covering the pores of mesoporous silica-based materials [354]. Finally, cancer cells present elevated levels of esterases in the cytosol, which can hydrolyze ester-containing gatekeepers. Examples of such esterase-responsive systems are the functionalization of MSNs with a poly(β-amino-ester) polymeric layer [355] and ester-containing stalks for supramolecular nanovalves [356,357]. Table 4 summarizes the different strategies applied for the design of enzyme-responsive MSNs.

Table 4. Strategies implemented into MSNs for achieving enzyme-responsive drug delivery.

Enzyme	Description	Reference
Peptides as Gatekeepers		
CatB MMP-2	Large peptidic sequences that close the mesopores and allow drug release upon enzymatic degradation	[341,345] [346,347]
Peptide as Linkers		
CatB MMP-2 MMP-9 MMP-13	Short peptidic sequences employed to graft different types of bulky gatekeepers (small nanoparticles, proteins, nanovalves) to the surface of MSNs	[342–344] [348] [349] [351]

Table 4. *Cont.*

Enzyme	Description	Reference
Other Enzyme-Degradable Gatekeepers		
MMP-9	MSNs covered with a gelatin that degrade in the presence of MMP-9	[350]
Hyaluronidase	MSNs functionalized with large carbohydrates (hyaluronic acid, chondroitin sulfate) that act simultaneously targeting agents and gatekeepers	[156,158,160, 162,352]
Trypsin	MSNs gated with BSA, which can be degraded by overexpressed trypsin in liver cancer	[353]
Alkaline phosphatase	ATP-capped mesoporous silica-based materials that allow drug release upon enzymatic degradation of ATP	[354]
Esterases	MSNs functionalized with ester-containing gatekeepers that are degraded in the presence of such enzymes	[355–357]

6.4. Light-Responsive MSNs

The use of light to unlock the pore entrances on MSNs has attracted much interest because of the ease of it application, since only a specific light source is needed. Researchers have focused on the use of ultraviolet (UV) (100–400 nm), visible (400–650 nm) and near-infrared (NIR) (650–1050 nm) light. The energy and, consequently, the capacity to penetrate in tissues depends on the wavelength employed. UV light presents the highest energy yet the lowest penetration capacity, which can lead to radiation-induced cellular damage. Conversely, low energetic NIR-light exhibits the deepest penetration capacity in living tissues, in addition to being harmless to the cells [358]. Overall, the design of light-responsive MSNs relies on the use of: (1) breakable bonds upon light irradiation and (2) conformational changes in molecules.

6.4.1. Light-Induced Cleavable Bonds

This kind of bonds can be employed as linkers to graft different gatekeepers to the surface of MSNs. In this manner, the drug release would only take place when the target cells were irradiated by the clinician, assuring lack of non-specific release to healthy cells. For instance, the o-nitrobenzyl group is cleaved upon 365 nm UV-light irradiation and can be employed to close the pore entrances with a targeting protein [140]. In addition, the pH-responsive polymer poly(2-(diethylamino)-ethyl methacrylate) has also be grafted using this linker, endowing MSNs with both pH- and light-responsiveness [359]. Similarly, cationic poly((2-dimethylamino)ethyl methacrylate)) has been anchored to MSNs through a 405 nm-sensitive coumarin group to achieve on-demand gene delivery [360]. Besides, it has been shown that ruthenium bipyridine-based compounds can act as gatekeepers by forming a thiolated coordination bond that can be cleaved upon 455 nm light irradiation [361]. Similarly, the mesopores can be capped with thymine derivatives that undergo reversible formation and cleavage of a cyclobutane dimer when irradiated with 240 nm and 365 nm light to open and close the pores, respectively [362].

As stated in Section 4, photosensitizers are compounds that generate ROS when irradiated with a particular wavelength. In this sense, it is possible to engineer gatekeepers grafted through ROS-responsive bonds that would only allow the release upon application of a given wavelength. For instance, our group has reported the use of a visible light-responsive porphyrin acting as gatekeeper through an aminoacrylate ROS-responsive bond. In this manner, the light irradiation would generate ROS that would then detach the gatekeeper, allowing the drug release [228]. In addition to porphyrins, the photosensitizer chlorin e6 generates ROS upon NIR-light irradiation (660 or 980 nm), and can be loaded in MSNs to mediate the cleavage of ROS-responsive bonds. For instance, β-CD [363] and BSA [364] can be attached using (alkylthio)alkene-based bonds. In addition, it is also possible to use small ROS-responsive thioketal-containing molecules as gatekeepers for MSNs [365].

Finally, the photosensitizer $AsPCs_{2a}$ can be employed to generate ROS able to oxidize the double bonds of the lipid bilayer of lipid-coated MSNs, modifying the permeability and triggering the release [229].

6.4.2. Light-Induced Conformational Changes

Another strategy for the design of light-responsive nanocarriers consists in functionalizing the surface of MSNs with polymers that undergo conformational changes in response to light. This behavior can be accomplished by introducing photoresponsive moieties throughout the polymer chain. In this manner, the light-mediated cleavage of such groups would induce a change from the hydrophobic to hydrophilic state, opening the pores and triggering the drug release. Examples of these groups are perylene (cleaved using 450 nm visible light) [366] and spiropyran (cleaved upon 365 nm UV-light exposure) [367]. A similar approach involves lowering the lower critical solution temperature (LCST) of a thermo-responsive polymer by introducing the o-nitrobenzyl group. In this manner, the bond cleavage upon UV light would increase the LCST of the polymer that would undergo a collapsed to extended conformational change, triggering drug release [368].

Some molecules undergo reversible *trans*-to-*cis* conformational changes upon light irradiation, behavior that many researchers have taken advantage of to engineer light-responsive nanovalves. For instance, using a cinnamamide derivative as stalk for cucurbit[7]uril allows to open and close the mesopores when irradiated with 300 nm and 254 UV-light, respectively [369]. Azobenzene derivatives show similar behavior, and can be employed as stalks for α- [370] and β-CDs [371] that only allow the drug release upon 365 nm UV-light irradiation. Similarly, azobenzene groups can be introduced as pendant groups throughout a polymer chain. In this manner, such groups can interact with the hydrophobic cavities of β-CD-coated MSNs, closing the pores. However, they undergo *trans*-to-*cis* transition when irradiated with 365 nm [372] or 520 nm light [373], ceasing the interactions and allowing the drug release. A nice approach to trigger the drug release consists in grafting fan-like azobenzene derivatives within the mesopores. In this manner, the *trans*-to-*cis* transition acts as a nanoimpeller that forces the payload diffusion outside the pores [374,375]. Table 5 summarizes the different strategies applied for the design of light-responsive MSNs.

Table 5. Different strategies implemented into MSNs for achieving light-responsive drug delivery.

Approach	Description	Reference
Light-Responsive Bonds		
o-nitrobenzyl group	Cleavable using 365 nm light. Used as linker for the grafting of proteins and pH-responsive polymers	[140,359]
Coumarin group	Cleavable using 405 nm light. Used as linker for the grafting of cationic polymers for gene delivery	[360]
Thiolated coordination bond	Cleavable using 455 nm light. Coordination bond formed by ruthenium bipyridine-based compounds that act as gatekeepers	[361]
Thymine derivatives	Reversible formation (365 nm) and cleavage (240 nm) of a cyclobutane dimer. Used as on-off gatekeeper	[362]
ROS-Responsive Bonds (ROS Generation upon Light Application)		
Aminoacrylate bond	Used as linker for the grafting of a porphyrin acting simultaneously as gatekeeper and ROS generator upon visible light irradiation	[228]
(alkylthio)alkene-based bond	Used as linker for the grafting of nanovalves and proteins. Cleaved when loaded photosensitizer chlorin e6 generates ROS upon NIR light irradiation	[363,364]
Thioketal group	Used as gatekeeper. Cleaved when chlorin e6 generates ROS upon NIR light irradiation	[365]
Double bonds	Photosensitizer $AsPCs_{2a}$ generates ROS upon NIR light irradiation that oxidize double bonds of the lipids and increase membrane permeability	[229]

Table 5. *Cont.*

Approach	Description	Reference
Light-Induced Conformational Changes		
Perylene group Spiropyran group o-nitrobenzyl group	Their removal from a polymer chain upon light irradiation, 450 nm (perylene) or 365 nm (spiropyran and o-nitrobenzyl), induce a conformational change that open the pores and triggers drug release	[366] [367] [368]
Cinnamamide derivative Azobenzene derivatives	Used as stalks for grafting of nanovalves (grafted on the surface or as pendant groups in polymers). Reversible *trans*-to-*cis* conformation change when irradiated, in general, with UV light	[369] [370–375]

6.5. Ultrasound-Responsive MSNs

US have long been applied in the clinic for the diagnosis and treatment of different pathologies. The main advantages of US are that their application requires minimal equipment and their non-invasiveness nature that allow deep and harmless penetration in living tissues. For that reason, there has been growing interest in developing US-triggered MSNs that rely on: (1) enhanced drug release owing to effects produced by US and (2) use bonds that can be disrupted by the action of this stimulus.

6.5.1. US-Enhanced Drug Release

Overall, the application of US leads to two main effects, namely acoustic cavitation (as noted in Section 2) and thermal effects, and it has been shown that both effects can lead to significantly higher drug release. In this regard, US can be effectively used to further enhance the effectiveness of functionalized nanoparticles, such as poly(dimethylsiloxane)-coated MSNs [376], polydopamine-coated MSNs [377] and β-CD-coated MSNs [378], achieving more amount of drugs released when used in combination with US.

6.5.2. US-Cleavable Bonds

US can also be employed to weaken chemical interactions, leading to on-off systems upon alternating application of US. Examples of this approach include alginate-coated MSNs that can be cross-linked through the formation of coordination bonds between alginate and calcium ions ($COO^{-}Ca^{2+}$) [379] and crown ether-modified MSNs that allow the drug release when hydrogen bonding with the gatekeeper decreases upon US application [380].

Another approximation consists in employing US-cleavable bonds. In this sense, it has been reported that PEG can be mechanically detached from MSNs after applying the stimulus [381]. Our group has reported the use of large co-polymers to seal the pore entrances of the particles. Such polymeric layer contains an US-cleavable acetal, so that when the stimulus is applied the bond is cleaved, leading to a phase transition from hydrophobic to hydrophilic that triggers the drug release [382]. In addition, the versatility of the system can be increased by modifying the synthetic procedure, as that allows the introduction of tunable targeting moieties [129].

6.6. Thermo-Responsive MSNs

The variation in temperature required for triggering the drug release from thermo-responsive MSNs can be macroscopically applied or induced by a secondary source, such as an alternating magnetic field or NIR light. The synthesis of this class of materials relies on using (1) gatekeepers that disassemble when there is an increment of temperature and (2) polymers that undergo phase transitions upon temperature variations. This stimulus is particularly interesting in some cases because treating cancer cells with moderate heat (40–43 °C), also known as hyperthermia, results in enhanced cell death and chemosensitivity [383]

6.6.1. Thermo-Responsive Disassembling Gatekeepers

A first strategy to endow MSNs with thermosensitive behavior consists in functionalizing the pore entrances with DNA strands that undergo reversible dehybridization at a given temperature. It would be

desirable that the MSNs increased the temperature locally by themselves, so external macroscopic heating would be unnecessary and no surrounding tissues would be affected. In this regard, the DNA nanogates can be grafted to MSNs containing superparamagnetic Fe_3O_4 nanoparticles able to generate heat upon application of an alternating magnetic field [384]. Similarly, indocyanine green-loaded MSNs generate heat upon NIR light irradiation, which can be employed to dehybridize DNA strands [231] or complementary base pairs [385]. It has been shown that DNA strands are unable to close the pore entrances below a certain size [386]. Nonetheless, such short sequences can be employed as linkers to block the mesopores with proteins [387], small gold nanoparticles [388] and magnetic γ- Fe_2O_3 nanoparticles [389].

In addition to nucleic acids, there are also some examples of thermo-responsive peptidic gatekeepers. For instance, the sequence Phe-Phe-Gly-Gly can be employed to seal the mesopores of MSNs, as it self-assembles at physiological temperature and undergo disassembly when heat is applied. Examples of this strategy include the use of superparamagnetic manganese- and cobalt-doped iron oxide nanoparticles [390] or microwaves [391] to elevate the temperature and trigger drug release. Similar behavior can be accomplished using poly(γ-benzyl-L-glutamate) as pore blocker [392]. Another example is based on using the heterodimeric peptide E/K, because it closes the pore entrances at physiological temperature owing to the coiled coil conformation, which is lost at higher temperature, triggering drug release [393].

MSNs can also be functionalized with thermo-responsive supramolecular nanovalves. For instance, the pores can be sealed using cucurbit[6]uril. Then, the heat generated upon application of a magnetic field is able to disrupt the stalk-nanovalve interaction, triggering the release [394]. Similarly, β-CDs can be attached to the surface using a Diels-Alder-based stalk, which is able to thermally open and close the pores on-demand upon application of the magnetic field [395].

6.6.2. Thermo-Responsive Polymers

There are several examples of polymers that undergo phase transition below and above their LCST. Polymers with a LCST > 37 °C are hydrophobic above physiological temperature. Then, if attached to the surface adopting a hairy conformation, the polymers will be hydrophobic above 37 °C, closing the pores. However, when the polymer is cross-linked and the system is above the transition temperature, that hydrophobic state leaves free spaces in the polymeric network that allow drug release [396]. Among this type of polymers, poly(N-isopropylacrylamide) (pNIPAM) is the most employed. Additional examples are MSNs functionalized with poly(urethane-amine) (LCST ca. 50 °C) [397] or p(MEO_2MA-co-OEGMA) (LCST ca. 37 °C) [398].

With regard to p(NIPAM), it can be directly engineered as gatekeeper for MSNs, although its coil-to-globule transition taking place at ca. 32 °C complicates its use in patients [399,400]. The LCST can be tuned by introducing different types of monomers. For instance, copolymerizing NIPAM with 3-(methacryloxypropyl)trimethoxysilane) (MPS) raises the LCST of p(NIPAM-co-MPS) up to 36 °C, which would entail better biological performance [401,402]. Similar behavior can be obtained introducing methacrylic acid (MAA), which increases the LCST of p(NIPAM-co-MAA) up to 44.4 °C, endowing magnetic MSNs with both pH- and thermo-responsiveness [403,404]. Our group recently reported magnetic MSNs functionalized with NIPAM and N-(hydroxymethyl)acrylamide) (NHMA). Thermosensitive p(NIPAM-co-NHMA) presented a LCST of ca. 42 °C, showing thermally controlled release and effective hyperthermia treatment in vivo [405,406]. Similarly, p(NIPAM-co-NHMA) can be engineered as gatekeeper for MSNs containing gold nanorods able to generate heat upon NIR light irradiation [137].

There are also polymers that present upper critical solution temperature (UCST). Polymers with UCST > 37 °C are hydrophobic below physiological temperature. For instance, poly(acrylamide-co-acrylonitrile) shows phase transition at 42 °C and can effectively block the pore entrances of MSNs at physiological temperature [407]. Another example is poly(N-acryloyl glycinamide-co-N-phenylacrylamide) (p(NAGAm-co-NPhAm)). This polymer undergoes phase transition at 45 °C and can be grafted to MSNs to accomplish effective drug delivery when the particles generate heat upon NIR-light irradiation [408]. Table 6 summarizes the different strategies applied for the design of thermo-responsive MSNs.

Table 6. Different strategies implemented into MSNs for achieving light-responsive drug delivery.

Approach	Description		Reference
Thermo-Responsive Disassembling Gatekeepers			
DNA	Large DNA strands acting as gatekeepers that dehybridize above a certain temperature, triggering drug release		[231,384–386]
	Short DNA strands used as linkers for grafting bulky gatekeepers (proteins, small nanoparticles) that allow drug release when strands dehybridize upon heating		[387–389]
Peptides	Peptide sequences used as gatekeepers that self-assemble at physiological temperature and undergo disassembly when heated		[390–392]
	Heterodimeric peptide acting as gatekeeper that present a coiled coil conformation at physiological temperature. That 3D structure is lost when heat is applied, triggering drug release		[393]
Nanovalves	Supramolecular nanovalves attached to the surface through thermo-sensitive stalks		[394,395]
LCST Polymers (Hydrophobic if T > LCST)			
poly(urethane-amine)	LCST ca. 50 °C	Polymers form a polymeric network. Below LCTS hydrophilic chains hamper drug release. When T > LCTS, polymers become hydrophobic and the polymeric network shrinks, facilitating drug release.	[397]
p(MEO_2MA-co-OEGMA)	LCST ca. 37 °C		[398]
p(NIPAM)	LCST ca. 32 °C		[399,400]
p(NIPAM-co-MPS)	LCST *ca*. 36 °C		[401,402]
p(NIPAM-co-MAA)	LCST ca. 44 °C		[403,404]
p(NIPAM-co-NHMA)	LCST ca. 42 °C		[137,405,406]
UCST Polymers (Hydrophilic if T > UCST)			
poly(acrylamide-co-acrylonitrile)	UCST ca. 42 °C	Polymers become hydrophilic above UCST, adopting an extended conformation that triggers drug release	[407]
p(NAGAm-co-NPhAm)	UCST ca. 45 °C		[408]

7. Future Perspectives

In the last decades, many researchers have taken advantage of the great physico-chemical and biocompatible features of MSNs to design many different nanocarriers for the treatment of different diseases, especially cancer. However, even though there are thousands of publications, the bench-to-bedside translation remains the bottleneck of the field.

Related to the role of industry, an important issue that should be addressed concerns the scalability and reproducibility of the synthesis of the particles. MSNs should be able to be produced on a large scale while showing size and colloidal stability reproducibility. Otherwise, the results derived from potential clinical studies would not have scientific relevance and consistency and health agencies would probably reject such mesoporous silica nanodevices. In this regard, the drug loading in the particles should be completely standardized, as it would be unacceptable that the amount of drug administered varied from one batch to another.

Assuming that the particles could be properly produced, a mandatory step should be the evaluation of these materials in humans, as no realistic translation might be accomplished until assuring the intrinsic toxicity that MSNs might have. Nonetheless, we should be encouraged by the fact that: (a) amorphous silica is "generally recognized as safe" by the FDA and (b) amorphous silica c-dots have been proved to be well tolerated and to accumulate in tumors in human trials. In view of that, both academia and industry should aim to validate in humans the remarkable preclinical results of these cost-effective silica materials.

Once the large-scale production and human safety of MSNs is validated, the next steps should be headed toward implementing the strategies described in this manuscript for overcoming the different biological barriers. In particular, researchers should mainly focus on achieving significant accumulation of nanoparticles in the tumors as, otherwise, they might not constitute a reliable alternative to the systemic administration of free drugs. More importantly, we should bear in mind that nanoparticle-based cancer treatments are not a magic bullet, meaning that they might not be applicable to every single type of cancer. Hence, the physiology of all types of cancer should be completely understood in order to decide whether it is worth treating them with nanomedicine.

In summary, the proper clinical translation of MSNs will require meeting, at least, the previous objectives along with the collaborative and interdisciplinary efforts of scientists and industry.

8. Conclusions

Experimental and translational research should focus on the different biological barriers that nanoparticles have to face upon administration, as they currently constitute a bottleneck that is preventing many nanomedicines for achieving effective translation into the clinic. In this sense, the great features that mesoporous silica nanoparticles offer have boosted their application for cancer treatment. It has been shown throughout this review that mesoporous silica nanoparticles can be conveniently engineered to enhance the accumulation in tumor tissues, improve the uptake by tumoral cells and prevent endosomal sequestration. In addition to effectively overcoming such biological barriers, mesoporous silica nanoparticles can be functionalized with many different stimuli-responsive gatekeepers, endowing them with on-demand and localized drug delivery to cancer cells. Furthermore, MSNs all well tolerated in vivo and it has been shown that they are mainly excreted through the urine. In view of the evidences, even more emphasis should be place on mesoporous silica nanoparticles research, as they are attractive candidates for clinic translation in the near future.

Author Contributions: All authors contributed equally. All authors have read and agreed to the published version of the manuscript.

Funding: The research was funded by the European Research Council through ERC-2015-AdG-694160 (VERDI) grant.

Acknowledgments: The authors acknowledge financial support from European Research Council through ERC-2015-AdG-694160 (VERDI) project.

Conflicts of Interest: The authors declare no conflict of interest.

References

1. Jain, K.K. Future of nanomedicine: Impact on healthcare & society. *Nanomedicine* **2015**, *10*, 3199–3202.
2. Fornaguera, C.; García-Celma, M.J. Personalized nanomedicine: A revolution at the nanoscale. *J. Pers. Med.* **2017**, *7*, 12. [CrossRef]
3. Pautler, M.; Brenner, S. Nanomedicine: Promises and challenges for the future of public health. *Int. J. Nanomed.* **2010**, *5*, 803–809.
4. Zhu, X.; Radovic-Moreno, A.F.; Wu, J.; Langer, R.; Shi, J. Nanomedicine in the management of microbial infection—Overview and perspectives. *Nano Today* **2014**, *9*, 478–498. [CrossRef]
5. Doane, T.L.; Burda, C. The unique role of nanoparticles in nanomedicine: Imaging, drug delivery and therapy. *Chem. Soc. Rev.* **2012**, *41*, 2885. [CrossRef]
6. Wicki, A.; Witzigmann, D.; Balasubramanian, V.; Huwyler, J. Nanomedicine in cancer therapy: Challenges, opportunities, and clinical applications. *J. Control. Release* **2015**, *200*, 138–157. [CrossRef]
7. Bozzuto, G.; Molinari, A. Liposomes as nanomedical devices. *Int. J. Nanomed.* **2015**, *10*, 975–999. [CrossRef]
8. Oerlemans, C.; Bult, W.; Bos, M.; Storm, G.; Nijsen, J.F.W.; Hennink, W.E. Polymeric Micelles in Anticancer Therapy: Targeting, Imaging and Triggered Release. *Pharm. Res.* **2010**, *27*, 2569–2589. [CrossRef]
9. Kumari, A.; Yadav, S.K.; Yadav, S.C. Biodegradable polymeric nanoparticles based drug delivery systems. *Colloids Surf. B Biointerfaces* **2010**, *75*, 1–18. [CrossRef]
10. Azharuddin, M.; Zhu, G.H.; Das, D.; Ozgur, E.; Uzun, L.; Turner, A.P.F.; Patra, H.K. A repertoire of biomedical applications of noble metal nanoparticles. *Chem. Commun.* **2019**, *55*, 6964–6996. [CrossRef]
11. Maiti, D.; Tong, X.; Mou, X.; Yang, K. Carbon-Based Nanomaterials for Biomedical Applications: A Recent Study. *Front. Pharmacol.* **2019**, *9*, 1401. [CrossRef]
12. Narayan, R.; Nayak, Y.U.; Raichur, M.A.; Garg, S. Mesoporous Silica Nanoparticles: A Comprehensive Review on Synthesis and Recent Advances. *Pharmaceutics* **2018**, *10*, 118. [CrossRef]
13. Yanagisawa, T.; Shimizu, T.; Kuroda, K.; Kato, C. The preparation of alkyltrimethylammonium-kanemite complexes and their conversion to microporous materials. *Bull. Chem. Soc. Jpn.* **1990**, *63*, 988–992. [CrossRef]
14. Kresge, C.T.; Leonowicz, M.E.; Roth, W.J.; Vartuli, J.C.; Beck, J.S. Ordered mesoporous molecular sieves synthesized by a liquid-crystal template mechanism. *Nature* **1992**, *359*, 710–712. [CrossRef]
15. Yan, Z.; Meng, H.; Shi, L.; Li, Z.; Kang, P. Synthesis of mesoporous hollow carbon hemispheres as highly efficient Pd electrocatalyst support for ethanol oxidation. *Electrochem. Commun.* **2010**, *12*, 689–692. [CrossRef]
16. Serrano, E.; Linares, N.; García-Martínez, J.; Berenguer, J.R. Sol–Gel Coordination Chemistry: Building Catalysts from the Bottom-Up. *ChemCatChem* **2013**, *5*, 844–860. [CrossRef]
17. Zhang, Y.; Zheng, S.; Zhu, S.; Ma, J.; Sun, Z.; Farid, M. Evaluation of paraffin infiltrated in various porous silica matrices as shape-stabilized phase change materials for thermal energy storage. *Energy Convers. Manag.* **2018**, *171*, 361–370. [CrossRef]
18. Mitran, R.A.; Berger, D.; Munteanu, C.; Matei, C. Evaluation of Different Mesoporous Silica Supports for Energy Storage in Shape-Stabilized Phase Change Materials with Dual Thermal Responses. *J. Org. Chem. C* **2015**, *119*, 15177–15184. [CrossRef]
19. Vallet-Regí, M.; Rámila, A.; del Real, R.P.; Pérez-Pariente, J. A new property of MCM-41: Drug delivery system. *Chem. Mater.* **2001**, *13*, 308–311. [CrossRef]
20. Vallet-Regí, M.; Balas, F.; Arcos, D. Mesoporous materials for drug delivery. *Angew. Chem. Int. Ed.* **2007**, *46*, 7548–7558. [CrossRef]
21. Manzano, M.; Vallet-Regí, M. Mesoporous silica nanoparticles for drug delivery. *Adv. Funct. Mater.* **2019**, 1902634. [CrossRef]
22. Rosenholm, J.M.; Mamaeva, V.; Sahlgren, C.; Lindén, M. Nanoparticles in targeted cancer therapy: Mesoporous silica nanoparticles entering preclinical development stage. *Nanomedicine* **2012**, *7*, 111–120. [CrossRef]
23. Napierska, D.; Thomassen, L.C.J.; Lison, D.; Martens, J.A.; Hoet, P.H. The nanosilica hazard: Another variable entity. *Part. Fibre Toxicol.* **2010**, *7*, 39. [CrossRef]
24. Croissant, J.G.; Fatieiev, Y.; Khashab, N.M. Degradability and clearance of silicon, organosilica, silsesquioxane, silica mixed oxide, and mesoporous silica nanoparticles. *Adv. Mater.* **2017**, *29*, 1604634. [CrossRef]

25. Yamada, H.; Urata, C.; Aoyama, Y.; Osada, S.; Yamauchi, Y.; Kuroda, K. Preparation of colloidal mesoporous silica nanoparticles with different diameters and their unique degradation behavior in static aqueous systems. *Chem. Mater.* **2012**, *24*, 1462–1471. [CrossRef]
26. Paris, J.L.; Colilla, M.; Izquierdo-barba, I.; Manzano, M.; Vallet-Regí, M. Tuning mesoporous silica dissolution in physiological environments: A review. *J. Mater. Sci.* **2017**, *52*, 8761–8771. [CrossRef]
27. Kempen, P.J.; Greasley, S.; Parker, K.A.; Campbell, J.L.; Chang, H.-Y.; Jones, J.R.; Sinclair, R.; Gambhir, S.S.; Jokerst, J. V Theranostic mesoporous silica nanoparticles biodegrade after pro-survival drug delivery and ultrasound/magnetic resonance imaging of stem cells. *Theranostics* **2015**, *5*, 631–642. [CrossRef]
28. Chen, G.; Teng, Z.; Su, X.; Liu, Y.; Lu, G. Unique biological degradation behavior of stöber mesoporous silica nanoparticles from their interiors to their exteriors. *J. Biomed. Nanotechnol.* **2015**, *11*, 722–729. [CrossRef]
29. Zhai, W.; He, C.; Wu, L.; Zhou, Y.; Chen, H.; Chang, J.; Zhang, H. Degradation of hollow mesoporous silica nanoparticles in human umbilical vein endothelial cells. *J. Biomed. Mater. Res. Part B Appl. Biomater.* **2012**, *100B*, 1397–1403. [CrossRef]
30. Gisbert-Garzarán, M.; Manzano, M.; Vallet-Regí, M. Mesoporous silica nanoparticles for the treatment of complex bone diseases: Bone cancer, bone infection and osteoporosis. *Pharmaceutics* **2020**, *12*, 83. [CrossRef]
31. Vallet-Regí, M.; González, B.; Izquierdo-Barba, I. Nanomaterials as promising alternative in the infection treatment. *Int. J. Mol. Sci.* **2019**, *20*, 3806. [CrossRef] [PubMed]
32. Tan, S.Y.; Teh, C.; Ang, C.Y.; Li, M.; Li, P.; Korzh, V.; Zhao, Y. Responsive mesoporous silica nanoparticles for sensing of hydrogen peroxide and simultaneous treatment toward heart failure. *Nanoscale* **2017**, *9*, 2253–2261. [CrossRef] [PubMed]
33. Cheng, J.; Ding, Q.; Wang, J.; Deng, L.; Yang, L.; Tao, L.; Lei, H.; Lu, S. 5-Azacytidine delivered by mesoporous silica nanoparticles regulates the differentiation of P19 cells into cardiomyocytes. *Nanoscale* **2016**, *8*, 2011–2021. [CrossRef] [PubMed]
34. Doadrio, A.L.; Sánchez-Montero, J.M.; Doadrio, J.C.; Salinas, A.J.; Vallet-Regí, M. Mesoporous silica nanoparticles as a new carrier methodology in the controlled release of the active components in a polypill. *Eur. J. Pharm. Sci.* **2017**, *97*, 1–8. [CrossRef]
35. Liao, Y.-T.; Lee, C.-H.; Chen, S.-T.; Lai, J.-Y.; Wu, K.C.-W. Gelatin-functionalized mesoporous silica nanoparticles with sustained release properties for intracameral pharmacotherapy of glaucoma. *J. Mater. Chem. B* **2017**, *5*, 7008–7013. [CrossRef]
36. Hu, C.; Sun, J.; Zhang, Y.; Chen, J.; Lei, Y.; Sun, X.; Deng, Y. Local delivery and sustained-release of nitric oxide donor loaded in mesoporous silica particles for efficient treatment of primary open-angle glaucoma. *Adv. Healthc. Mater.* **2018**, *7*, 1801047. [CrossRef]
37. Hou, L.; Zheng, Y.; Wang, Y.; Hu, Y.; Shi, J.; Liu, Q.; Zhang, H.; Zhang, Z. Self-regulated carboxyphenylboronic acid-modified mesoporous silica nanoparticles with "touch switch" releasing property for insulin delivery. *ACS Appl. Mater. Interfaces* **2018**, *10*, 21927–21938. [CrossRef]
38. Xu, B.; Jiang, G.; Yu, W.; Liu, D.; Zhang, Y.; Zhou, J.; Sun, S.; Liu, Y. H_2O_2-Responsive mesoporous silica nanoparticles integrated with microneedle patches for the glucose-monitored transdermal delivery of insulin. *J. Mater. Chem. B* **2017**, *5*, 8200–8208. [CrossRef]
39. Bray, F.; Ferlay, J.; Soerjomataram, I.; Siegel, R.L.; Torre, L.A.; Jemal, A. Global cancer statistics 2018: GLOBOCAN estimates of incidence and mortality worldwide for 36 cancers in 185 countries. *CA. Cancer J. Clin.* **2018**, *68*, 394–424. [CrossRef]
40. Wilhelm, S.; Tavares, A.J.; Dai, Q.; Ohta, S.; Audet, J.; Dvorak, H.F.; Chan, W.C.W. Analysis of nanoparticle delivery to tumours. *Nat. Rev. Mater.* **2016**, *1*, 16014. [CrossRef]
41. Matsumura, Y.; Maeda, H. A new concept for macromolecular therapeutics in cancer chemotherapy: Mechanism of tumoritropic accumulation of proteins and the antitumor agent smancs. *Cancer Res.* **1986**, *46*, 6387–6392. [PubMed]
42. Grodzinski, P.; Kircher, M.; Goldberg, M.; Gabizon, A. Integrating nanotechnology into cancer care. *ACS Nano* **2019**, *13*, 7370–7376. [CrossRef] [PubMed]
43. Fang, J.; Nakamura, H.; Maeda, H. The EPR effect: Unique features of tumor blood vessels for drug delivery, factors involved, and limitations and augmentation of the effect. *Adv. Drug Deliv. Rev.* **2011**, *63*, 136–151. [CrossRef]

44. Dogra, P.; Adolphi, N.L.; Wang, Z.; Lin, Y.S.; Butler, K.S.; Durfee, P.N.; Croissant, J.G.; Noureddine, A.; Coker, E.N.; Bearer, E.L.; et al. Establishing the effects of mesoporous silica nanoparticle properties on in vivo disposition using imaging-based pharmacokinetics. *Nat. Commun.* **2018**, *9*, 1–14. [CrossRef]
45. Etheridge, M.L.; Campbell, S.A.; Erdman, A.G.; Haynes, C.L.; Wolf, S.M.; McCullough, J. The big picture on nanomedicine: The state of investigational and approved nanomedicine products. *Nanomedicine Nanotechnol. Biol. Med.* **2013**, *9*, 1–14. [CrossRef]
46. Zhao, Y.; Wang, Y.; Ran, F.; Cui, Y.; Liu, C.; Zhao, Q.; Gao, Y.; Wang, D.; Wang, S. A comparison between sphere and rod nanoparticles regarding their in vivo biological behavior and pharmacokinetics. *Sci. Rep.* **2017**, *7*, 4131. [CrossRef]
47. Toy, R.; Peiris, P.M.; Ghaghada, K.B. Shaping cancer nanomedicine: The effect of particle shape on the in vivo journey of nanoparticles. *Nanomedicine* **2014**, *9*, 121–134. [CrossRef] [PubMed]
48. Zhao, J.; Stenzel, M.H. Entry of Nanoparticles into Cells: The Importance of Nanoparticle Properties. *Polym. Chem.* **2018**, *9*, 259–272. [CrossRef]
49. Behzadi, S.; Serpooshan, V.; Tao, W.; Hamaly, M.A.; Alkawareek, M.Y.; Dreaden, E.C.; Brown, D.; Alkilany, A.M.; Farokhzad, O.C.; Mahmoudi, M. Cellular uptake of nanoparticles: Journey inside the cell. *Chem. Soc. Rev.* **2017**, *46*, 4218–4244. [CrossRef]
50. Ge, C.; Tian, J.; Zhao, Y.; Chen, C.; Zhou, R.; Chai, Z. Towards understanding of nanoparticle–protein corona. *Arch. Toxicol.* **2015**, *89*, 519–539. [CrossRef]
51. Jokerst, J.V.; Lobovkina, T.; Zare, R.N.; Gambhir, S.S. Nanoparticle PEGylation for imaging and therapy. *Nanomedicine* **2011**, *6*, 715–728. [CrossRef] [PubMed]
52. Clemments, A.M.; Muniesa, C.; Landry, C.C.; Botella, P. Effect of surface properties in protein corona development on mesoporous silica nanoparticles. *RSC Adv.* **2014**, *4*, 29134–29138. [CrossRef]
53. Yildirim, A.; Ozgur, E.; Bayindir, M. Impact of mesoporous silica nanoparticle surface functionality on hemolytic activity, thrombogenicity and non-specific protein adsorption. *J. Mater. Chem. B* **2013**, *1*, 1909–1920. [CrossRef] [PubMed]
54. Chen, S.; Li, L.; Zhao, C.; Zheng, J. Surface hydration: Principles and applications toward low-fouling/nonfouling biomaterials. *Polymer (Guildf.)* **2010**, *51*, 5283–5293. [CrossRef]
55. Encinas, N.; Angulo, M.; Astorga, C.; Colilla, M.; Izquierdo-Barba, I.; Vallet-Regí, M. Mixed-charge pseudo-zwitterionic mesoporous silica nanoparticles with low-fouling and reduced cell uptake properties. *Acta Biomater.* **2019**, *84*, 317–327. [CrossRef] [PubMed]
56. Sanchez-Salcedo, S.; Vallet-Regí, M.; Shahin, S.A.; Glackin, C.A.; Zink, J.I. Mesoporous core-shell silica nanoparticles with anti-fouling properties for ovarian cancer therapy. *Chem. Eng. J.* **2018**, *340*, 114–124. [CrossRef]
57. Rosen, J.E.; Gu, F.X. Surface functionalization of silica nanoparticles with cysteine: A low-fouling zwitterionic surface. *Langmuir* **2011**, *27*, 10507–10513. [CrossRef]
58. Xuan, M.; Shao, J.; Zhao, J.; Li, Q.; Dai, L.; Li, J. Magnetic mesoporous silica nanoparticles cloaked by red blood cell membranes: Applications in cancer therapy. *Angew. Chem. Int. Ed.* **2018**, *57*, 6049–6053. [CrossRef]
59. Cai, D.; Liu, L.; Han, C.; Ma, X.; Qian, J.; Zhou, J.; Zhu, W. Cancer cell membrane-coated mesoporous silica loaded with superparamagnetic ferroferric oxide and Paclitaxel for the combination of Chemo/Magnetocaloric therapy on MDA-MB-231 cells. *Sci. Rep.* **2019**, *9*, 14475. [CrossRef]
60. Yue, J.; Wang, Z.; Shao, D.; Chang, Z.; Hu, R.; Li, L.; Luo, S.; Dong, W. Cancer cell membrane-modified biodegradable mesoporous silica nanocarriers for berberine therapy of liver cancer. *RSC Adv.* **2018**, *8*, 40288–40297. [CrossRef]
61. Yang, J.; Teng, Y.; Fu, Y.; Zhang, C. Chlorins e6 loaded silica nanoparticles coated with gastric cancer cell membrane for tumor specific photodynamic therapy of gastric cancer. *Int. J. Nanomedicine* **2019**, *14*, 5061–5071. [CrossRef] [PubMed]
62. van Rijt, S.H.; Bölükbas, D.A.; Argyo, C.; Wipplinger, K.; Naureen, M.; Datz, S.; Eickelberg, O.; Meiners, S.; Bein, T.; Schmid, O.; et al. Applicability of avidin protein coated mesoporous silica nanoparticles as drug carriers in the lung. *Nanoscale* **2016**, *8*, 8058–8069. [CrossRef] [PubMed]
63. Luo, Z.; Hu, Y.; Xin, R.; Zhang, B.; Li, J.; Ding, X.; Hou, Y.; Yang, L.; Cai, K. Surface functionalized mesoporous silica nanoparticles with natural proteins for reduced immunotoxicity. *J. Biomed. Mater. Res. Part A* **2014**, *102*, 3781–3794. [CrossRef] [PubMed]

64. Natfji, A.A.; Ravishankar, D.; Osborn, H.M.I.; Greco, F. Parameters affecting the enhanced permeability and retention effect: The need for patient selection. *J. Pharm. Sci.* **2017**, *106*, 3179–3187. [CrossRef] [PubMed]
65. Villaverde, G.; Baeza, A. Targeting strategies for improving the efficacy of nanomedicine in oncology. *Beilstein J. Nanotechnol.* **2019**, *10*, 168–181. [CrossRef]
66. Wang, Y.; Xie, Y.; Kilchrist, K.V.; Li, J.; Duvall, C.L.; Oupický, D. Endosomolytic and tumor-penetrating mesoporous silica nanoparticles for siRNA/miRNA combination cancer therapy. *ACS Appl. Mater. Interfaces* **2020**, *12*, 4308–4322. [CrossRef]
67. Liu, X.; Lin, P.; Perrett, I.; Lin, J.; Liao, Y.-P.; Chang, C.H.; Jiang, J.; Wu, N.; Donahue, T.; Wainberg, Z.; et al. Tumor-penetrating peptide enhances transcytosis of silicasome-based chemotherapy for pancreatic cancer. *J. Clin. Invest.* **2017**, *127*, 2007–2018. [CrossRef]
68. Kuang, J.; Song, W.; Yin, J.; Zeng, X.; Han, S.; Zhao, Y.-P.; Tao, J.; Liu, C.-J.; He, X.-H.; Zhang, X.-Z. iRGD modified chemo-immunotherapeutic nanoparticles for enhanced immunotherapy against glioblastoma. *Adv. Funct. Mater.* **2018**, *28*, 1800025. [CrossRef]
69. Liu, X.; Jiang, J.; Ji, Y.; Lu, J.; Chan, R.; Meng, H. Targeted drug delivery using iRGD peptide for solid cancer treatment. *Mol. Syst. Des. Eng.* **2017**, *2*, 370–379. [CrossRef]
70. Ruoslahti, E. Tumor penetrating peptides for improved drug delivery. *Adv. Drug Deliv. Rev.* **2017**, *110–111*, 3–12. [CrossRef]
71. Kang, T.; Gao, X.; Hu, Q.; Jiang, D.; Feng, X.; Zhang, X.; Song, Q.; Yao, L.; Huang, M.; Jiang, X.; et al. iNGR-modified PEG-PLGA nanoparticles that recognize tumor vasculature and penetrate gliomas. *Biomaterials* **2014**, *35*, 4319–4332. [CrossRef]
72. Pawelek, J.M.; Low, K.B.; Bermudes, D. Bacteria as tumour-targeting vectors. *Lancet Oncol.* **2003**, *4*, 548–556. [CrossRef]
73. Li, Z.; Fan, D.; Xiong, D. Mesenchymal stem cells as delivery vectors for anti-tumor therapy. *Stem Cell Investig.* **2015**, *2*, 6. [PubMed]
74. Vallet-Regí, M.; Paris, J.L.; de la Torre, P.; Cabañas, M.V.; Manzano, M.; Flores, A.I. Mesenchymal stem cells from human placenta as nanoparticle delivery vectors. *Insights Stem Cells* **2018**, *4*, 1.
75. Das, S.; Raj, R. Prospects of bacteriotherapy with nanotechnology in nanoparticledrug conjugation approach for cancer therapy. *Curr. Med. Chem.* **2016**, *23*, 1477–1494.
76. Suh, S.B.; Jo, A.; Traore, M.A.; Zhan, Y.; Coutermarsh-Ott, S.L.; Ringel-Scaia, V.M.; Allen, I.C.; Davis, R.M.; Behkam, B. Nanoscale bacteria-enabled autonomous drug delivery system (NanoBEADS) enhances intratumoral transport of nanomedicine. *Adv. Sci.* **2019**, *6*, 1801309. [CrossRef]
77. Moreno, V.M.; Álvarez, E.; Izquierdo-Barba, I.; Baeza, A.; Serrano-López, J.; Vallet-Regí, M. Bacteria as Nanoparticles Carrier for Enhancing Penetration in a Tumoral Matrix Model. *Adv. Mater. Interfaces* **2020**, in press. [CrossRef]
78. Paris, J.L.; de la Torre, P.; Cabañas, M.V.; Manzano, M.; Grau, M.; Flores, A.I.; Vallet-Regí, M. Vectorization of ultrasound-responsive nanoparticles in placental mesenchymal stem cells for cancer therapy. *Nanoscale* **2017**, *9*, 5528–5537. [CrossRef]
79. Paris, J.L.; de la Torre, P.; Manzano, M.; Cabañas, M.V.; Flores, A.I.; Vallet-Regí, M. Decidua-derived mesenchymal stem cells as carriers of mesoporous silica nanoparticles. In vitro and in vivo evaluation on mammary tumors. *Acta Biomater.* **2016**, *33*, 275–282. [CrossRef]
80. Huang, X.; Zhang, F.; Wang, H.; Niu, G.; Choi, K.Y.; Swierczewska, M.; Zhang, G.; Gao, H.; Wang, Z.; Zhu, L.; et al. Mesenchymal stem cell-based cell engineering with multifunctional mesoporous silica nanoparticles for tumor delivery. *Biomaterials* **2013**, *34*, 1772–1780. [CrossRef]
81. Netti, P.A.; Berk, D.A.; Swartz, M.A.; Grodzinsky, A.J.; Jain, R.K. Role of Extracellular Matrix Assembly in Interstitial Transport in Solid Tumors. *Cancer Res.* **2000**, *60*, 2497–2503.
82. Walker, C.; Mojares, E.; Del Río Hernández, A. Role of extracellular matrix in development and cancer progression. *Int. J. Mol. Sci.* **2018**, *19*, 3028. [CrossRef]
83. Parodi, A.; Haddix, S.G.; Taghipour, N.; Scaria, S.; Taraballi, F.; Cevenini, A.; Yazdi, I.K.; Corbo, C.; Palomba, R.; Khaled, S.Z.; et al. Bromelain surface modification increases the diffusion of silica nanoparticles in the tumor extracellular matrix. *ACS Nano* **2014**, *8*, 9874–9883. [CrossRef]
84. Villegas, M.R.; Baeza, A.; Noureddine, A.; Durfee, P.N.; Butler, K.S.; Agola, J.O.; Brinker, C.J.; Vallet-Regí, M. Multifunctional Protocells for Enhanced Penetration in 3D Extracellular Tumoral Matrices. *Chem. Mater.* **2018**, *30*, 112–120. [CrossRef]

85. Villegas, M.R.; Baeza, A.; Vallet-Regí, M. Hybrid Collagenase Nanocapsules for Enhanced Nanocarrier Penetration in Tumoral Tissues. *ACS Appl. Mater. Interfaces* **2015**, *7*, 24075–24081. [CrossRef] [PubMed]
86. Zhang, Y.-R.; Lin, R.; Li, H.-J.; He, W.; Du, J.-Z.; Wang, J. Strategies to improve tumor penetration of nanomedicines through nanoparticle design. *WIREs Nanomed. Nanobiotechnol.* **2019**, *11*, e1519. [CrossRef] [PubMed]
87. He, X.; Wang, D.; Chen, P.; Qiao, Y.; Yang, T.; Yu, Z.; Wang, C.; Wu, H. Construction of a novel "ball-and-rod" MSNs-pp-PEG system: A promising antitumor drug delivery system with a particle size switchable function. *Chem. Commun.* **2020**, in press. [CrossRef]
88. Coussios, C.C.; Roy, R.A. Applications of acoustics and cavitation to noninvasive therapy and drug delivery. *Annu. Rev. Fluid Mech.* **2008**, *40*, 395–420. [CrossRef]
89. Arvanitis, C.D.; Bazan-Peregrino, M.; Rifai, B.; Seymour, L.W.; Coussios, C.C. Cavitation-enhanced extravasation for drug delivery. *Ultrasound Med. Biol.* **2011**, *37*, 1838–1852. [CrossRef]
90. Ho, Y.-J.; Wu, C.-H.; Jin, Q.; Lin, C.-Y.; Chiang, P.-H.; Wu, N.; Fan, C.-H.; Yang, C.-M.; Yeh, C.-K. Superhydrophobic drug-loaded mesoporous silica nanoparticles capped with β-cyclodextrin for ultrasound image-guided combined antivascular and chemo-sonodynamic therapy. *Biomaterials* **2020**, *232*, 119723. [CrossRef]
91. Paris, J.L.; Mannaris, C.; Cabañas, M.V.; Carlisle, R.; Manzano, M.; Vallet-Regí, M.; Coussios, C.C. Ultrasound-mediated cavitation-enhanced extravasation of mesoporous silica nanoparticles for controlled-release drug delivery. *Chem. Eng. J.* **2018**, *340*, 2–8. [CrossRef]
92. Gustafson, H.H.; Holt-Casper, D.; Grainger, D.W.; Ghandehari, H. Nanoparticle uptake: The phagocyte problem. *Nano Today* **2015**, *10*, 487–510. [CrossRef] [PubMed]
93. Arvizo, R.R.; Miranda, O.R.; Moyano, D.F.; Walden, C.A.; Giri, K.; Robertson, J.D.; Rotello, V.M.; Reid, J.M.; Mukherjee, P. Modulating pharmacokinetics, tumor uptake and biodistribution by engineered nanoparticles. *PLoS ONE* **2011**, *6*, 24374. [CrossRef] [PubMed]
94. Lu, H.; Stenzel, M.H. Multicellular tumor spheroids (MCTS) as a 3D in vitro evaluation tool of nanoparticles. *Small* **2018**, *14*, 1702858. [CrossRef]
95. Alkilany, A.M.; Zhu, L.; Weller, H.; Mews, A.; Parak, W.J.; Barz, M.; Feliu, N. Ligand density on nanoparticles: A parameter with critical impact on nanomedicine. *Adv. Drug Deliv. Rev.* **2019**, *143*, 22–36. [CrossRef]
96. Yamaguchi, H.; Hayama, K.; Sasagawa, I.; Okada, Y.; Kawase, T.; Tsubokawa, N.; Tsuchimochi, M. HER2-targeted multifunctional silica nanoparticles specifically enhance the radiosensitivity of HER2-overexpressing breast cancer cells. *Int. J. Mol. Sci.* **2018**, *19*, 908. [CrossRef] [PubMed]
97. Li, L.; Lu, Y.; Jiang, C.; Zhu, Y.; Yang, X.; Hu, X.; Lin, Z.; Zhang, Y.; Peng, M.; Xia, H.; et al. Actively targeted deep tissue imaging and photothermal-chemo therapy of breast cancer by antibody-functionalized drug-loaded X-ray-responsive bismuth sulfide@mesoporous silica core–shell nanoparticles. *Adv. Funct. Mater.* **2018**, *28*, 1704623. [CrossRef]
98. Ngamcherdtrakul, W.; Morry, J.; Gu, S.; Castro, D.J.; Goodyear, S.M.; Sangvanich, T.; Reda, M.M.; Lee, R.; Mihelic, S.A.; Beckman, B.L.; et al. Cationic polymer modified mesoporous silica nanoparticles for targeted siRNA delivery to HER2+ breast cancer. *Adv. Funct. Mater.* **2015**, *25*, 2646–2659. [CrossRef]
99. Tsai, C.-P.; Chen, C.-Y.; Hung, Y.; Chang, F.-H.; Mou, C.-Y. Monoclonal antibody-functionalized mesoporous silica nanoparticles (MSN) for selective targeting breast cancer cells. *J. Mater. Chem.* **2009**, *19*, 5737–5743. [CrossRef]
100. Ngamcherdtrakul, W.; Sangvanich, T.; Reda, M.; Gu, S.; Bejan, D.; Yantasee, W. Lyophilization and stability of antibody-conjugated mesoporous silica nanoparticle with cationic polymer and PEG for siRNA delivery. *Int. J. Nanomed.* **2018**, *13*, 4015–4027. [CrossRef]
101. Wang, X.; Liu, Y.; Wang, S.; Shi, D.; Zhou, X.; Wang, C.; Wu, J.; Zeng, Z.; Li, Y.; Sun, J.; et al. CD44-engineered mesoporous silica nanoparticles for overcoming multidrug resistance in breast cancer. *Appl. Surf. Sci.* **2015**, *332*, 308–317. [CrossRef]
102. Chen, F.; Hong, H.; Shi, S.; Goel, S.; Valdovinos, H.F.; Hernandez, R.; Theuer, C.P.; Barnhart, T.E.; Cai, W. Engineering of hollow mesoporous silica nanoparticles for remarkably enhanced tumor active targeting efficacy. *Sci. Rep.* **2014**, *4*, 5080. [CrossRef]
103. Goel, S.; Chen, F.; Luan, S.; Valdovinos, H.F.; Shi, S.; Graves, S.A.; Ai, F.; Barnhart, T.E.; Theuer, C.P.; Cai, W. Engineering intrinsically zirconium-89 radiolabeled self-destructing mesoporous silica nanostructures for in vivo biodistribution and tumor targeting studies. *Adv. Sci.* **2016**, *3*, 1600122. [CrossRef] [PubMed]

104. Chen, F.; Hong, H.; Zhang, Y.; Valdovinos, H.F.; Shi, S.; Kwon, G.S.; Theuer, C.P.; Barnhart, T.E.; Cai, W. In vivo tumor targeting and image-guided drug delivery with antibody-conjugated, radiolabeled mesoporous silica nanoparticles. *ACS Nano* **2013**, *7*, 9027–9039. [CrossRef] [PubMed]
105. Qu, W.; Meng, B.; Yu, Y.; Wang, S. EpCAM antibody-conjugated mesoporous silica nanoparticles to enhance the anticancer efficacy of carboplatin in retinoblastoma. *Mater. Sci. Eng. C* **2017**, *76*, 646–651. [CrossRef] [PubMed]
106. Dréau, D.; Moore, L.J.; Alvarez-Berrios, M.P.; Tarannum, M.; Mukherjee, P.; Vivero-Escoto, J.L. Mucin-1-antibody-conjugated mesoporous silica nanoparticles for selective breast cancer detection in a Mucin-1 transgenic murine mouse model. *J. Biomed. Nanotechnol.* **2016**, *12*, 2172–2184. [CrossRef]
107. Zhang, X.; Li, Y.; Wei, M.; Liu, C.; Yu, T.; Yang, J. Cetuximab-modified silica nanoparticle loaded with ICG for tumor-targeted combinational therapy of breast cancer. *Drug Deliv.* **2019**, *26*, 129–136. [CrossRef]
108. Wang, Y.; Huang, H.-Y.; Yang, L.; Zhang, Z.; Ji, H. Cetuximab-modified mesoporous silica nano-medicine specifically targets EGFR-mutant lung cancer and overcomes drug resistance. *Sci. Rep.* **2016**, *6*, 25468. [CrossRef]
109. Er, Ö.; Colak, G.S.; Ocakoglu, K.; Ince, M.; Bresolí-Obach, R.; Mora, M.; Sagristá, L.M.; Yurt, F.; Nonell, S. Selective photokilling of human pancreatic cancer cells using cetuximab-targeted mesoporous silica nanoparticles for delivery of zinc phthalocyanine. *Molecules* **2018**, *23*, 2749. [CrossRef]
110. Farokhzad, O.C.; Karp, J.M.; Langer, R. Nanoparticle–aptamer bioconjugates for cancer targeting. *Expert Opin. Drug Deliv.* **2006**, *3*, 311–324. [CrossRef]
111. Dineshkumar, S.; Raj, A.; Srivastava, A.; Mukherjee, S.; Pasha, S.S.; Kachwal, V.; Fageria, L.; Chowdhury, R.; Laskar, I.R. Facile incorporation of "aggregation-induced emission"-active conjugated polymer into mesoporous silica hollow nanospheres: Synthesis, characterization, photophysical studies, and application in bioimaging. *ACS Appl. Mater. Interfaces* **2019**, *11*, 31270–31282. [CrossRef]
112. Babaei, M.; Abnous, K.; Taghdisi, S.M.; Amel Farzad, S.; Peivandi, M.T.; Ramezani, M.; Alibolandi, M. Synthesis of theranostic epithelial cell adhesion molecule targeted mesoporous silica nanoparticle with gold gatekeeper for hepatocellular carcinoma. *Nanomedicine* **2017**, *12*, 1261–1279. [CrossRef] [PubMed]
113. Xie, X.; Li, F.; Zhang, H.; Lu, Y.; Lian, S.; Lin, H.; Gao, Y.; Jia, L. EpCAM aptamer-functionalized mesoporous silica nanoparticles for efficient colon cancer cell-targeted drug delivery. *Eur. J. Pharm. Sci.* **2016**, *83*, 28–35. [CrossRef] [PubMed]
114. Li, Y.; Duo, Y.; Bao, S.; He, L.; Ling, K.; Luo, J.; Zhang, Y.; Huang, H.; Zhang, H.; Yu, X. EpCAM aptamer-functionalized polydopamine-coated mesoporous silica nanoparticles loaded with DM1 for targeted therapy in colorectal cancer. *Int. J. Nanomedicine* **2017**, *12*, 6239–6257. [CrossRef] [PubMed]
115. Pascual, L.; Cerqueira-Coutinho, C.; García-Fernández, A.; de Luis, B.; Bernardes, E.S.; Albernaz, M.S.; Missailidis, S.; Martínez-Máñez, R.; Santos-Oliveira, R.; Orzaez, M.; et al. MUC1 aptamer-capped mesoporous silica nanoparticles for controlled drug delivery and radio-imaging applications. *Nanomed. Nanotechnol. Biol. Med.* **2017**, *13*, 2495–2505. [CrossRef] [PubMed]
116. Hanafi-Bojd, M.Y.; Moosavian Kalat, S.A.; Taghdisi, S.M.; Ansari, L.; Abnous, K.; Malaekeh-Nikouei, B. MUC1 aptamer-conjugated mesoporous silica nanoparticles effectively target breast cancer cells. *Drug Dev. Ind. Pharm.* **2018**, *44*, 13–18. [CrossRef] [PubMed]
117. Zhang, P.; Cheng, F.; Zhou, R.; Cao, J.; Li, J.; Burda, C.; Min, Q.; Zhu, J.-J. DNA-hybrid-gated multifunctional mesoporous silica nanocarriers for dual-targeted and microRNA-responsive controlled drug delivery. *Angew. Chem. Int. Ed.* **2014**, *53*, 2371–2375. [CrossRef]
118. Alizadeh, L.; Alizadeh, E.; Zarebkohan, A.; Ahmadi, E.; Rahmati-Yamchi, M.; Salehi, R. AS1411 aptamer-functionalized chitosan-silica nanoparticles for targeted delivery of epigallocatechin gallate to the SKOV-3 ovarian cancer cell lines. *J. Nanoparticle Res.* **2020**, *22*, 5. [CrossRef]
119. Tang, Y.; Hu, H.; Zhang, M.G.; Song, J.; Nie, L.; Wang, S.; Niu, G.; Huang, P.; Lu, G.; Chen, X. An aptamer-targeting photoresponsive drug delivery system using "off–on" graphene oxide wrapped mesoporous silica nanoparticles. *Nanoscale* **2015**, *7*, 6304–6310. [CrossRef]
120. Li, L.-L.; Yin, Q.; Cheng, J.; Lu, Y. Polyvalent mesoporous silica nanoparticle-aptamer bioconjugates target breast cancer cells. *Adv. Healthc. Mater.* **2012**, *1*, 567–572. [CrossRef]
121. Nejabat, M.; Mohammadi, M.; Abnous, K.; Taghdisi, S.M.; Ramezani, M.; Alibolandi, M. Fabrication of acetylated carboxymethylcellulose coated hollow mesoporous silica hybrid nanoparticles for nucleolin targeted delivery to colon adenocarcinoma. *Carbohydr. Polym.* **2018**, *197*, 157–166. [CrossRef]

122. Tan, J.; Yang, N.; Zhong, L.; Tan, J.; Hu, Z.; Zhao, Q.; Gong, W.; Zhang, Z.; Zheng, R.; Lai, Z.; et al. A new theranostic system based on endoglin aptamer conjugated fluorescent silica nanoparticles. *Theranostics* **2017**, *7*, 4862–4876. [CrossRef]
123. Wang, K.; Yao, H.; Meng, Y.; Wang, Y.; Yan, X.; Huang, R. Specific aptamer-conjugated mesoporous silica-carbon nanoparticles for HER2-targeted chemo-photothermal combined therapy. *Acta Biomater.* **2015**, *16*, 196–205. [CrossRef]
124. Habault, J.; Poyet, J.L. Recent advances in cell penetrating peptide-based anticancer therapies. *Molecules* **2019**, *24*, 927. [CrossRef]
125. Guidotti, G.; Brambilla, L.; Rossi, D. Cell-penetrating peptides: From basic research to clinics. *Trends Pharmacol. Sci.* **2017**, *38*, 406–424. [CrossRef]
126. Pan, L.; He, Q.; Liu, J.; Chen, Y.; Ma, M.; Zhang, L.; Shi, J. Nuclear-targeted drug delivery of tat peptide-conjugated monodisperse mesoporous silica nanoparticles. *J. Am. Chem. Soc.* **2012**, *134*, 5722–5725. [CrossRef]
127. Li, X.; Chen, Y.; Wang, M.; Ma, Y.; Xia, W.; Gu, H. A mesoporous silica nanoparticle – PEI – Fusogenic peptide system for siRNA delivery in cancer therapy. *Biomaterials* **2013**, *34*, 1391–1401. [CrossRef]
128. Wu, X.; Han, Z.; Schur, R.M.; Lu, Z. Targeted Mesoporous Silica Nanoparticles Delivering Arsenic Trioxide with Environment Sensitive Drug Release for E ffective Treatment of Triple Negative Breast Cancer. *ACS Biomater. Sci.* **2016**, *2*, 501–507. [CrossRef]
129. Paris, J.L.; Villaverde, G.; Cabañas, M.V.; Manzano, M.; Vallet-Regí, M. From proof-of-concept material to PEGylated and modularly targeted ultrasound-responsive mesoporous silica nanoparticles. *J. Mater. Chem. B* **2018**, *6*, 2785–2794. [CrossRef]
130. Lu, Y.; Li, L.; Lin, Z.; Li, M.; Hu, X.; Zhang, Y.; Peng, M. Enhancing osteosarcoma killing and CT imaging using ultrahigh drug loading and nir-responsive bismuth sulfide@mesoporous silica nanoparticles. *Adv. Healthc. Mater.* **2018**, *7*, 1800602. [CrossRef]
131. Li, H.; Li, K.; Zeng, Q.; Zeng, Y.; Chen, D.; Pang, L.; Chen, X.; Zhan, Y. Novel vinyl-modified RGD conjugated silica nanoparticles based on photo click chemistry for in vivo prostate cancer targeted fluorescence imaging. *RSC Adv.* **2019**, *9*, 25318–25325. [CrossRef]
132. Xu, X.; Li, H.; Li, K.; Zeng, Q.; Liu, Y.; Zeng, Y.; Chen, D.; Liang, J.; Chen, X.; Zhan, Y. A photo-triggered conjugation approach for attaching RGD ligands to biodegradable mesoporous silica nanoparticles for the tumor fluorescent imaging. *Nanomed. Nanotechnol. Biol. Med.* **2019**, *19*, 136–144. [CrossRef] [PubMed]
133. Paris, J.L.; Villaverde, G.; Gómez-Graña, S.; Vallet-Regí, M. Nanoparticles for multimodal antivascular therapeutics: Dual drug release, photothermal and photodynamic therapy. *Acta Biomater.* **2020**, *101*, 459–468. [CrossRef] [PubMed]
134. Zhang, P.; Tang, M.; Huang, Q.; Zhao, G.; Huang, N.; Zhang, X.; Tan, Y.; Cheng, Y. Combination of 3-methyladenine therapy and Asn-Gly-Arg (NGR)-modified mesoporous silica nanoparticles loaded with temozolomide for glioma therapy in vitro. *Biochem. Biophys. Res. Commun.* **2019**, *509*, 549–556. [CrossRef]
135. Lee, J.; Oh, E.-T.; Han, Y.; Kim, H.G.; Park, H.J.; Kim, C. Mesoporous silica nanocarriers with cyclic peptide gatekeeper: Specific targeting of aminopeptidase n and triggered drug release by stimuli-responsive conformational transformation. *Chem. Eur. J.* **2017**, *23*, 16966–16971. [CrossRef]
136. Hu, J.; Zhang, X.; Wen, Z.; Tan, Y.; Huang, N.; Cheng, S.; Zheng, H.; Cheng, Y. Asn-Gly-Arg-modified polydopamine-coated nanoparticles for dual-targeting therapy of brain glioma in rats. *Oncotarget* **2016**, *7*, 73681–73696. [CrossRef]
137. Villaverde, G.; Gómez-Graña, S.; Guisasola, E.; García, I.; Hanske, C.; Liz-Marzán, L.M.; Baeza, A.; Vallet-Regí, M. Targeted chemo-photothermal therapy: A nanomedicine approximation to selective melanoma treatment. *Part. Part. Syst. Charact.* **2018**, *35*, 1800148. [CrossRef]
138. Wei, Y.; Gao, L.; Wang, L.; Shi, L.; Wei, E.; Zhou, B.; Zhou, L.; Ge, B. Polydopamine and peptide decorated doxorubicin-loaded mesoporous silica nanoparticles as a targeted drug delivery system for bladder cancer therapy. *Drug Deliv.* **2017**, *24*, 681–691. [CrossRef]
139. Shi, J.; Hou, S.; Huang, J.; Wang, S.; Huan, W.; Huang, C.; Liu, X.; Jiang, R.; Qian, W.; Lu, J.; et al. An MSN-PEG-IP drug delivery system and IL13Rα2 as targeted therapy for glioma. *Nanoscale* **2017**, *9*, 8970–8981. [CrossRef]

140. Martínez-Carmona, M.; Baeza, A.; Rodríguez-Milla, M.A.; García-Castro, J.; Vallet-Regí, M. Mesoporous silica nanoparticles grafted with a light-responsive protein shell for highly cytotoxic antitumoral therapy. *J. Mater. Chem. B* **2015**, *3*, 5746–5752. [CrossRef]
141. Montalvo-Quiros, S.; Aragoneses-Cazorla, G.; Garcia-Alcalde, L.; Vallet-Regí, M.; González, B.; Luque-Garcia, J.L. Cancer cell targeting and therapeutic delivery of silver nanoparticles by mesoporous silica nanocarriers: Insights into the action mechanisms using quantitative proteomics. *Nanoscale* **2019**, *11*, 4531–4545. [CrossRef] [PubMed]
142. Chen, X.; Sun, H.; Hu, J.; Han, X.; Liu, H.; Hu, Y. Transferrin gated mesoporous silica nanoparticles for redox-responsive and targeted drug delivery. *Colloids Surf., B* **2017**, *152*, 77–84. [CrossRef] [PubMed]
143. Zhou, J.; Li, M.; Lim, W.Q.; Luo, Z.; Phua, S.Z.F.; Huo, R.; Li, L.; Li, K.; Dai, L.; Liu, J.; et al. A transferrin-conjugated hollow nanoplatform for redox-controlled and targeted chemotherapy of tumor with reduced inflammatory reactions. *Theranostics* **2018**, *8*, 518–532. [CrossRef] [PubMed]
144. Jiao, Y.; Shen, S.; Sun, Y.; Jiang, X.; Yang, W. A functionalized hollow mesoporous silica nanoparticles-based controlled dual-drug delivery system for improved tumor cell cytotoxicity. *Part. Part. Syst. Char.* **2015**, *32*, 222–233. [CrossRef]
145. Saini, K.; Bandyopadhyaya, R. Transferrin-conjugated polymer-coated mesoporous silica nanoparticles loaded with gemcitabine for killing pancreatic cancer cells. *ACS Appl. Nano Mater.* **2020**, *3*, 229–240. [CrossRef]
146. Gurka, M.K.; Pender, D.; Chuong, P.; Fouts, B.L.; Sobelov, A.; McNally, M.W.; Mezera, M.; Woo, S.Y.; McNally, L.R. Identification of pancreatic tumors in vivo with ligand-targeted, pH responsive mesoporous silica nanoparticles by multispectral optoacoustic tomography. *J. Control. Release* **2016**, *231*, 60–67. [CrossRef]
147. Martínez-Carmona, M.; Lozano, D.; Colilla, M.; Vallet-Regí, M. Lectin-conjugated pH-responsive mesoporous silica nanoparticles for targeted bone cancer treatment. *Acta Biomater.* **2018**, *65*, 393–404. [CrossRef]
148. Bhat, R.; García, I.; Aznar, E.; Arnaiz, B.; Martínez-Bisbal, M.C.; Liz-Marzán, L.M.; Penadés, S.; Martínez-Máñez, R. Lectin-gated and glycan functionalized mesoporous silica nanocontainers for targeting cancer cells overexpressing Lewis X antigen. *Nanoscale* **2018**, *10*, 239–249. [CrossRef]
149. Wu, Y.; Xu, Z.; Sun, W.; Yang, Y.; Jin, H.; Qiu, L.; Chen, J.; Chen, J. Co-responsive smart cyclodextrin-gated mesoporous silica nanoparticles with ligand-receptor engagement for anti-cancer treatment. *Mater. Sci. Eng. C* **2019**, *103*, 109831. [CrossRef]
150. Zhao, R.; Li, T.; Zheng, G.; Jiang, K.; Fan, L.; Shao, J. Simultaneous inhibition of growth and metastasis of hepatocellular carcinoma by co-delivery of ursolic acid and sorafenib using lactobionic acid modified and pH-sensitive chitosan-conjugated mesoporous silica nanocomplex. *Biomaterials* **2017**, *143*, 1–16. [CrossRef]
151. Wang, Z.; Wu, P.; He, Z.; He, H.; Rong, W.; Li, J.; Zhou, D.; Huang, Y. Mesoporous silica nanoparticles with lactose-mediated targeting effect to deliver platinum(iv) prodrug for liver cancer therapy. *J. Mater. Chem. B* **2017**, *5*, 7591–7597. [CrossRef] [PubMed]
152. Luo, Z.; Cai, K.; Hu, Y.; Zhao, L.; Liu, P.; Duan, L.; Yang, W. Mesoporous silica nanoparticles end-capped with collagen: Redox-responsive nanoreservoirs for targeted drug delivery. *Angew. Chem. Int. Ed.* **2011**, *50*, 640–643. [CrossRef] [PubMed]
153. Huang, L.; Zhang, Q.; Dai, L.; Shen, X.; Chen, W.; Cai, K. Phenylboronic acid-modified hollow silica nanoparticles for dual-responsive delivery of doxorubicin for targeted tumor therapy. *Regen. Biomater.* **2017**, *4*, 111–124. [CrossRef] [PubMed]
154. Sodagar Taleghani, A.; Ebrahimnejad, P.; Heidarinasab, A.; Akbarzadeh, A. Sugar-conjugated dendritic mesoporous silica nanoparticles as pH-responsive nanocarriers for tumor targeting and controlled release of deferasirox. *Mater. Sci. Eng. C* **2019**, *98*, 358–368. [CrossRef]
155. Niemelä, E.; Desai, D.; Nkizinkiko, Y.; Eriksson, J.E.; Rosenholm, J.M. Sugar-decorated mesoporous silica nanoparticles as delivery vehicles for the poorly soluble drug celastrol enables targeted induction of apoptosis in cancer cells. *Eur. J. Pharm. Biopharm.* **2015**, *96*, 11–21. [CrossRef]
156. Chen, Z.; Li, Z.; Lin, Y.; Yin, M.; Ren, J.; Qu, X. Bioresponsive hyaluronic acid-capped mesoporous silica nanoparticles for targeted drug delivery. *Chem. Eur. J.* **2013**, *19*, 1778–1783. [CrossRef]
157. Yu, M.; Jambhrunkar, S.; Thorn, P.; Chen, J.; Gu, W.; Yu, C. Hyaluronic acid modified mesoporous silica nanoparticles for targeted drug delivery to CD44-overexpressing cancer cells. *Nanoscale* **2013**, *5*, 178–183. [CrossRef]

158. Zhao, Q.; Liu, J.; Zhu, W.; Sun, C.; Di, D.; Zhang, Y.; Wang, P.; Wang, Z.; Wang, S. Dual-stimuli responsive hyaluronic acid-conjugated mesoporous silica for targeted delivery to CD44-overexpressing cancer cells. *Acta Biomater.* **2015**, *23*, 147–156. [CrossRef]
159. Chen, C.; Tang, W.; Jiang, D.; Yang, G.; Wang, X.; Zhou, L.; Zhang, W.; Wang, P. Hyaluronic acid conjugated polydopamine functionalized mesoporous silica nanoparticles for synergistic targeted chemo-photothermal therapy. *Nanoscale* **2019**, *11*, 11012–11024. [CrossRef]
160. Radhakrishnan, K.; Tripathy, J.; Datey, A.; Chakravortty, D.; Raichur, A.M. Mesoporous silica–chondroitin sulphate hybrid nanoparticles for targeted and bio-responsive drug delivery. *New J. Chem.* **2015**, *39*, 1754–1760. [CrossRef]
161. Oommen, O.P.; Duehrkop, C.; Nilsson, B.; Hilborn, J.; Varghese, O.P. Multifunctional hyaluronic acid and chondroitin sulfate nanoparticles: Impact of glycosaminoglycan presentation on receptor mediated cellular uptake and immune activation. *ACS Appl. Mater. Interfaces* **2016**, *8*, 20614–20624. [CrossRef] [PubMed]
162. Liu, M.; Du, H.; Khan, A.R.; Ji, J.; Yu, A.; Zhai, G. Redox/enzyme sensitive chondroitin sulfate-based self-assembled nanoparticles loading docetaxel for the inhibition of metastasis and growth of melanoma. *Carbohydr. Polym.* **2018**, *184*, 82–93. [CrossRef] [PubMed]
163. Russell-Jones, G.; Mctavish, K.; Mcewan, J.; Rice, J.; Nowotnik, D. Vitamin-mediated targeting as a potential mechanism to increase drug uptake by tumours. *J. Inorg. Biochem.* **2004**, *98*, 1625–1633. [CrossRef] [PubMed]
164. Liong, M.; Zink, J.I.; Lu, J.; Tamanoi, F.; Kovochich, M.; Xia, T.; Nel, A.E.; Ruehm, S.G. Multifunctional inorganic nanoparticles for imaging, targeting, and drug delivery. *ACS Nano* **2008**, *2*, 889–896. [CrossRef]
165. Sun, X.; Wang, N.; Yang, L.-Y.; Ouyang, X.-K.; Huang, F. Folic acid and PEI modified mesoporous silica for targeted delivery of curcumin. *Pharmaceutics* **2019**, *11*, 430. [CrossRef]
166. Cabañas, M.V.; Lozano, D.; Torres-Pardo, A.; Sobrino, C.; González-Calbet, J.; Arcos, D.; Vallet-Regí, M. Features of aminopropyl modified mesoporous silica nanoparticles. Implications on the active targeting capability. *Mater. Chem. Phys.* **2018**, *220*, 260–269. [CrossRef]
167. Datz, S.; Argyo, C.; Gattner, M.; Weiss, V.; Brunner, K.; Bretzler, J.; von Schirnding, C.; Torrano, A.A.; Spada, F.; Vrabel, M.; et al. Genetically designed biomolecular capping system for mesoporous silica nanoparticles enables receptor-mediated cell uptake and controlled drug release. *Nanoscale* **2016**, *8*, 8101–8110. [CrossRef]
168. Martínez-Carmona, M.; Lozano, D.; Colilla, M.; Vallet-Regí, M. Selective topotecan delivery to cancer cells by targeted pH-sensitive mesoporous silica nanoparticles. *RSC Adv.* **2016**, *6*, 50923–50932. [CrossRef]
169. Cheng, W.; Nie, J.; Xu, L.; Liang, C.; Peng, Y.; Liu, G.; Wang, T.; Mei, L.; Huang, L.; Zeng, X. pH-sensitive delivery vehicle based on folic acid-conjugated polydopamine-modified mesoporous silica nanoparticles for targeted cancer therapy. *ACS Appl. Mater. Interfaces* **2017**, *9*, 18462–18473. [CrossRef]
170. Qu, W.; Meng, B.; Yu, Y.; Wang, S. Folic acid-conjugated mesoporous silica nanoparticles for enhanced therapeutic efficacy of topotecan in retina cancers. *Int. J. Nanomedicine* **2018**, *13*, 4379–4389. [CrossRef]
171. Li, Y.; Wang, S.; Song, F.X.; Zhang, L.; Yang, W.; Wang, H.X.; Chen, Q.L. A pH-sensitive drug delivery system based on folic acid-targeted HBP-modified mesoporous silica nanoparticles for cancer therapy. *Colloids Surf., A.* **2020**, *590*, 124470. [CrossRef]
172. Song, Y.; Zhou, B.; Du, X.; Wang, Y.; Zhang, J.; Ai, Y.; Xia, Z.; Zhao, G. Folic acid (FA)-conjugated mesoporous silica nanoparticles combined with MRP-1 siRNA improves the suppressive effects of myricetin on non-small cell lung cancer (NSCLC). *Biomed. Pharmacother.* **2020**, *125*, 109561. [CrossRef] [PubMed]
173. Lv, G.; Qiu, L.; Liu, G.; Wang, W.; Li, K.; Zhao, X.; Lin, J. pH sensitive chitosan-mesoporous silica nanoparticles for targeted delivery of a ruthenium complex with enhanced anticancer effects. *Dalt. Trans.* **2016**, *45*, 18147–18155. [CrossRef] [PubMed]
174. Li, Z.; Zhang, Y.; Zhang, K.; Wu, Z.; Feng, N. Biotinylated-lipid bilayer coated mesoporous silica nanoparticles for improving the bioavailability and anti-leukaemia activity of Tanshinone IIA. *Artif. Cells Nanomed. Biotechnol.* **2018**, *46*, 578–587. [CrossRef] [PubMed]
175. Lv, G.; Li, K.; Qiu, L.; Peng, Y.; Zhao, X.; Li, X.; Liu, Q.; Wang, S.; Lin, J. Enhanced tumor diagnostic and therapeutic effect of mesoporous silica nanoparticle-mediated pre-targeted strategy. *Pharm. Res.* **2018**, *35*, 63. [CrossRef] [PubMed]
176. Thepphankulngarm, N.; Wonganan, P.; Sapcharoenkun, C.; Tuntulani, T.; Leeladee, P. Combining vitamin B12 and cisplatin-loaded porous silica nanoparticles via coordination: A facile approach to prepare a targeted drug delivery system. *New J. Chem.* **2017**, *41*, 13823–13829. [CrossRef]
177. Xiong, Y.; Li, M.; Lu, Q.; Qing, G.; Sun, T. Sialic acid-targeted biointerface materials and bio-applications. *Polymers* **2017**, *9*, 249. [CrossRef]

178. Liu, J.; Zhang, B.; Luo, Z.; Ding, X.; Li, J.; Dai, L.; Zhou, J.; Zhao, X.; Ye, J.; Cai, K. Enzyme responsive mesoporous silica nanoparticles for targeted tumor therapy in vitro and in vivo. *Nanoscale* **2015**, *7*, 3614–3626. [CrossRef]
179. Liu, L.; Zhang, Y.; Zhang, L.; Yan, G.; Yao, J.; Yang, P.; Lu, H. Highly specific revelation of rat serum glycopeptidome by boronic acid-functionalized mesoporous silica. *Anal. Chim. Acta* **2012**, *753*, 64–72. [CrossRef]
180. Villaverde, G.; Baeza, A.; Melen, G.J.; Alfranca, A.; Ramírez, M.; Vallet-Regí, M. A new targeting agent for the selective drug delivery of nanocarriers for treating neuroblastoma. *J. Mater. Chem. B* **2015**, *3*, 4831–4842. [CrossRef] [PubMed]
181. Xu, H.; Wang, Z.; Li, Y.; Guo, Y.; Zhou, H.; Li, Y.; Wu, F.; Zhang, L.; Yang, X.; Lu, B.; et al. Preparation and characterization of a dual-receptor mesoporous silica nanoparticle–hyaluronic acid–RGD peptide targeting drug delivery system. *RSC Adv.* **2016**, *6*, 40427–40435. [CrossRef]
182. Zhou, H.; Xu, H.; Li, X.; Lv, Y.; Ma, T.; Guo, S.; Huang, Z.; Wang, X.; Xu, P. Dual targeting hyaluronic acid—RGD mesoporous silica coated gold nanorods for chemo-photothermal cancer therapy. *Mater. Sci. Eng. C* **2017**, *81*, 261–270. [CrossRef] [PubMed]
183. Daglioglu, C. Environmentally Responsive Dual-Targeting Nanoparticles: Improving Drug Accumulation in Cancer Cells as a Way of Preventing Anticancer Drug Efflux. *J. Pharm. Sci.* **2018**, *107*, 934–941. [CrossRef] [PubMed]
184. Li, Y.; Duo, Y.; Zhai, P.; He, L.; Zhong, K.; Zhang, Y.; Huang, K.; Luo, J.; Zhang, H.; Yu, X. Dual targeting delivery of miR-328 by functionalized mesoporous silica nanoparticles for colorectal cancer therapy. *Nanomedicine* **2018**, *13*, 14. [CrossRef] [PubMed]
185. Villaverde, G.; Alfranca, A.; Gonzalez-Murillo, Á.; Melen, G.J.; Castillo, R.R.; Ramírez, M.; Baeza, A.; Vallet-Regí, M. Molecular scaffolds as double-targeting agents for the diagnosis and treatment of neuroblastoma. *Angew. Chem. Int. Ed.* **2019**, *58*, 3067–3072. [CrossRef]
186. Pan, L.; Liu, J.; He, Q.; Shi, J. MSN-mediated sequential vascular-to-cell nuclear-targeted drug delivery for efficient tumor regression. *Adv. Mater.* **2014**, *26*, 6742–6748. [CrossRef]
187. Xiong, L.; Du, X.; Kleitz, F.; Qiao, S.Z. Cancer-cell-specific nuclear-targeted drug delivery by dual-ligand-modified mesoporous silica nanoparticles. *Small* **2015**, *11*, 5919–5926. [CrossRef]
188. Naz, S.; Wang, M.; Han, Y.; Hu, B.; Teng, L.; Zhou, J.; Zhang, H.; Chen, J. Enzyme-responsive mesoporous silica nanoparticles for tumor cells and mitochondria multistage-targeted drug delivery. *Int. J. Nanomed.* **2019**, *14*, 2533–2542. [CrossRef]
189. Liu, Y.; Dai, R.; Wei, Q.; Li, W.; Zhu, G.; Chi, H.; Guo, Z.; Wang, L.; Cui, C.; Xu, J.; et al. Dual-functionalized janus mesoporous silica nanoparticles with active targeting and charge reversal for synergistic tumor-targeting therapy. *ACS Appl. Mater. Interfaces* **2019**, *11*, 44582–44592. [CrossRef]
190. López, V.; Villegas, M.R.; Rodríguez, V.; Villaverde, G.; Lozano, D.; Baeza, A.; Vallet-Regí, M. Janus mesoporous silica nanoparticles for dual targeting of tumor cells and mitochondria. *ACS Appl. Mater. Interfaces* **2017**, *9*, 26697–26706. [CrossRef]
191. Fang, Y.; Xue, J.; Gao, S.; Lu, A.; Yang, D.; Jiang, H.; He, Y.; Shi, K. Cleavable PEGylation: A strategy for overcoming the "PEG dilemma" in efficient drug delivery. *Drug Deliv.* **2017**, *24*, 22–32. [CrossRef] [PubMed]
192. Qu, X.; Yang, Z. Benzoic-Imine-Based Physiological-pH-Responsive Materials for Biomedical Applications. *Chem. Asian J.* **2016**, *11*, 2633–2641. [CrossRef] [PubMed]
193. Liu, J.; Luo, Z.; Zhang, J.; Luo, T.; Zhou, J.; Zhao, X.; Cai, K. Hollow mesoporous silica nanoparticles facilitated drug delivery via cascade pH stimuli in tumor microenvironment for tumor therapy. *Biomaterials* **2016**, *83*, 51–65. [CrossRef] [PubMed]
194. Chen, H.; Kuang, Y.; Liu, R.; Chen, Z.; Jiang, B.; Sun, Z.; Chen, X.; Li, C. Dual-pH-sensitive mesoporous silica nanoparticle-based drug delivery system for tumor-triggered intracellular drug release. *J. Mater. Sci.* **2018**, *53*, 10653–10665. [CrossRef]
195. Gao, Y.; Yang, C.; Liu, X.; Ma, R.; Kong, D.; Shi, L. A Multifunctional nanocarrier based on nanogated mesoporous silica for enhanced tumor-specific uptake and intracellular delivery. *Macromol. Biosci.* **2012**, *12*, 251–259. [CrossRef]
196. Xiao, D.; Jia, H.Z.; Zhang, J.; Liu, C.W.; Zhuo, R.X.; Zhang, X.Z. A dual-responsive mesoporous silica nanoparticle for tumor-triggered targeting drug delivery. *Small* **2014**, *10*, 591–598. [CrossRef]

197. Paris, J.L.; Manzano, M.; Cabañas, M.V.; Vallet-Regí, M. Mesoporous silica nanoparticles engineered for ultrasound-induced uptake by cancer cells. *Nanoscale* **2018**, *10*, 6402–6408. [CrossRef]
198. Zhang, Y.; Xu, J. Mesoporous silica nanoparticle-based intelligent drug delivery system for bienzyme-responsive tumour targeting and controlled release. *R. Soc. open Sci.* **2018**, *5*, 170986. [CrossRef]
199. Zou, Z.; He, X.; He, D.; Wang, K.; Qing, Z.; Yang, X.; Wen, L.; Xiong, J.; Li, L.; Cai, L. Programmed packaging of mesoporous silica nanocarriers for matrix metalloprotease 2-triggered tumor targeting and release. *Biomaterials* **2015**, *58*, 35–45. [CrossRef]
200. Lei, Q.; Qiu, W.-X.; Hu, J.-J.; Cao, P.-X.; Zhu, C.-H.; Cheng, H.; Zhang, X.-Z. Multifunctional mesoporous silica nanoparticles with thermal-responsive gatekeeper for nir light-triggered chemo/photothermal-therapy. *Small* **2016**, *12*, 4286–4298. [CrossRef] [PubMed]
201. Yuan, Z.-F.; Chen, W.-H.; Zhang, X.-Z.; Zhuo, R.-X.; Zhang, J.; Wang, Y.; Cheng, S.-X.; Luo, G.-F. Multifunctional envelope-type mesoporous silica nanoparticles for tumor-triggered targeting drug delivery. *J. Am. Chem. Soc.* **2013**, *135*, 5068–5073.
202. Smith, S.A.; Selby, L.I.; Johnston, A.P.R.; Such, G.K. The endosomal escape of nanoparticles: Toward more efficient cellular delivery. *Bioconjug. Chem.* **2019**, *30*, 263–272. [CrossRef] [PubMed]
203. Gisbert-Garzarán, M.; Manzano, M.; Vallet-Regí, M. pH-responsive mesoporous silica and carbon nanoparticles for drug delivery. *Bioengineering* **2017**, *4*, 3. [CrossRef] [PubMed]
204. Weiss, V.; Argyo, C.; Torrano, A.A.; Strobel, C.; Mackowiak, S.A.; Schmidt, A.; Datz, S.; Gatzenmeier, T.; Hilger, I.; Bräuchle, C.; et al. Dendronized mesoporous silica nanoparticles provide an internal endosomal escape mechanism for successful cytosolic drug release. *Microporous Mesoporous Mater.* **2016**, *227*, 242–251. [CrossRef]
205. Tu, J.; Wang, T.; Shi, W.; Wu, G.; Tian, X.; Wang, Y.; Ge, D.; Ren, L. Multifunctional ZnPc-loaded mesoporous silica nanoparticles for enhancement of photodynamic therapy efficacy by endolysosomal escape. *Biomaterials* **2012**, *33*, 7903–7914. [CrossRef]
206. Rosenholm, J.M.; Peuhu, E.; Eriksson, J.E.; Sahlgren, C.; Lindén, M. Targeted intracellular delivery of hydrophobic agents using mesoporous hybrid silica nanoparticles as carrier systems. *Nano Lett.* **2009**, *9*, 3308–3311. [CrossRef]
207. Benjaminsen, R.V.; Mattebjerg, M.A.; Henriksen, J.R.; Moghimi, S.M.; Andresen, T.L. The possible "proton sponge" effect of polyethylenimine (PEI) does not include change in lysosomal pH. *Mol. Ther.* **2013**, *21*, 149–157. [CrossRef]
208. Shen, J.; Kim, H.-C.; Su, H.; Wang, F.; Wolfram, J.; Kirui, D.; Mai, J.; Mu, C.; Ji, L.-N.; Mao, Z.-W.; et al. Cyclodextrin and polyethylenimine functionalized mesoporous silica nanoparticles for delivery of siRNA cancer therapeutics. *Theranostics* **2014**, *4*, 487–497. [CrossRef]
209. Prabhakar, N.; Zhang, J.; Desai, D.; Casals, E.; Gulin-Sarfraz, T.; Näreoja, T.; Westermarck, J.; Rosenholm, J.M. Stimuli-responsive hybrid nanocarriers developed by controllable integration of hyperbranched PEI with mesoporous silica nanoparticles for sustained intracellular siRNA delivery. *Int. J. Nanomedicine* **2016**, *11*, 6591–6608. [CrossRef]
210. Hom, C.; Lu, J.; Liong, M.; Luo, H.; Li, Z.; Zink, J.I.; Tamanoi, F. Mesoporous silica nanoparticles facilitate delivery of siRNA to shutdown signaling pathways in mammalian cells. *Small* **2010**, *6*, 1185–1190. [CrossRef]
211. Chen, Z.; Zhu, P.; Zhang, Y.; Liu, Y.; He, Y.; Zhang, L.; Gao, Y. Enhanced sensitivity of cancer stem cells to chemotherapy using functionalized mesoporous silica nanoparticles. *Mol. Pharm.* **2016**, *13*, 2749–2759. [CrossRef] [PubMed]
212. Moghimi, S.M.; Symonds, P.; Murray, J.C.; Hunter, A.C.; Debska, G.; Szewczyk, A. A two-stage poly(ethylenimine)-mediated cytotoxicity: Implications for gene transfer/therapy. *Mol. Ther.* **2005**, *11*, 990–995. [CrossRef] [PubMed]
213. Shahbazi, M.-A.; Almeida, P.V.; Mäkilä, E.M.; Kaasalainen, M.H.; Salonen, J.J.; Hirvonen, J.T.; Santos, H.A. Augmented cellular trafficking and endosomal escape of porous silicon nanoparticles via zwitterionic bilayer polymer surface engineering. *Biomaterials* **2014**, *35*, 7488–7500. [CrossRef] [PubMed]
214. Li, S.; Hong, M. Protonation, tautomerization, and rotameric structure of histidine: A comprehensive study by magic-angle-spinning solid-state NMR. *J. Am. Chem. Soc.* **2011**, *133*, 1534–1544. [CrossRef]

215. Bilalis, P.; Tziveleka, L.-A.; Varlas, S.; Iatrou, H. pH-Sensitive nanogates based on poly(L-histidine) for controlled drug release from mesoporous silica nanoparticles. *Polym. Chem.* **2016**, *7*, 1475–1485. [CrossRef]
216. Li, Z.; Zhang, L.; Tang, C.; Yin, C. Co-delivery of doxorubicin and survivin shRNA-expressing plasmid via microenvironment-responsive dendritic mesoporous silica nanoparticles for synergistic cancer therapy. *Pharm. Res.* **2017**, *34*, 2829–2841. [CrossRef]
217. Ashley, C.E.; Carnes, E.C.; Phillips, G.K.; Padilla, D.; Durfee, P.N.; Brown, P.A.; Hanna, T.N.; Liu, J.; Phillips, B.; Carter, M.B.; et al. The targeted delivery of multicomponent cargos to cancer cells by nanoporous particle-supported lipid bilayers. *Nat. Mater.* **2011**, *10*, 389–397. [CrossRef]
218. Ashley, C.E.; Carnes, E.C.; Epler, K.E.; Padilla, D.P.; Phillips, G.K.; Castillo, R.E.; Wilkinson, D.C.; Wilkinson, B.S.; Burgard, C.A.; Kalinich, R.M.; et al. Delivery of small interfering RNA by peptide-targeted mesoporous silica nanoparticle-supported lipid bilayers. *ACS Nano* **2012**, *6*, 2174–2188. [CrossRef]
219. Sun, X.; Luo, Y.; Huang, L.; Yu, B.Y.; Tian, J. A peptide-decorated and curcumin-loaded mesoporous silica nanomedicine for effectively overcoming multidrug resistance in cancer cells. *RSC Adv.* **2017**, *7*, 16401–16409. [CrossRef]
220. Zhang, J.; Wu, D.; Li, M.F.; Feng, J. Multifunctional mesoporous silica nanoparticles based on charge-reversal plug-gate nanovalves and acid-decomposable ZnO quantum dots for intracellular drug delivery. *ACS Appl. Mater. Interfaces* **2015**, *7*, 26666–26673. [CrossRef] [PubMed]
221. Li, Z.-Y.; Liu, Y.; Hu, J.-J.; Xu, Q.; Liu, L.-H.; Jia, H.-Z.; Chen, W.-H.; Lei, Q.; Rong, L.; Zhang, X.-Z. Stepwise-acid-active multifunctional mesoporous silica nanoparticles for tumor-specific nucleus-targeted drug delivery. *ACS Appl. Mater. Interfaces* **2014**, *6*, 14568–14575. [CrossRef] [PubMed]
222. Lee, J.; Han, S.; Lee, J.; Choi, M.; Kim, C. Stimuli-responsive α-helical peptide gatekeepers for mesoporous silica nanocarriers. *New J. Chem.* **2017**, *41*, 6969–6972. [CrossRef]
223. Qu, Q.; Ma, X.; Zhao, Y. Anticancer effect of α-tocopheryl succinate delivered by mitochondria-targeted mesoporous silica nanoparticles. *ACS Appl. Mater. Interfaces* **2016**, *8*, 34261–34269. [CrossRef] [PubMed]
224. Qu, Q.; Ma, X.; Zhao, Y. Targeted delivery of doxorubicin to mitochondria using mesoporous silica nanoparticle nanocarriers. *Nanoscale* **2015**, *7*, 16677–16686. [CrossRef] [PubMed]
225. Yadav, D.K.; Kumar, S.; Choi, E.-H.; Chaudhary, S.; Kim, M.-H. Molecular dynamic simulations of oxidized skin lipid bilayer and permeability of reactive oxygen species. *Sci. Rep.* **2019**, *9*, 4496. [CrossRef] [PubMed]
226. Dobay, M.P.; Schmidt, A.; Mendoza, E.; Bein, T.; Rädler, J.O. Cell type determines the light-induced endosomal escape kinetics of multifunctional mesoporous silica nanoparticles. *Nano Lett.* **2013**, *13*, 1047–1052. [CrossRef]
227. Schloßbauer, A.; Sauer, A.M.; Cauda, V.; Schmidt, A.; Engelke, H.; Rothbauer, U.; Zolghadr, K.; Leonhardt, H.; Bräuchle, C.; Bein, T. Cascaded photoinduced drug delivery to cells from multifunctional core–shell mesoporous silica. *Adv. Healthc. Mater.* **2012**, *1*, 316–320. [CrossRef]
228. Martínez-Carmona, M.; Lozano, D.; Baeza, A.; Colilla, M.; Vallet-Regí, M. A novel visible light responsive nanosystem for cancer treatment. *Nanoscale* **2017**, *9*, 15967–15973. [CrossRef]
229. Mackowiak, S.A.; Schmidt, A.; Weiss, V.; Argyo, C.; von Schirnding, C.; Bein, T.; Bräuchle, C. Targeted drug delivery in cancer cells with red-light photoactivated mesoporous silica nanoparticles. *Nano Lett.* **2013**, *13*, 2576–2583. [CrossRef]
230. Niedermayer, S.; Weiss, V.; Herrmann, A.; Schmidt, A.; Datz, S.; Müller, K.; Wagner, E.; Bein, T.; Bräuchle, C. Multifunctional polymer-capped mesoporous silica nanoparticles for pH-responsive targeted drug delivery. *Nanoscale* **2015**, *7*, 7953–7964. [CrossRef]
231. Hai, L.; Jia, X.; He, D.; Zhang, A.; Wang, T.; Cheng, H.; He, X.; Wang, K. DNA-functionalized hollow mesoporous silica nanoparticles with dual cargo loading for near-infrared-responsive synergistic chemo-photothermal treatment of cancer cells. *ACS Appl. Nano Mater.* **2018**, *1*, 3486–3497. [CrossRef]
232. Horcajada, P.; Rámila, A.; Férey, G.; Vallet-Regí, M. Influence of superficial organic modification of MCM-41 matrices on drug delivery rate. *Solid State Sci.* **2006**, *8*, 1243–1249. [CrossRef]
233. Balas, F.; Manzano, M.; Horcajada, P.; Vallet-Regí, M. Confinement and controlled release of bisphosphonates on ordered mesoporous silica-based materials. *J. Am. Chem. Soc.* **2006**, *128*, 8116–8117. [CrossRef] [PubMed]
234. Nieto, A.; Balas, F.; Manzano, M.; Vallet-Regí, M. Functionalization degree of SBA-15 as key factor to modulate sodium alendronate dosage. *Microporous Mesoporous Mater.* **2008**, *116*, 4–13. [CrossRef]
235. Doadrio, J.C.; Sousa, E.M.B.; Izquierdo-Barba, I.; Doadrio, A.L.; Perez-Pariente, J.; Vallet-Regí, M. Functionalization of mesoporous materials with long alkyl chains as a strategy for controlling drug delivery pattern. *J. Mater. Chem.* **2006**, *16*, 462–466. [CrossRef]

236. López-Noriega, A.; Arcos, D.; Vallet-Regí, M. Functionalizing mesoporous bioglasses for long-term anti-osteoporotic drug delivery. *Chem. A Eur. J.* **2010**, *16*, 10879–10886. [CrossRef]
237. Varache, M.; Bezverkhyy, I.; Weber, G.; Saviot, L.; Chassagnon, R.; Baras, F.; Bouyer, F. Loading of cisplatin into mesoporous silica nanoparticles: Effect of surface functionalization. *Langmuir* **2019**, *35*, 8984–8995. [CrossRef]
238. Wani, A.; Muthuswamy, E.; Savithra, G.H.L.; Mao, G.; Brock, S.; Oupický, D. Surface functionalization of mesoporous silica nanoparticles controls loading and release behavior of mitoxantrone. *Pharm. Res.* **2012**, *29*, 2407–2418. [CrossRef]
239. Chang, B.; Guo, J.; Liu, C.; Qian, J.; Yang, W. Surface functionalization of magnetic mesoporous silica nanoparticles for controlled drug release. *J. Mater. Chem.* **2010**, *20*, 9941–9947. [CrossRef]
240. She, X.; Chen, L.; Li, C.; He, C.; He, L.; Kong, L. Functionalization of hollow mesoporous silica nanoparticles for improved 5-FU loading. *J. Nanomater.* **2015**, *2015*, 872035. [CrossRef]
241. Bahrami, Z.; Badiei, A.; Atyabi, F.; Darabi, H.R.; Mehravi, B. Piperazine and its carboxylic acid derivatives-functionalized mesoporous silica as nanocarriers for gemcitabine: Adsorption and release study. *Mater. Sci. Eng. C* **2015**, *49*, 66–74. [CrossRef]
242. Aggad, D.; Jimenez, C.M.; Dib, S.; Croissant, J.G.; Lichon, L.; Laurencin, D.; Richeter, S.; Maynadier, M.; Alsaiari, S.K.; Boufatit, M.; et al. Gemcitabine delivery and photodynamic therapy in cancer cells via porphyrin-ethylene-based periodic mesoporous organosilica nanoparticles. *ChemNanoMat* **2018**, *4*, 46–51. [CrossRef]
243. Croissant, J.; Cattoën, X.; Man, M.W.C.; Gallud, A.; Raehm, L.; Trens, P.; Maynadier, M.; Durand, J.-O. Biodegradable ethylene-bis(propyl)disulfide-based periodic mesoporous organosilica nanorods and nanospheres for efficient in-vitro drug delivery. *Adv. Mater.* **2014**, *26*, 6174–6180. [CrossRef]
244. Croissant, J.G.; Fatieiev, Y.; Julfakyan, K.; Lu, J.; Emwas, A.-H.; Anjum, D.H.; Omar, H.; Tamanoi, F.; Zink, J.I.; Khashab, N.M. Biodegradable oxamide-phenylene-based mesoporous organosilica nanoparticles with unprecedented drug payloads for delivery in cells. *Chem. Eur. J.* **2016**, *22*, 14806–14811. [CrossRef] [PubMed]
245. Vander Heiden, M.G.; Cantley, L.C.; Thompson, C.B. Understanding the Warburg effect: The metabolic requirements of cell proliferation. *Science* **2009**, *324*, 1029–1033. [CrossRef]
246. Kato, Y.; Ozawa, S.; Miyamoto, C.; Maehata, Y.; Suzuki, A.; Maeda, T.; Baba, Y. Acidic extracellular microenvironment and cancer. *Cancer Cell Int.* **2013**, *13*, 89. [CrossRef] [PubMed]
247. Casey, J.R.; Grinstein, S.; Orlowski, J. Sensors and regulators of intracellular pH. *Nat. Rev. Mol. Cell Biol.* **2010**, *11*, 50–61. [CrossRef] [PubMed]
248. Cui, L.; Lin, H.; Yang, C.; Han, X.; Zhang, T.; Qu, F. Synthesis of multifunctional Fe_3O_4@mSiO_2@Au core-shell nanocomposites for pH-responsive drug delivery. *Eur. J. Inorg. Chem.* **2014**, *2014*, 6156–6164. [CrossRef]
249. Chen, S.; Yang, Y.; Li, H.; Zhou, X.; Liu, M. pH-Triggered Au-fluorescent mesoporous silica nanoparticles for 19F MR/fluorescent multimodal cancer cellular imaging. *Chem. Commun.* **2014**, *50*, 283–285. [CrossRef]
250. Dai, L.; Zhang, Q.; Shen, X.; Sun, Q.; Mu, C.; Gu, H.; Cai, K. pH-responsive nanocontainer based on hydrazone-bearing hollow silica nanoparticles for targeting tumor therapy. *J. Mater. Chem. B* **2016**, *4*, 4594–4604. [CrossRef]
251. Yuan, X.; Peng, S.; Lin, W.; Wang, J.; Zhang, L. Multistage pH-responsive mesoporous silica nanohybrids with charge reversal and intracellular release for efficient anticancer drug delivery. *J. Colloid Interface Sci.* **2019**, *555*, 82–93. [CrossRef] [PubMed]
252. Liu, R.; Zhang, Y.; Zhao, X.; Agarwal, A.; Mueller, L.J.; Feng, P. pH-responsive nanogated ensemble based on gold-capped mesoporous silica through an acid-labile acetal linker. *J. Am. Chem. Soc.* **2010**, *132*, 1500–1501. [CrossRef] [PubMed]
253. Chen, Y.; Ai, K.; Liu, J.; Sun, G.; Yin, Q.; Lu, L. Multifunctional envelope-type mesoporous silica nanoparticles for pH-responsive drug delivery and magnetic resonance imaging. *Biomaterials* **2015**, *60*, 111–120. [CrossRef] [PubMed]
254. Chen, T.; Yu, H.; Yang, N.; Wang, M.; Ding, C.; Fu, J. Graphene quantum dot-capped mesoporous silica nanoparticles through an acid-cleavable acetal bond for intracellular drug delivery and imaging. *J. Mater. Chem. B* **2014**, *2*, 4979–4982. [CrossRef] [PubMed]

255. Chen, M.; He, X.; Wang, K.; He, D.; Yang, S.; Qiu, P.; Chen, S. A pH-responsive polymer/mesoporous silica nano-container linked through an acid cleavable linker for intracellular controlled release and tumor therapy in vivo. *J. Mater. Chem. B* **2014**, *2*, 428–436. [CrossRef]
256. Yang, K.; Luo, H.; Zeng, M.; Jiang, Y.; Li, J.; Fu, X. Intracellular pH-triggered, targeted drug delivery to cancer cells by multifunctional envelope-type mesoporous silica nanocontainers. *ACS Appl. Mater. Interfaces* **2015**, *7*, 17399–17447. [CrossRef]
257. Bull, S.D.; Davidson, M.G.; Van Den Elsen, J.M.H.; Fossey, J.S.; Jenkins, A.T.A.; Jiang, Y.B.; Kubo, Y.; Marken, F.; Sakurai, K.; Zhao, J.; et al. Exploiting the reversible covalent bonding of boronic acids: Recognition, sensing, and assembly. *Acc. Chem. Res.* **2013**, *46*, 312–326. [CrossRef]
258. Aznar, E.; Marcos, M.D.; Martínez-Máñez, R.; Sancenón, F.; Soto, J.; Amorós, P.; Guillem, C. pH- and photo-switched release of guest molecules from mesoporous silica supports. *J. Am. Chem. Soc.* **2009**, *131*, 6833–6843. [CrossRef]
259. Gan, Q.; Lu, X.; Yuan, Y.; Qian, J.; Zhou, H.; Lu, X.; Shi, J.; Liu, C. A magnetic, reversible pH-responsive nanogated ensemble based on Fe_3O_4 nanoparticles-capped mesoporous silica. *Biomaterials* **2011**, *32*, 1932–1942. [CrossRef]
260. Salinas, Y.; Hoerhager, C.; García-Fernández, A.; Resmini, M.; Sancenón, F.; Matínez-Máñez, R.; Brueggemann, O. Biocompatible phenylboronic-acid-capped ZnS nanocrystals designed As caps in mesoporous silica hybrid materials for on-demand pH-triggered release in cancer cells. *ACS Appl. Mater. Interfaces* **2018**, *10*, 34029–34038. [CrossRef]
261. Luo, Z.; Cai, K.; Hu, Y.; Zhang, B.; Xu, D. Cell-specific intracellular anticancer drug delivery from mesoporous silica nanoparticles with pH sensitivity. *Adv. Healthc. Mater.* **2012**, *1*, 321–325. [CrossRef] [PubMed]
262. Wang, J.; Liu, H.; Leng, F.; Zheng, L.; Yang, J.; Wang, W.; Huang, C.Z. Autofluorescent and pH-responsive mesoporous silica for cancer-targeted and controlled drug release. *Microporous Mesoporous Mater.* **2014**, *186*, 187–193. [CrossRef]
263. Chen, H.; Zheng, D.; Liu, J.; Kuang, Y.; Li, Q.; Zhang, M.; Ye, H.; Qin, H.; Xu, Y.; Li, C.; et al. pH-Sensitive drug delivery system based on modified dextrin coated mesoporous silica nanoparticles. *Int. J. Biol. Macromol.* **2016**, *85*, 596–603. [CrossRef] [PubMed]
264. Wang, T.T.; Lan, J.; Zhang, Y.; Wu, Z.L.; Li, C.M.; Wang, J.; Huang, C.Z. Reduced graphene oxide gated mesoporous silica nanoparticles as a versatile chemo-photothermal therapy system through pH controllable release. *J. Mater. Chem. B* **2015**, *3*, 6377–6384. [CrossRef]
265. Muhammad, F.; Guo, M.; Qi, W.; Sun, F.; Wang, A.; Guo, Y.; Zhu, G. pH-triggered controlled drug release from mesoporous silica nanoparticles via intracellular dissolution of ZnO nanolids. *J. Am. Chem. Soc.* **2011**, *133*, 8778–8781. [CrossRef]
266. Wu, S.; Huang, X.; Du, X. pH- and redox-triggered synergistic controlled release of a ZnO-gated hollow mesoporous silica drug delivery system. *J. Mater. Chem. B* **2015**, *3*, 1426–1432. [CrossRef]
267. Muhammad, F.; Wang, A.; Guo, M.; Zhao, J.; Qi, W.; Yingjie, G.; Gu, J.; Zhu, G. PH dictates the release of hydrophobic drug cocktail from mesoporous nanoarchitecture. *ACS Appl. Mater. Interfaces* **2013**, *5*, 11828–11835. [CrossRef]
268. Li, Z.; Li, H.; Liu, L.; You, X.; Zhang, C.; Wang, Y. A pH-sensitive nanocarrier for co-delivery of doxorubicin and camptothecin to enhance chemotherapeutic efficacy and overcome multidrug resistance in vitro. *RSC Adv.* **2015**, *5*, 77097–77105. [CrossRef]
269. Chen, Y.; Yin, Q.; Ji, X.; Zhang, S.; Chen, H.; Zheng, Y.; Sun, Y.; Qu, H.; Wang, Z.; Li, Y.; et al. Manganese oxide-based multifunctionalized mesoporous silica nanoparticles for pH-responsive MRI, ultrasonography and circumvention of MDR in cancer cells. *Biomaterials* **2012**, *33*, 7126–7137. [CrossRef]
270. Zhang, S.; Qian, X.; Zhang, L.; Peng, W.; Chen, Y. Composition-property relationships in multifunctional hollow mesoporous carbon nanosystems for PH-responsive magnetic resonance imaging and on-demand drug release. *Nanoscale* **2015**, *7*, 7632–7643. [CrossRef]
271. Jin, L.; Huang, Q.-J.; Zeng, H.-Y.; Du, J.-Z.; Xu, S.; Chen, C.-R. Hydrotalcite-gated hollow mesoporous silica delivery system for controlled drug release. *Microporous Mesoporous Mater.* **2019**, *274*, 304–312. [CrossRef]
272. Shao, M.; Chang, C.; Liu, Z.; Chen, K.; Zhou, Y.; Zheng, G.; Huang, Z.; Xu, H.; Xu, P.; Lu, B. Polydopamine coated hollow mesoporous silica nanoparticles as pH-sensitive nanocarriers for overcoming multidrug resistance. *Colloids Surfaces B Biointerfaces* **2019**, *183*, 110427. [CrossRef] [PubMed]

273. Gisbert-Garzarán, M.; Manzano, M.; Vallet-Regí, M. Self-immolative chemistry in nanomedicine. *Chem. Eng. J.* **2017**, *340*, 24–31. [CrossRef]
274. Juárez, L.A.; Añón, E.; Giménez, C.; Sancenón, F.; Martínez-Máñez, R.; Costero, A.M.; Gaviña, P.; Parra, M.; Bernardos, A. Self-immolative linkers as caps for the design of gated silica mesoporous supports. *Chem. Eur. J.* **2016**, *22*, 14126–14130. [CrossRef] [PubMed]
275. Gisbert-Garzarán, M.; Lozano, D.; Vallet-Regí, M.; Manzano, M. Self-Immolative Polymers as novel pH-responsive gate keepers for drug delivery. *RSC Adv.* **2017**, *7*, 132–136. [CrossRef]
276. Gisbert-Garzarán, M.; Berkmann, J.C.; Giasafaki, D.; Lozano, D.; Spyrou, K.; Manzano, M.; Steriotis, T.; Duda, G.N.; Schmidt-Bleek, K.; Charalambopoulou, G.; et al. Engineered pH-responsive mesoporous carbon nanoparticles for drug delivery. *ACS Appl. Mater. Interfaces* **2020**, *12*, 14946–14957. [CrossRef]
277. Birault, A.; Giret, S.; Théron, C.; Gallud, A.; Da Silva, A.; Durand, D.; Nguyen, C.; Bettache, N.; Gary-Bobo, M.; Bartlett, J.R.; et al. Sequential delivery of synergistic drugs by silica nanocarriers for enhanced tumour treatment. *J. Mater. Chem. B* **2020**, *8*, 1472–1480. [CrossRef]
278. Meng, H.; Xue, M.; Xia, T.; Zhao, Y.L.; Tamanoi, F.; Stoddart, J.F.; Zink, J.I.; Nel, A.E. Autonomous in vitro anticancer drug release from mesoporous silica nanoparticles by pH-sensitive nanovalves. *J. Am. Chem. Soc.* **2010**, *132*, 12690–12697. [CrossRef]
279. Li, Z.; Clemens, D.L.; Lee, B.Y.; Dillon, B.J.; Horwitz, M.A.; Zink, J.I. Mesoporous silica nanoparticles with pH-sensitive nanovalves for delivery of moxifloxacin provide improved treatment of lethal pneumonic tularemia. *ACS Nano* **2015**, *9*, 10778–10789. [CrossRef]
280. Pourjavadi, A.; Tehrani, Z.M. Poly(N-isopropylacrylamide)-coated β-cyclodextrin–capped magnetic mesoporous silica nanoparticles exhibiting thermal and pH dual response for triggered anticancer drug delivery. *Int. J. Polym. Mater. Polym. Biomater.* **2017**, *66*, 336–348. [CrossRef]
281. Théron, C.; Gallud, A.; Carcel, C.; Gary-Bobo, M.; Maynadier, M.; García, M.; Lu, J.; Tamanoi, F.; Zink, J.I.; Wong Chi Man, M. Hybrid mesoporous silica nanoparticles with pH-operated and complementary H-bonding caps as an autonomous drug-delivery system. *Chem. Eur. J.* **2014**, *20*, 9372–9380. [CrossRef] [PubMed]
282. Sun, J.T.; Hong, C.Y.; Pan, C.Y. Fabrication of PDEAEMA-coated mesoporous silica nanoparticles and pH-responsive controlled release. *J. Phys. Chem. C* **2010**, *114*, 12481–12486. [CrossRef]
283. Yu, F.; Tang, X.; Pei, M. Facile synthesis of PDMAEMA-coated hollow mesoporous silica nanoparticles and their pH-responsive controlled release. *Microporous Mesoporous Mater.* **2013**, *173*, 64–69. [CrossRef]
284. Gao, Q.; Xu, Y.; Wu, D.; Shen, W.; Deng, F. Synthesis, characterization, and in vitro pH-controllable drug release from mesoporous silica spheres with switchable gates. *Langmuir* **2010**, *26*, 17133–17138. [CrossRef] [PubMed]
285. Xu, X.; Lü, S.; Gao, C.; Wang, X.; Bai, X.; Gao, N.; Liu, M. Facile preparation of pH-sensitive and self-fluorescent mesoporous silica nanoparticles modified with PAMAM dendrimers for label-free imaging and drug delivery. *Chem. Eng. J.* **2015**, *266*, 171–178. [CrossRef]
286. Pourjavadi, A.; Tehrani, Z.M.; Moghanaki, A.A. Folate-Conjugated pH-Responsive Nanocarrier Designed for Active Tumor Targeting and Controlled Release of Gemcitabine. *Pharm. Res.* **2015**, 417–432. [CrossRef]
287. Liu, R.; Liao, P.; Liu, J.; Feng, P. Responsive polymer-coated mesoporous silica as a pH-sensitive nanocarrier for controlled release. *Langmuir* **2011**, *27*, 3095–3099. [CrossRef]
288. Rafi, A.A.; Mahkam, M.; Davaran, S.; Hamishehkar, H. A Smart pH-responsive Nano-Carrier as a Drug Delivery System: A hybrid system comprised of mesoporous nanosilica MCM-41 (as a nano-container) & a pH-sensitive polymer (as smart reversible gatekeepers): Preparation, characterization and in vitro release. *Eur. J. Pharm. Sci.* **2016**, *93*, 64–73.
289. Peng, H.; Dong, R.; Wang, S.; Zhang, Z.; Luo, M.; Bai, C.; Zhao, Q.; Li, J.; Chen, L.; Xiong, H. A pH-responsive nano-carrier with mesoporous silica nanoparticles cores and poly(acrylic acid) shell-layers: Fabrication, characterization and properties for controlled release of salidroside. *Int. J. Pharm.* **2013**, *446*, 153–159. [CrossRef]
290. Samart, C.; Prawingwong, P.; Amnuaypanich, S.; Zhang, H.; Kajiyoshi, K.; Reubroycharoen, P. Preparation of poly(Acrylic Acid) grafted-mesoporous silica as pH responsive releasing material. *J. Ind. Eng. Chem.* **2014**, *20*, 2153–2158. [CrossRef]
291. Hong, C.-Y.; Li, X.; Pan, C.-Y. Fabrication of smart nanocontainers with a mesoporous core and a pH-responsive shell for controlled uptake and release. *J. Mater. Chem.* **2009**, *19*, 5155–5160. [CrossRef]

292. Choi, J.Y.; Gupta, B.; Ramasamy, T.; Jeong, J.-H.; Jin, S.G.; Choi, H.-G.; Yong, C.S.; Kim, J.O. PEGylated polyaminoacid-capped mesoporous silica nanoparticles for mitochondria-targeted delivery of celastrol in solid tumors. *Colloids Surfaces B Biointerfaces* **2018**, *165*, 56–66. [CrossRef] [PubMed]
293. Nguyen, C.T.H.; Webb, R.I.; Lambert, L.K.; Strounina, E.; Lee, E.C.; Parat, M.-O.; McGuckin, M.A.; Popat, A.; Cabot, P.J.; Ross, B.P. Bifunctional succinylated ε-polylysine-coated mesoporous silica nanoparticles for pH-responsive and intracellular drug delivery targeting the colon. *ACS Appl. Mater. Interfaces* **2017**, *9*, 9470–9483. [CrossRef] [PubMed]
294. Chen, L.; Di, J.; Cao, C.; Zhao, Y.; Ma, Y.; Luo, J.; Wen, Y.; Song, W.; Song, Y.; Jiang, L. A pH-driven DNA nanoswitch for responsive controlled release. *Chem. Commun.* **2011**, *47*, 2850–2852. [CrossRef]
295. Chen, M.; Yang, S.; He, X.; Wang, K.; Qiu, P.; He, D. Co-loading of coralyne and indocyanine green into adenine DNA-functionalized mesoporous silica nanoparticles for pH- and near-infrared-responsive chemothermal treatment of cancer cells. *J. Mater. Chem. B* **2014**, *2*, 6064–6071. [CrossRef] [PubMed]
296. He, D.G.; He, X.X.; Wang, K.M.; Chen, M.A.; Zhao, Y.X.; Zou, Z. Intracellular acid-triggered drug delivery system using mesoporous silica nanoparticles capped with T-Hg2+-T base pairs mediated duplex DNA. *J. Mater. Chem. B* **2013**, *1*, 1552–1560. [CrossRef] [PubMed]
297. Murai, K.; Higuchi, M.; Kinoshita, T.; Nagata, K.; Kato, K. Design of a nanocarrier with regulated drug release ability utilizing a reversible conformational transition of a peptide, responsive to slight changes in pH. *Phys. Chem. Chem. Phys.* **2013**, *15*, 11454–11460. [CrossRef]
298. Chen, C.; Pu, F.; Huang, Z.; Liu, Z.; Ren, J.; Qu, X. Stimuli-responsive controlled-release system using quadruplex DNA-capped silica nanocontainers. *Nucleic Acids Res.* **2011**, *39*, 1638–1644. [CrossRef]
299. Xue, M.; Findenegg, G.H. Lysozyme as a pH-responsive valve for the controlled release of guest molecules from mesoporous silica. *Langmuir* **2012**, *28*, 17578–17584. [CrossRef]
300. Mishra, A.K.; Pandey, H.; Agarwal, V.; Ramteke, P.W.; Pandey, A.C. Nanoengineered mesoporous silica nanoparticles for smart delivery of doxorubicin. *J. Nanoparticle Res.* **2014**, *16*, 2515. [CrossRef]
301. Pourjavadi, A.; Tehrani, Z.M.; Bennett, C. PEG-co-polyvinyl pyridine coated magnetic mesoporous silica nanoparticles for pH-responsive controlled release of doxorubicin. *Int. J. Polym. Mater. Polym. Biomater.* **2015**, *64*, 570–577. [CrossRef]
302. Pourjavadi, A.; Tehrani, Z.M. Mesoporous silica nanoparticles with bilayer coating of poly(acrylic acid-co-itaconic acid) and human serum albumin (HSA): A pH-sensitive carrier for gemcitabine delivery. *Mater. Sci. Eng. C* **2016**, *61*, 782–790. [CrossRef] [PubMed]
303. Pourjavadi, A.; Mazaheri Tehrani, Z.; Jokar, S. Chitosan based supramolecular polypseudorotaxane as a pH-responsive polymer and their hybridization with mesoporous silica-coated magnetic graphene oxide for triggered anticancer drug delivery. *Polym. (United Kingdom)* **2015**, *76*, 52–61. [CrossRef]
304. Liu, W.T.; Yang, Y.; Shen, P.H.; Gao, X.J.; He, S.Q.; Liu, H.; Zhu, C.S. Facile and simple preparation of pH-sensitive chitosan-mesoporous silica nanoparticles for future breast cancer treatment. *Express Polym. Lett.* **2015**, *9*, 1068–1075. [CrossRef]
305. Pourjavadi, A.; Tehrani, Z.M. Mesoporous silica nanoparticles (MCM-41) coated PEGylated chitosan as a pH-responsive nanocarrier for triggered release of erythromycin. *Int. J. Polym. Mater. Polym. Biomater.* **2014**, *63*, 692–697. [CrossRef]
306. Chen, F.; Zhu, Y. Chitosan enclosed mesoporous silica nanoparticles as drug nano-carriers: Sensitive response to the narrow pH range. *Microporous Mesoporous Mater.* **2012**, *150*, 83–89. [CrossRef]
307. Sun, Y.; Sun, Y.L.; Wang, L.; Ma, J.; Yang, Y.W.; Gao, H. Nanoassembles constructed from mesoporous silica nanoparticles and surface-coated multilayer polyelectrolytes for controlled drug delivery. *Microporous Mesoporous Mater.* **2014**, *185*, 245–253. [CrossRef]
308. Wan, X.; Zhang, G.; Liu, S. PH-disintegrable polyelectrolyte multilayer-coated mesoporous silica nanoparticles exhibiting triggered co-release of cisplatin and model drug molecules. *Macromol. Rapid Commun.* **2011**, *32*, 1082–1089. [CrossRef]
309. Du, P.; Zhao, X.; Zeng, J.; Guo, J.; Liu, P. Layer-by-layer engineering fluorescent polyelectrolyte coated mesoporous silica nanoparticles as pH-sensitive nanocarriers for controlled release. *Appl. Surf. Sci.* **2015**, *345*, 90–98. [CrossRef]
310. Feng, W.; Nie, W.; He, C.; Zhou, X.; Chen, L.; Qiu, K.; Wang, W.; Yin, Z. Effect of pH-responsive alginate/chitosan multilayers coating on delivery efficiency, cellular uptake and biodistribution of mesoporous silica nanoparticles based nanocarriers. *ACS Appl. Mater. Interfaces* **2014**, *6*, 8447–8460. [CrossRef]

311. Traverso, N.; Ricciarelli, R.; Nitti, M.; Marengo, B.; Furfaro, A.L.; Pronzato, M.A.; Marinari, U.M.; Domenicotti, C. Role of glutathione in cancer progression and chemoresistance. *Oxid. Med. Cell. Longev.* **2013**, 972913. [CrossRef] [PubMed]
312. Cheng, R.; Feng, F.; Meng, F.; Deng, C.; Feijen, J.; Zhong, Z. Glutathione-responsive nano-vehicles as a promising platform for targeted intracellular drug and gene delivery. *J. Control. Release* **2011**, *152*, 2–12. [CrossRef] [PubMed]
313. Estrela, J.M.; Ortega, A.; Obrador, E. Glutathione in cancer biology and therapy. *Crit. Rev. Clin. Lab. Sci.* **2006**, *43*, 143–181. [CrossRef] [PubMed]
314. Balendiran, G.K.; Dabur, R.; Fraser, D. The role of glutathione in cancer. *Cell Biochem. Funct.* **2004**, *22*, 343–352. [CrossRef] [PubMed]
315. Guo, X.; Cheng, Y.; Zhao, X.; Luo, Y.; Chen, J.; Yuan, W.E. Advances in redox-responsive drug delivery systems of tumor microenvironment. *J. Nanobiotechnol.* **2018**, *16*, 74–83. [CrossRef]
316. Maggini, L.; Cabrera, I.; Ruiz-Carretero, A.; Prasetyanto, E.A.; Robinet, E.; De Cola, L. Breakable mesoporous silica nanoparticles for targeted drug delivery. *Nanoscale* **2016**, *8*, 7240–7247. [CrossRef] [PubMed]
317. Mai, N.X.D.; Birault, A.; Matsumoto, K.; Ta, H.K.T.; Intasa-ard, S.G.; Morrison, K.; Thang, P.B.; Doan, T.L.H.; Tamanoi, F. Biodegradable periodic mesoporous organosilica (BPMO) loaded with daunorubicin: A promising nanoparticle-based anticancer drug. *ChemMedChem* **2020**, *15*, 593–599. [CrossRef] [PubMed]
318. Chen, L.; Zhou, X.; Nie, W.; Zhang, Q.; Wang, W.; Zhang, Y.; He, C. Multifunctional redox-responsive mesoporous silica nanoparticles for efficient targeting drug delivery and magnetic resonance imaging. *ACS Appl. Mater. Interfaces* **2016**, *8*, 33829–33841. [CrossRef] [PubMed]
319. Zhang, B.; Luo, Z.; Liu, J.; Ding, X.; Li, J.; Cai, K. Cytochrome c end-capped mesoporous silica nanoparticles as redox-responsive drug delivery vehicles for liver tumor-targeted triplex therapy in vitro and in vivo. *J. Control. Release* **2014**, *192*, 192–201. [CrossRef] [PubMed]
320. Zhao, Q.; Wang, S.; Yang, Y.; Li, X.; Di, D.; Zhang, C.; Jiang, T.; Wang, S. Hyaluronic acid and carbon dots-gated hollow mesoporous silica for redox and enzyme-triggered targeted drug delivery and bioimaging. *Mater. Sci. Eng. C* **2017**, *78*, 475–484. [CrossRef]
321. Jiao, J.; Liu, C.; Li, X.; Liu, J.; Di, D.; Zhang, Y.; Zhao, Q.; Wang, S. Fluorescent carbon dot modified mesoporous silica nanocarriers for redox-responsive controlled drug delivery and bioimaging. *J. Colloid Interface Sci.* **2016**, *483*, 343–352. [CrossRef]
322. Yang, Y.; Lin, Y.; Di, D.; Zhang, X.; Wang, D.; Zhao, Q.; Wang, S. Gold nanoparticle-gated mesoporous silica as redox-triggered drug delivery for chemo-photothermal synergistic therapy. *J. Colloid Interface Sci.* **2017**, *508*, 323–331. [CrossRef]
323. Zhang, Z.; Liu, C.; Bai, J.; Wu, C.; Xiao, Y.; Li, Y.; Zheng, J.; Yang, R.; Tan, W. Silver nanoparticle gated, mesoporous silica coated gold nanorods (AuNR@MS@AgNPs): Low premature release and multifunctional cancer theranostic platform. *ACS Appl. Mater. Interfaces* **2015**, *7*, 6211–6219. [CrossRef] [PubMed]
324. Muhammad, F.; Wang, A.; Qi, W.; Zhang, S.; Zhu, G. Intracellular antioxidants dissolve man-made antioxidant nanoparticles: Using redox vulnerability of nanoceria to develop a responsive drug delivery system. *ACS Appl. Mater. Interfaces* **2014**, *6*, 19424–19433. [CrossRef]
325. Kim, H.; Kim, S.; Park, C.; Lee, H.; Park, H.J.; Kim, C. Glutathione-induced intracellular release of guests from mesoporous silica nanocontainers with cyclodextrin gatekeepers. *Adv. Mater.* **2010**, *22*, 4280–4283. [CrossRef]
326. Zhang, Q.; Liu, F.; Nguyen, K.T.; Ma, X.; Wang, X.; Xing, B.; Zhao, Y. Multifunctional mesoporous silica nanoparticles for cancer-targeted and controlled drug delivery. *Adv. Funct. Mater.* **2012**, *22*, 5144–5156. [CrossRef]
327. Nguyen Thi, T.T.; Tran, T.V.; Tran, N.Q.; Nguyen, C.K.; Nguyen, D.H. Hierarchical self-assembly of heparin-PEG end-capped porous silica as a redox sensitive nanocarrier for doxorubicin delivery. *Mater. Sci. Eng. C* **2017**, *70*, 947–954. [CrossRef] [PubMed]
328. Luo, Z.; Ding, X.; Hu, Y.; Wu, S.; Xiang, Y.; Zeng, Y.; Zhang, B.; Yan, H.; Zhang, H.; Zhu, L.; et al. Engineering a Hollow Nanocontainer Platform with Multifunctional Molecular Machines for Tumor-Targeted Therapy in Vitro and in Vivo. *ACS Nano* **2013**, *7*, 10271–10284. [CrossRef] [PubMed]
329. Liu, J.; Liu, X.; Yuan, Y.; Li, Q.; Chang, B.; Xu, L.; Cai, B.; Qi, C.; Li, C.; Jiang, X.; et al. Supramolecular modular approach toward conveniently constructing and multifunctioning a pH/redox dual-responsive drug

delivery nanoplatform for improved cancer chemotherapy. *ACS Appl. Mater. Interfaces* **2018**, *10*, 26473–26484. [CrossRef] [PubMed]
330. Lin, J.-T.; Liu, Z.-K.; Zhu, Q.-L.; Rong, X.-H.; Liang, C.-L.; Wang, J.; Ma, D.; Sun, J.; Wang, G.-H. Redox-responsive nanocarriers for drug and gene co-delivery based on chitosan derivatives modified mesoporous silica nanoparticles. *Colloids Surfaces B Biointerfaces* **2017**, *155*, 41–50. [CrossRef]
331. Zhou, X.; Chen, L.; Nie, W.; Wang, W.; Qin, M.; Mo, X.; Wang, H.; He, C. Dual-Responsive Mesoporous Silica Nanoparticles Mediated Codelivery of Doxorubicin and Bcl-2 SiRNA for Targeted Treatment of Breast Cancer. *J. Phys. Chem. C* **2016**, *120*, 22375–22387. [CrossRef]
332. Palanikumar, L.; Kim, J.; Oh, J.Y.; Choi, H.; Park, M.-H.; Kim, C.; Ryu, J.-H. Hyaluronic Acid-Modified Polymeric Gatekeepers on Biodegradable Mesoporous Silica Nanoparticles for Targeted Cancer Therapy. *ACS Biomater. Sci. Eng.* **2018**, *4*, 1716–1722. [CrossRef]
333. Li, H.; Zhang, J.Z.; Tang, Q.; Du, M.; Hu, J.; Yang, D. Reduction-responsive drug delivery based on mesoporous silica nanoparticle core with crosslinked poly(acrylic acid) shell. *Mater. Sci. Eng. C* **2013**, *33*, 3426–3431. [CrossRef]
334. Li, Q.L.; Xu, S.H.; Zhou, H.; Wang, X.; Dong, B.; Gao, H.; Tang, J.; Yang, Y.W. PH and Glutathione Dual-Responsive Dynamic Cross-Linked Supramolecular Network on Mesoporous Silica Nanoparticles for Controlled Anticancer Drug Release. *ACS Appl. Mater. Interfaces* **2015**, *7*, 28656–28664. [CrossRef] [PubMed]
335. Yang, C.; Guo, W.; Cui, L.; An, N.; Zhang, T.; Guo, G.; Lin, H.; Qu, F. Fe_3O_4@$mSiO_2$ core–shell nanocomposite capped with disulfide gatekeepers for enzyme-sensitive controlled release of anti-cancer drugs. *J. Mater. Chem. B* **2015**, *3*, 1010–1019. [CrossRef] [PubMed]
336. Li, Z.-Y.; Hu, J.-J.; Xu, Q.; Chen, S.; Jia, H.-Z.; Sun, Y.-X.; Zhuo, R.-X.; Zhang, X.-Z. A redox-responsive drug delivery system based on RGD containing peptide-capped mesoporous silica nanoparticles. *J. Mater. Chem. B* **2015**, *3*, 39–44. [CrossRef]
337. Cheng, Y.J.; Zhang, A.Q.; Hu, J.J.; He, F.; Zeng, X.; Zhang, X.Z. Multifunctional peptide-amphiphile end-capped mesoporous silica nanoparticles for tumor targeting drug delivery. *ACS Appl. Mater. Interfaces* **2017**, *9*, 2093–2103. [CrossRef]
338. Sha, L.; Wang, D.; Mao, Y.; Shi, W.; Gao, T.; Zhao, Q.; Wang, S. Hydrophobic interaction mediated coating of pluronics on mesoporous silica nanoparticle with stimuli responsiveness for cancer therapy. *Nanotechnology* **2018**, *29*, 345101. [CrossRef]
339. Xiao, D.; Jia, H.-Z.; Ma, N.; Zhuo, R.-X.; Zhang, X.-Z. A redox-responsive mesoporous silica nanoparticle capped with amphiphilic peptides by self-assembly for cancer targeting drug delivery. *Nanoscale* **2015**, *7*, 10071–10077. [CrossRef] [PubMed]
340. Ruan, H.; Hao, S.; Young, P.; Zhang, H. Targeting cathepsin B for cancer therapies. *Horizons Cancer Res.* **2015**, *56*, 23–40.
341. de la Torre, C.; Mondragón, L.; Coll, C.; Sancenón, F.; Marcos, M.D.; Martínez-Máñez, R.; Amorós, P.; Pérez-Payá, E.; Orzáez, M. Cathepsin-B induced controlled release from peptide-capped mesoporous silica nanoparticles. *Chem. Eur. J.* **2014**, *20*, 15309–15314. [CrossRef] [PubMed]
342. Li, J.; Liu, F.; Shao, Q.; Min, Y.; Costa, M.; Yeow, E.K.L.; Xing, B. Enzyme-responsive cell-penetrating peptide conjugated mesoporous silica quantum dot nanocarriers for controlled release of nucleus-targeted drug molecules and real-time intracellular fluorescence imaging of tumor cells. *Adv. Healthc. Mater.* **2014**, *3*, 1230–1239. [CrossRef] [PubMed]
343. Cheng, Y.J.; Luo, G.F.; Zhu, J.Y.; Xu, X.D.; Zeng, X.; Cheng, D.B.; Li, Y.M.; Wu, Y.; Zhang, X.Z.; Zhuo, R.X.; et al. Enzyme-induced and tumor-targeted drug delivery system based on multifunctional mesoporous silica nanoparticles. *ACS Appl. Mater. Interfaces* **2015**, *7*, 9078–9087. [CrossRef] [PubMed]
344. Zheng, F.; Zhang, P.; Xi, Y.; Huang, K.; Min, Q.; Zhu, J.-J. Peptide-mediated core/satellite/shell multifunctional nanovehicles for precise imaging of cathepsin B activity and dual-enzyme controlled drug release. *NPG Asia Mater.* **2017**, *9*, e366. [CrossRef]
345. Tukappa, A.; Ultimo, A.; de la Torre, C.; Pardo, T.; Sancenón, F.; Martínez-Máñez, R. Polyglutamic acid-gated mesoporous silica nanoparticles for enzyme-controlled drug delivery. *Langmuir* **2016**, *32*, 8507–8515. [CrossRef]
346. Li, E.; Yang, Y.; Hao, G.; Yi, X.; Zhang, S.; Pan, Y.; Xing, B.; Gao, M. Multifunctional magnetic mesoporous silica nanoagents for in vivo enzyme-responsive drug delivery and MR imaging. *Nanotheranostics* **2018**, *2*, 233–242. [CrossRef]

347. Hu, J.-J.; Liu, L.-H.; Li, Z.-Y.; Zhuo, R.-X.; Zhang, X.-Z. MMP-responsive theranostic nanoplatform based on mesoporous silica nanoparticles for tumor imaging and targeted drug delivery. *J. Mater. Chem. B* **2016**, *4*, 1932–1940. [CrossRef]
348. Eskandari, P.; Bigdeli, B.; Porgham Daryasari, M.; Baharifar, H.; Bazri, B.; Shourian, M.; Amani, A.; Sadighi, A.; Goliaei, B.; Khoobi, M.; et al. Gold-capped mesoporous silica nanoparticles as an excellent enzyme-responsive nanocarrier for controlled doxorubicin delivery. *J. Drug Target.* **2019**, *27*, 1084–1093. [CrossRef]
349. van Rijt, S.H.; Bölükbas, D.A.; Argyo, C.; Datz, S.; Lindner, M.; Eickelberg, O.; Königshoff, M.; Bein, T.; Meiners, S. Protease-mediated release of chemotherapeutics from mesoporous silica nanoparticles to ex vivo human and mouse lung tumors. *ACS Nano* **2015**, *9*, 2377–2389. [CrossRef]
350. Xu, J.-H.; Gao, F.-P.; Li, L.-L.; Ma, H.L.; Fan, Y.-S.; Liu, W.; Guo, S.-S.; Zhao, X.-Z.; Wang, H. Gelatin–mesoporous silica nanoparticles as matrix metalloproteinases-degradable drug delivery systems in vivo. *Microporous Mesoporous Mater.* **2013**, *182*, 165–172. [CrossRef]
351. Liu, Y.; Ding, X.; Li, J.; Luo, Z.; Hu, Y.; Liu, J.; Dai, L.; Zhou, J.; Hou, C.; Cai, K. Enzyme responsive drug delivery system based on mesoporous silica nanoparticles for tumor therapy in vivo. *Nanotechnology* **2015**, *26*, 145102. [CrossRef]
352. Ding, J.; Liang, T.; Zhou, Y.; He, Z.; Min, Q.; Jiang, L.; Zhu, J. Hyaluronidase-triggered anticancer drug and siRNA delivery from cascaded targeting nanoparticles for drug-resistant breast cancer therapy. *Nano Res.* **2017**, *10*, 690–703. [CrossRef]
353. Srivastava, P.; Hira, S.K.; Srivastava, D.N.; Gupta, U.; Sen, P.; Singh, R.A.; Manna, P.P. Protease-Responsive Targeted Delivery of Doxorubicin from Bilirubin-BSA-Capped Mesoporous Silica Nanoparticles against Colon Cancer. *ACS Biomater. Sci. Eng.* **2017**, *3*, 3376–3385. [CrossRef]
354. Polo, L.; Gómez-Cerezo, N.; Aznar, E.; Vivancos, J.L.; Sancenón, F.; Arcos, D.; Vallet-Regí, M.; Martínez-Máñez, R. Molecular gates in mesoporous bioactive glasses for the treatment of bone tumors and infection. *Acta Biomater.* **2017**, *50*, 114–126. [CrossRef]
355. Fernando, I.R.; Ferris, D.P.; Frasconi, M.; Malin, D.; Strekalova, E.; Yilmaz, M.D.; Ambrogio, M.W.; Algaradah, M.M.; Hong, M.P.; Chen, X.; et al. Esterase- and pH-responsive poly(β-amino ester)-capped mesoporous silica nanoparticles for drug delivery. *Nanoscale* **2015**, *7*, 7178–7183. [CrossRef] [PubMed]
356. Sun, Y.-L.; Zhou, Y.; Li, Q.-L.; Yang, Y.-W. Enzyme-responsive supramolecular nanovalves crafted by mesoporous silica nanoparticles and choline-sulfonatocalix[4]arene [2]pseudorotaxanes for controlled cargo release. *Chem. Commun.* **2013**, *49*, 9033–9035. [CrossRef]
357. Patel, K.; Angelos, S.; Dichtel, W.R.; Coskun, A.; Yang, Y.-W.; Zink, J.I.; Stoddart, J.F. Enzyme-responsive snap-top covered silica nanocontainers. *J. Am. Chem. Soc.* **2008**, *130*, 2382–2383. [CrossRef]
358. Linsley, C.S.; Wu, B.M. Recent advances in light-responsive on-demand drug-delivery systems. *Ther. Deliv.* **2017**, *8*, 89–107. [CrossRef] [PubMed]
359. Zhang, Y.; Ang, C.Y.; Li, M.; Tan, S.Y.; Qu, Q.; Luo, Z.; Zhao, Y. Polymer-coated hollow mesoporous silica nanoparticles for triple-responsive drug delivery. *ACS Appl. Mater. Interfaces* **2015**, *7*, 18179–18187. [CrossRef]
360. Lin, X.; Wu, M.; Li, M.; Cai, Z.; Sun, H.; Tan, X.; Li, J.; Zeng, Y.; Liu, X.; Liu, J. Photo-responsive hollow silica nanoparticles for light-triggered genetic and photodynamic synergistic therapy. *Acta Biomater.* **2018**, *76*, 178–192. [CrossRef]
361. Knežević, N.Ž.; Trewyn, B.G.; Lin, V.S.-Y. Functionalized mesoporous silica nanoparticle-based visible light responsive controlled release delivery system. *Chem. Commun.* **2011**, *47*, 2817–2819. [CrossRef] [PubMed]
362. He, D.; He, X.; Wang, K.; Cao, J.; Zhao, Y. A light-responsive reversible molecule-gated system using thymine-modified mesoporous silica nanoparticles. *Langmuir* **2012**, *28*, 4003–4008. [CrossRef] [PubMed]
363. Chai, S.; Guo, Y.; Zhang, Z.; Chai, Z.; Ma, Y.; Qi, L. Cyclodextrin-gated mesoporous silica nanoparticles as drug carriers for red light-induced drug release. *Nanotechnology* **2017**, *28*, 145101. [CrossRef] [PubMed]
364. Yang, G.; Sun, X.; Liu, J.; Feng, L.; Liu, Z. Light-responsive, singlet-oxygen-triggered on-demand drug release from photosensitizer-doped mesoporous silica nanorods for cancer combination therapy. *Adv. Funct. Mater.* **2016**, *26*, 4722–4732. [CrossRef]
365. Zhang, T.; Lin, H.; Cui, L.; An, N.; Tong, R.; Chen, Y.; Yang, C.; Li, X.; Liu, J.; Qu, F. Near infrared light triggered reactive oxygen species responsive upconversion nanoplatform for drug delivery and photodynamic therapy. *Eur. J. Inorg. Chem.* **2016**, *2016*, 1206–1213. [CrossRef]

366. Wang, G.; Dong, J.; Yuan, T.; Zhang, J.; Wang, L.; Wang, H. Visible light and pH responsive polymer-coated mesoporous silica nanohybrids for controlled release. *Macromol. Biosci.* **2016**, *16*, 990–994. [CrossRef]
367. Xing, Q.; Li, N.; Chen, D.; Sha, W.; Jiao, Y.; Qi, X.; Xu, Q.; Lu, J. Light-responsive amphiphilic copolymer coated nanoparticles as nanocarriers and real-time monitors for controlled drug release. *J. Mater. Chem. B* **2014**, *2*, 1182–1189. [CrossRef]
368. Lai, J.; Mu, X.; Xu, Y.; Wu, X.; Wu, C.; Li, C.; Chen, J.; Zhao, Y. Light-responsive nanogated ensemble based on polymer grafted mesoporous silica hybrid nanoparticles. *Chem. Commun.* **2010**, *46*, 7370–7372. [CrossRef]
369. Sun, Y.-L.; Yang, B.-J.; Zhang, S.X.-A.; Yang, Y.-W. Cucurbit[7]uril Pseudorotaxane-Based Photoresponsive Supramolecular Nanovalve. *Chem.—A Eur. J.* **2012**, *18*, 9212–9216. [CrossRef]
370. Wang, M.; Wang, T.; Wang, D.; Jiang, W.; Fu, J. Acid and light stimuli-responsive mesoporous silica nanoparticles for controlled release. *J. Mater. Sci.* **2019**, *54*, 6199–6211. [CrossRef]
371. Zhao, J.; He, Z.; Li, B.; Cheng, T.; Liu, G. AND logic-like pH- and light-dual controlled drug delivery by surface modified mesoporous silica nanoparticles. *Mater. Sci. Eng. C* **2017**, *73*, 1–7. [CrossRef] [PubMed]
372. Mei, X.; Yang, S.; Chen, D.; Li, N.; Li, H.; Xu, Q.; Ge, J.; Lu, J. Light-triggered reversible assemblies of azobenzene-containing amphiphilic copolymer with β-cyclodextrin-modified hollow mesoporous silica nanoparticles for controlled drug release. *Chem. Commun.* **2012**, *48*, 10010–10012. [CrossRef] [PubMed]
373. Bian, Q.; Xue, Z.; Sun, P.; Shen, K.; Wang, S.; Jia, J. Visible-light-triggered supramolecular valves based on β-cyclodextrin-modified mesoporous silica nanoparticles for controlled drug release. *RSC Adv.* **2019**, *9*, 17179–17182. [CrossRef]
374. Lu, J.; Choi, E.; Tamanoi, F.; Zink, J.I. Light-activated nanoimpeller-controlled drug release in cancer cells. *Small* **2008**, *4*, 421–426. [CrossRef]
375. Croissant, J.; Maynadier, M.; Gallud, A.; Peindy N'Dongo, H.; Nyalosaso, J.L.; Derrien, G.; Charnay, C.; Durand, J.-O.; Raehm, L.; Serein-Spirau, F.; et al. Two-photon-triggered drug delivery in cancer cells using nanoimpellers. *Angew. Chem. Int. Ed.* **2013**, *52*, 13813–13817. [CrossRef]
376. Kim, H.-J.; Matsuda, H.; Zhou, H.; Honma, I. Ultrasound-triggered smart drug release from a poly(dimethylsiloxane)– Mesoporous silica composite. *Adv. Mater.* **2006**, *18*, 3083–3088. [CrossRef]
377. Li, X.; Xie, C.; Xia, H.; Wang, Z. pH and ultrasound dual-responsive polydopamine-coated mesoporous silica nanoparticles for controlled drug delivery. *Langmuir* **2018**, *34*, 9974–9981. [CrossRef]
378. Wang, J.; Jiao, Y.; Shao, Y. Mesoporous silica nanoparticles for dual-mode chemo-sonodynamic therapy by low-energy ultrasound. *Materials* **2018**, *11*, 2041. [CrossRef]
379. Li, X.; Wang, Z.; Xia, H. Ultrasound reversible response nanocarrier based on sodium alginate modified mesoporous silica nanoparticles. *Front. Chem.* **2019**, *7*, 59. [CrossRef]
380. Lee, S.-F.; Zhu, X.-M.; Wang, Y.-X.J.; Xuan, S.-H.; You, Q.; Chan, W.-H.; Wong, C.-H.; Wang, F.; Yu, J.C.; Cheng, C.H.K.; et al. Ultrasound, pH, and magnetically responsive crown-ether-coated core/shell nanoparticles as drug encapsulation and release systems. *ACS Appl. Mater. Interfaces* **2013**, *5*, 1566–1574. [CrossRef]
381. Cheng, C.-A.; Chen, W.; Zhang, L.; Wu, H.H.; Zink, J.I. A responsive mesoporous silica nanoparticle platform for magnetic resonance imaging-guided high-intensity focused ultrasound-stimulated cargo delivery with controllable location, time, and dose. *J. Am. Chem. Soc.* **2019**, *141*, 17670–17684. [CrossRef] [PubMed]
382. Paris, J.L.; Cabañas, M.V.; Manzano, M.; Vallet-Regí, M. Polymer-grafted mesoporous silica nanoparticles as ultrasound-responsive drug carriers. *ACS Nano* **2015**, *9*, 11023–11033. [CrossRef] [PubMed]
383. Jose, J.; Kumar, R.; Harilal, S.; Mathew, G.E.; Parambi, D.G.T.; Prabhu, A.; Uddin, M.S.; Aleya, L.; Kim, H.; Mathew, B. Magnetic nanoparticles for hyperthermia in cancer treatment: An emerging tool. *Environ. Sci. Pollut. Res.* **2019**. [CrossRef] [PubMed]
384. Zhu, Y.; Tao, C. DNA-capped Fe_3O_4/SiO_2 magnetic mesoporous silica nanoparticles for potential controlled drug release and hyperthermia. *RSC Adv.* **2015**, *5*, 22365–22372. [CrossRef]
385. Li, X.; Wang, X.; Hua, M.; Yu, H.; Wei, S.; Wang, A.; Zhou, J. Photothermal-triggered controlled drug release from mesoporous silica nanoparticles based on base-pairing rules. *ACS Biomater. Sci. Eng.* **2019**, *5*, 2399–2408. [CrossRef]
386. Yu, Z.; Li, N.; Zheng, P.; Pan, W.; Tang, B. Temperature-responsive DNA-gated nanocarriers for intracellular controlled release. *Chem. Commun.* **2014**, *50*, 3494–3497. [CrossRef]

387. Schlossbauer, A.; Warncke, S.; Gramlich, P.M.E.; Kecht, J.; Manetto, A.; Carell, T.; Bein, T. A programmable DNA-based molecular valve for colloidal mesoporous silica. *Angew. Chem. Int. Ed.* **2010**, *49*, 4734–4737. [CrossRef]
388. Zhou, L.; Liu, G.; Wang, Y.; Liu, J.; Zhang, Y.; Ma, Y. AuNP and ssDNA capped mesoporous silica nanoparticles for laser controlled drug release. *RSC Adv.* **2019**, *9*, 34958–34962. [CrossRef]
389. Ruiz-Hernández, E.; Baeza, A.; Vallet-Regí, M. Smart drug delivery through DNA/magnetic nanoparticle gates. *ACS Nano* **2011**, *5*, 1259–1266. [CrossRef]
390. Ruan, L.; Chen, W.; Wang, R.; Lu, J.; Zink, J.I. Magnetically stimulated drug release using nanoparticles capped by self-assembling peptides. *ACS Appl. Mater. Interfaces* **2019**, *11*, 43835–43842. [CrossRef]
391. Shi, Z.; Yang, C.; Li, R.; Ruan, L. Microwave thermal-triggered drug delivery using thermosensitive peptide-coated core–shell mesoporous silica nanoparticles. *J. Mater. Sci.* **2020**, *55*, 6118–6129. [CrossRef]
392. Cui, Y.; Deng, R.; Li, X.; Wang, X.; Jia, Q.; Bertrand, E.; Meguellati, K.; Yang, Y.-W. Temperature-sensitive polypeptide brushes-coated mesoporous silica nanoparticles for dual-responsive drug release. *Chinese Chem. Lett.* **2019**, *30*, 2291–2294. [CrossRef]
393. Martelli, G.; Zope, H.R.; Bròvia Capell, M.; Kros, A. Coiled-coil peptide motifs as thermoresponsive valves for mesoporous silica nanoparticles. *Chem. Commun.* **2013**, *49*, 9932–9934. [CrossRef] [PubMed]
394. Thomas, C.R.; Ferris, D.P.; Lee, J.-H.; Choi, E.; Cho, M.H.; Kim, E.S.; Stoddart, J.F.; Shin, J.-S.; Cheon, J.; Zink, J.I. Noninvasive remote-controlled release of drug molecules in vitro using magnetic actuation of mechanized nanoparticles. *J. Am. Chem. Soc.* **2010**, *132*, 10623–10625. [CrossRef] [PubMed]
395. Rühle, B.; Datz, S.; Argyo, C.; Bein, T.; Zink, J.I. A molecular nanocap activated by superparamagnetic heating for externally stimulated cargo release. *Chem. Commun.* **2016**, *52*, 1843–1846. [CrossRef] [PubMed]
396. Guisasola, E.; Baeza, A.; Talelli, M.; Arcos, D.; Vallet-Regí, M. Design of thermoresponsive polymeric gates with opposite controlled release behaviors. *RSC Adv.* **2016**, *6*, 42510–42516. [CrossRef]
397. Song, Z.; Shi, J.; Zhang, Z.; Qi, Z.; Han, S.; Cao, S. Mesoporous silica-coated gold nanorods with a thermally responsive polymeric cap for near-infrared-activated drug delivery. *J. Mater. Sci.* **2018**, *53*, 7165–7179. [CrossRef]
398. Ribeiro, T.; Coutinho, E.; Rodrigues, A.S.; Baleizão, C.; Farinha, J.P.S. Hybrid mesoporous silica nanocarriers with thermovalve-regulated controlled release. *Nanoscale* **2017**, *9*, 13485–13494. [CrossRef]
399. Su, Y.; Ojo, O.F.; Tsengam, I.K.M.; He, J.; McPherson, G.L.; John, V.T.; Valla, J.A. Thermoresponsive coatings on hollow particles with mesoporous shells serve as stimuli-responsive gates to species encapsulation and release. *Langmuir* **2018**, *34*, 14608–14616. [CrossRef]
400. Hegazy, M.; Zhou, P.; Wu, G.; Wang, L.; Rahoui, N.; Taloub, N.; Huang, X.; Huang, Y. Construction of polymer coated core–shell magnetic mesoporous silica nanoparticles with triple responsive drug delivery. *Polym. Chem.* **2017**, *8*, 5852–5864. [CrossRef]
401. Brunella, V.; Jadhav, S.A.; Miletto, I.; Berlier, G.; Ugazio, E.; Sapino, S.; Scalarone, D. Hybrid drug carriers with temperature-controlled on–off release: A simple and reliable synthesis of PNIPAM-functionalized mesoporous silica nanoparticles. *React. Funct. Polym.* **2016**, *98*, 31–37. [CrossRef]
402. Peralta, M.E.; Jadhav, S.A.; Magnacca, G.; Scalarone, D.; Mártire, D.O.; Parolo, M.E.; Carlos, L. Synthesis and in vitro testing of thermoresponsive polymer-grafted core-shell magnetic mesoporous silica nanoparticles for efficient controlled and targeted drug delivery. *J. Colloid Interface Sci.* **2019**, *544*, 198–205. [CrossRef] [PubMed]
403. Chang, B.; Sha, X.; Guo, J.; Jiao, Y.; Wang, C.; Yang, W. Thermo and pH dual responsive, polymer shell coated, magnetic mesoporous silica nanoparticles for controlled drug release. *J. Mater. Chem.* **2011**, *21*, 9239–9247. [CrossRef]
404. Tian, Z.; Yu, X.; Ruan, Z.; Zhu, M.; Zhu, Y.; Hanagata, N. Magnetic mesoporous silica nanoparticles coated with thermo-responsive copolymer for potential chemo- and magnetic hyperthermia therapy. *Microporous Mesoporous Mater.* **2018**, *256*, 1–9. [CrossRef]
405. Guisasola, E.; Baeza, A.; Talelli, M.; Arcos, D.; Moros, M.; de la Fuente, J.M.; Vallet-Regí, M. Magnetic-responsive release controlled by hot spot effect. *Langmuir* **2015**, *31*, 12777–12782. [CrossRef]
406. Guisasola, E.; Asín, L.; Beola, L.; de la Fuente, J.M.; Baeza, A.; Vallet-Regí, M. Beyond traditional hyperthermia: In vivo cancer treatment with magnetic-responsive mesoporous silica nanocarriers. *ACS Appl. Mater. Interfaces* **2018**, *10*, 12518–12525. [CrossRef]

407. Hei, M.; Wang, J.; Wang, K.; Zhu, W.; Ma, P.X. Dually responsive mesoporous silica nanoparticles regulated by upper critical solution temperature polymers for intracellular drug delivery. *J. Mater. Chem. B* **2017**, *5*, 9497–9501. [CrossRef]
408. Hu, W.; Bai, X.; Wang, Y.; Lei, Z.; Luo, H.; Tong, Z. Upper critical solution temperature polymer-grafted hollow mesoporous silica nanoparticles for near-infrared-irradiated drug release. *J. Mater. Chem. B* **2019**, *7*, 5789–5796. [CrossRef]